MARTIN MARIETTA ENERGY SYSTEMS LIBRARIES
3 4456 0049758 5

CENTRAL RESEARCH LIBRARY
DOCUMENT COLLECTION

ORNL-2920
UC-81 - Reactors-Power

HOMOGENEOUS REACTOR PROGRAM

QUARTERLY PROGRESS REPORT

FOR PERIOD ENDING JANUARY 31, 1960

CENTRAL RESEARCH LIBRARY
DOCUMENT COLLECTION
LIBRARY LOAN COPY
DO NOT TRANSFER TO ANOTHER PERSON
If you wish someone else to see this document, send in name with document and the library will arrange a loan.

OAK RIDGE NATIONAL LABORATORY
operated by
UNION CARBIDE CORPORATION
for the
U.S. ATOMIC ENERGY COMMISSION

Printed in USA. Price $3.00. Available from the
Office of Technical Services
Department of Commerce
Washington 25, D.C.

LEGAL NOTICE

This report was prepared as an account of Government sponsored work. Neither the United States, nor the Commission, nor any person acting on behalf of the Commission:

A. Makes any warranty or representation, expressed or implied, with respect to the accuracy, completeness, or usefulness of the information contained in this report, or that the use of any information, apparatus, method, or process disclosed in this report may not infringe privately owned rights; or

B. Assumes any liabilities with respect to the use of, or for damages resulting from the use of any information, apparatus, method, or process disclosed in this report.

As used in the above, "person acting on behalf of the Commission" includes any employee or contractor of the Commission, or employee of such contractor, to the extent that such employee or contractor of the Commission, or employee of such contractor prepares, disseminates, or provides access to, any information pursuant to his employment or contract with the Commission, or his employment with such contractor.

cy 8

Date: April 28, 1960

To: Distribution

From: W. D. Reel

Subject: Errata for HRP Quar. Prog. Rep. Jan. 31, 1960 (ORNL-2920)

Please make the following changes in your copy of the subject report:

Page 29, Fig. 7.2, change:

"CASE I - DIFFUSION NEGLECTED"

to

"CASE I - DIFFUSION INCLUDED"

Page 30, Fig. 7.3, change:

"II - HEAT FLUX TO REMOVE FRICTION HEATING IN CORE FLUID"

to

"II - HEAT FLUX TO REMOVE FISSION HEATING IN CORE FLUID"

WDR/ds

Distribution

Same as Internal Distribution for ORNL-2920

ORNL-2920
Reactors-Power
TID-4500 (15th ed.)

Contract No. W-7405-eng-26

HOMOGENEOUS REACTOR PROGRAM

QUARTERLY PROGRESS REPORT

for Period Ending January 31, 1960

Program Director - R. B. Briggs

Homogeneous Reactor Test - S. E. Beall
Reactor Analysis and Engineering Development - R. N. Lyon
Reactor Materials Research - E. G. Bohlmann
Chemical Engineering Development - D. E. Ferguson
Supporting Chemical Research - H. F. McDuffie
Analytical Chemistry - M. T. Kelley

DATE ISSUED

APR 2 . 1960

OAK RIDGE NATIONAL LABORATORY
Oak Ridge, Tennessee
operated by
UNION CARBIDE CORPORATION
for the
U. S. ATOMIC ENERGY COMMISSION

MARTIN MARIETTA ENERGY SYSTEMS LIBRARIES

3 4456 0049758 5

SUMMARY

PART I. HOMOGENEOUS REACTOR TEST

1. HRT Operations

During run 21, which occupied the greater portion of the report period, the reactor operated continuously for 105 days and generated approximately 5600 Mwhr(th). The major objective of the run was the investigation of fuel stability. The reactor operated for long periods at the design power of 5 Mw with none of the usual indications of instability while the system pressure was kept at 1250 psig. At higher pressures instabilities were encountered at 5 Mw. The amount of excess acid in the fuel also affected the instability threshold. There was an approximate 1-Mw elevation in the power threshold when the acid level was increased from an acid-to-sulfate ratio of 0.25 to a ratio of 0.35. This improvement is consistent with the elevation of the heavy-liquid-phase separation temperature with increasing acidity.

The O_2 addition rate was varied but had no detectable effect on reactor stability. In an experiment to observe effects of suspended solids which might be in the core, it appeared that suspended solids were not present in sufficient quantity to be measurable as a reactivity change.

Experiments on internal recombination indicated specific rate constants for copper 2.5 times those determined in early operation of the HRT and in out-of-pile experiments.

Run 21 ended on January 22, so that the reason for an abrupt change in the mixing rate of fuel between the core and blanket could be investigated and a reactor steam-system valve could be repaired.

2. HRT Processing Plant

The multiclone-hydroclone solids separation system was operated in two periods for a total of 410 hr in run 21. Solids removal rates were a factor of 3 to 5 lower than in comparable periods in run 20, substantiating earlier evidence that the malfunction which was indicated later in run 20 was not corrected by replacement of the hydroclone with a spare prior to run 21. The zirconium content of the solids removed increased significantly, indicating additional corrosion of the core tank, amounting to 1 to 3 kg through the first 1200 hr of run 21.

The xenon poisoning at 5 Mw, determined by measuring the increased Xe^{136} content in the off-gas stream due to capture of neutrons by Xe^{135}, was 0.95%. The discrepancy between this figure and the expected value of 2%, based on available knowledge of iodine behavior in the reactor, has not been resolved.

3. HRT Engineering Development

The Zircaloy wear rings of a test pump ignited while the pump was being operated as a steam-oxygen blower with rubbing contact of the wear rings. Ignition occurred after the pump had been cooled to 72°C and the vapor was essentially pure oxygen. Sets of titanium wear rings, with no rubbing contact, and stainless steel wear rings, with rubbing contact, were not damaged under similar test conditions.

A universal periscope manipulator which provides for gear-driven movements and smooth rotation of various optical core-inspection devices was designed, constructed, and tested. A simplified shielding assembly was designed to permit many HRT maintenance operations to be performed dry, making it unnecessary to flood the reactor cell with water for shielding.

4. HRT Design

A design was completed for a new line to simplify the return of condensate from the fuel low-pressure system to the blanket dump tank in the HRT.

A method was proposed for venting to the reactor cell the space between the steam block and flow-control valves in the event of high activity in reactor steam.

5. HRT Controls and Instrumentation

Shop tests of a Laub Electrocaloric (heat balance) flowmeter revealed that the fluctuations in indicated flow rate observed in previous operational tests on the HRT mockup were due to oscillations produced by a large distance-velocity lag which is present at low flow rates. Investigation of the Laub flowmeter was discontinued, and study of a magnetic flowmeter was begun.

Radiation tests of a miniature television camera were repeated by using a nonbrowning lens; 9.6×10^7 r of gamma radiation was accumulated over a period of 248.5 hr. The only effect of the irradiation was a gradual loss of sensitivity, which was compensated by adjustment of the target control. Tests of the camera after decontamination showed that 80% of the loss in sensitivity was due to loss of Vidicon sensitivity, 14% was due to browning of the lamps which provided illumination, and only 6% was due to lens browning.

Two Eberline model RM-2 radiation monitors were installed in the 7500 Area to give better coverage of radiation hazards to personnel.

Revisions were made to the HRT control system to permit operation of the turbine with reactor steam.

PART II. REACTOR ANALYSIS AND ENGINEERING DEVELOPMENT

6. Reactor Analysis

A two-group, two-dimensional criticality calculation for cylindrical geometry was programmed for the IBM-704. The code facilitates the writing of programs that utilize two-dimensional calculations as subroutines.

7. Development of Fuel- and Slurry-System Components

The stator of the 20-cfm blower was examined and was found to have failed by the short to ground of a stator slot. The irradiation test stator failed after a dosage of 5.4×10^9 rads, which is a satisfactory life for pump-motor insulation.

Failures of the third-stage diaphragm of the oxygen compressor, for recycling contaminated gas, are reported. The increased-capacity solution feed pumps continued to perform satisfactorily in their undurance test. Trouble-free operation of diaphragm pumps for slurries was continued.

A simple slurry feed-tank - feed-pump piping connection was developed and demonstrated.

Satisfactory performance of slurry check valves and letdown chokes continued. A shutoff valve, utilizing an alumina ball and seat, was developed; initial tests were quite promising.

Tests of a 5-in. model of the cylindrical core design, with a swirling annular inlet, indicated that the cool inlet fluid could be maintained in contact with the entire core wall. A 2-ft-dia, 6-ft-long model of this core is being constructed to provide quantitative information on velocity distribution.

Calculations were made of the temperature distribution in a 4- by 12-ft cylindrical core with straight-through flow. Internal core-wall cooling was required to maintain the wall at 260°C or below for the temperature-power system selected.

Preliminary tests were conducted on models of the slurry blanket of a cylindrical reactor.

The preliminary mechanical design of a 380-Mw(thermal) two-region breeder reactor having a slurry blanket and solution core was completed. The core is a 4- by 12-ft cylinder with a swirling annular inlet. Provision is made for internally cooling the core tank, if that becomes necessary, to maintain a wall temperature of 260°C. A thermal shield for the pressure vessel was not required, according to stress computations.

8. Development of Reactor Slurry Systems

Effects of ThO_2 concentration, temperature, and flow rate on the homogeneity of slurry flowing in a horizontal 3-1/2-in. pipe are being studied in run 21A in the 200A loop.

Run 3B in the 200B loop, in which a mixed U-Th oxide was circulated, was interrupted by the formation of an intractable plug in a long vertical line during a shutdown period. Following mechanical removal of the sludge, the run was completed with no additional caking or plugging.

In order to investigate further the caking and plugging observed with mixed U-Th oxide in run 3B, run 4B was initiated with a pure 1600°C-fired thoria believed immune to caking and plugging. Indeed, no difficulties have been encountered during the early part of the run.

Construction and shakedown of a 50A loop were completed, and the first slurry run has been started with a 3.65-μ 1600°C-fired thoria.

Dilatant characteristics of a number of slurries were investigated in the laboratory. The 8% U-Th mixed oxide was found to be extremely dilatant, while pumped 1600°C-fired thoria had little or no dilatancy. A theoretical correlation,

$$P = \frac{\tau_y}{c}\left(e^{4c\,L/D} - 1\right),$$

was developed for predicting the pressure required to blow out plugs, depending on geometry and physical properties, and was confirmed experimentally.

Following completion of run SM-8 in the 300-SM system, the high pressure system was diluted to less than 0.1 g of Th-U per liter and drained. Some major revisions and improvements are being made to the system.

9. Instrument and Valve Development

As part of a program to test and evaluate electronic instrumentation systems for possible use in future reactor systems, a Foxboro model M/62 universal controller was tested. Test results indicated that the controller gain is down 3 db at 10 cps with derivative off and that line voltage effects and long-term control drift were negligible. Further tests will be made on additional components of the Foxboro electronic Consotrol instrumentation system and on representative components of electronic instrumentation systems manufactured by the Taylor, Minneapolis-Honeywell, and Swartwout Instrument Companies.

Sample coupons of Coors Procelain Company Al_2O_3 were tested in high-temperature oxygenated water to determine the suitability of Al_2O_3 for use as a liner material for magnetic flowmeters. Test results indicate an average corrosion rate of 1.3 mpy in 100°C oxygenated water and 9.4 mpy in 300°C oxygenated water. Porosity tests showed that there was not more than a 0.01% increase in weight after being exposed to water at room temperature and at 300°C. The feasibility of lining a Foxboro magnetic flowmeter with an Al_2O_3 sleeve is being investigated.

A prototype flush-diaphragm differential-pressure transmitter, which was constructed by the Foxboro Instrument Company on a best-effort basis, was rereived and tested. Test results indicate that the transmitter was linear within 1/2% of full scale when the range was set at 100-0-100 in. of H_2O. Hysteresis was 1% of full scale when the transmitter was mounted in the horizontal position and was negligible in the vertical position. The zero shift due to pressure was 2% of full scale at 2000 psia. Zero shift due to temperature was negligible at 100°C.

A Hammel-Dahl flushed-bellows, high-pressure slurry control valve was removed from service and inspected following failure of the stem-sealing bellows. Failure of the bellows was attributed to an inability to keep the differential pressure across the bellows wall below 450 psi. At the time of failure the valve had accumulated 4695 hr of service at 1600 psig and 280°C. Examination of the valve trim revealed pitting of the Zircaloy-2 seat and extensive uniform erosion in the guide region of the plug shank. The Zircaloy-2 plug appeared to be in good condition.

Six isolation valves between the high- and low-pressure systems of the slurry mockup loop were removed and leak tested. One valve, which utilized a Stellite No. 6 plug and a Stellite No. 12 seat, had suffered severe damage

in the plug-seating region. Another valve, which utilized Armco 17-4 PH for both plug and seat, exhibited a leak rate of 4 cc/min when water was applied under the valve seat for 10 min.

Three Annin Company split-body valves are being modified to accept a standard ring gasket between the body sections.

PART III. SOLUTION FUELS

10. Reactions in Aqueous Solutions

In the temperature range 79-114°C typical reactor fuel solutions were found to respond to the sudden addition of H_2O_2 or solid uranium peroxide in a manner which was consistent with a rapid establishment of the two equilibria:

$$UO_4 \text{ (solid)} \rightleftharpoons UO_4 \text{ (in solution)}$$

$$UO_4 \text{ (in solution)} + 2H^+ \rightleftharpoons UO_2^{++} + H_2O_2$$

to give a saturated solution of uranium peroxide. Following the rapid equilibrium with solid-phase uranium peroxide, the course of the slower peroxide-decomposition reaction was followed, and this course was altered by changes in acidity and uranium concentration, as expected.

The maximum permissible power density for a homogeneous reactor solution was related to the uranyl ion concentration, the acidity, the UO_4 solubility, the equilibrium constant for the second equilibrium given above, and the rate of peroxide decomposition in the solution by an equation which reduces to the form

$$W_{max} = \left(1.05 + 378 \frac{\left[H^+\right]^2}{\left[UO_2^{++}\right]}\right) k_{obs}$$

This equation is known to be strictly valid only over the range of the experimental conditions, although the extrapolation to reactor operating conditions is believed to be reasonable.

11. Heterogeneous Equilibria in Aqueous Systems

Laboratory experiments to determine temperatures of immiscibility for synthetic HRT fuels and their concentrates were continued. The temperatures of second-liquid-phase formation were obtained for three series of solutions and concentrates having mole ratios, $UO_2SO_4:CuSO_4:D_2SO_4$, of 1:1:1, 1:1:1.5, and 1:1:2. These series showed minimum temperatures of 326, 340, and 350°C at six, four, and three times, respectively, the concentration of solutions initially 0.025 M in UO_2SO_4.

The heavy-liquid phase from a synthetic HRE-2 fuel solution was found to redissolve only slowly just below the immiscibility temperature unless good mixing was provided. The rate of solution increased as the temperature was lowered until, finally, the interface disappeared. It was proposed that the temperature of disappearance of the interface corresponded to the minimal immiscibility temperature of the multicomponent phase diagram of the system.

Over-all solubility data are presented for the system UO_3-CuO-NiO-SO_3-H_2O, its D_2O analog, and its included four- and three-component systems. In previous reports, solubility data at 300°C at a fixed concentration of SO_3, that is, either at 0.06 or 0.08 m SO_3, were presented. In this report the data are given for solubilities of the solid phases as a function of SO_3 concentration from 0.04 to 0.5 m. From these over-all data, skeletal diagrams at fixed SO_3 concentration can be constructed in order to specify solubility limitations for HRT fuel compositions.

The precise measurement of the pH of intensely radioactive solutions using a glass electrode is difficult because of radiation effects on glass. If the radioactive solutions are diluted considerably and the pH of the diluted solution determined, then perhaps the effect of radiation on the electrode would be reduced. The pH of dilutions of compositions approximating HRT fuel solutions was measured. These data showed, to a close approximation, that a single measurement of pH of the diluted, synthetic HRT fuel solution could be related to the free-acid concentration of the undiluted solution; the method may be of potential use for determination of free D_2SO_4 in HR fuel compositions.

A previous observation on the effect of hydraulic pressure on the two-liquid-phase boundary temperature indicated that the temperature-pressure coefficient may be large. In order to establish an order of magnitude for this effect, exploratory experiments were performed on UO_2SO_4 solutions by sealing a solution in a platinum tube, pressurizing the tube and contents in an autoclave, and maintaining the tube above the usual two-liquid phase boundary temperature. After cooling the tube, removing the pressure, and removing the tube from the autoclave, the contents were examined to establish whether liquid-liquid immiscibility had been eliminated. Results indicated $\Delta t/\Delta p$ values greater than 1.9°C but less than 8.7°C per 1000 psi for aqueous UO_2SO_4 solutions approximating 1 M in concentration.

The effect of the mole ratio, UO_3/SO_3, on immiscibility temperatures of 0.02, 0.05, and 0.20 m SO_3 solutions was determined. As in the previous study of solutions 0.1 M in SO_3, plots of temperature vs the mole ratio, UO_3/SO_3, gave approximately linear relationships down to low ratios. At even lower ratios the UO_3 component was found to be soluble in the supercritical fluid as expected.

The previous investigation of the system UO_3-N_2O_5-H_2O from 135 to 300°C and from 0.00025 to 5 m HNO_3 was extended by measurements at 25, 325, and 350°C from 0.005 to 5 m HNO_3. Upon increasing the temperature from 25 to 350°C, the mole ratio, UO_3/HNO_3, at saturation was found to decrease from 0.6 to 0.54 at 5 m HNO_3 and from 1.2 to 0.15 at 0.005 m HNO_3.

In two-liquid-phase composition studies made by REED, a heavy second-liquid phase was collected from 0.034 M UO_2SO_4, 0.0194 M $CuSO_4$, 0.0097 M $NiSO_4$, 0.0275 M D_2SO_4 in D_2O at 325°C and shown to be 4.56 M U, 1.53 M Cu, 0.413 M Ni, 6.52 M sulfate, and less than 0.01 M acid. If sulfate equivalent to the nickel is subtracted from the total sulfate, the uranium, copper, and remaining sulfate are in the ratio 3:1:4 in the heavy phase.

12. Solution Corrosion

The critical velocity for cast type CD4MCu stainless steel was shown to be about the same as that for cast type 347 stainless steel in 0.04 m UO_2SO_4, 0.025 m D_2SO_4, 0.02 m $CuSO_4$ at 250°C. The critical velocity for type 304 + 0.5% Pt stainless steel was 5 to 10 fps higher than for type 304 or 347 under the same conditions.

13. Radiation Corrosion

Batch-type experiments were performed to study the sorption of uranium on hydrous zirconium oxide from UO_2SO_4 solutions at 250°C. Refined techniques yielded quite reproducible data which indicate the dependence of sorption on uranium concentration in the range 1 to 30 g/liter. These data should serve as a base line for a study of the effects of other variables which may affect the amount or nature of the sorption.

PART IV. SLURRY FUELS

14. Engineering and Physical Properties

The rheological characteristics of two suspensions of spherical thoria particles were determined for comparison with earlier results on irregularly crystalline ThO_2. One of the suspensions consisted of 1.4-μ-dia particles prepared by flame calcination; the second contained 17-μ-dia "standard slurry" spheres refired at 1200°C. Assuming that suspensions of spheroids follow the cubic relationship between the yield stress and the concentration observed previously with irregularly shaped material, the effect of particle diameter was found to be independent of particle shape. On the other hand, the yield stress of suspensions of spheroids may be as low as one-tenth that of suspensions of irregularly crystalline material with the same particle size.

Previously determined laminar heat-transfer coefficients were recorrelated using a recently published theoretical analysis; the data scatter was reduced to half its previous value.

The effects of slurry velocity (5, 10, and 20 fps) and confining-metal surface (stainless steel, nickel, and copper) on cake formation were investigated in the 30-gpm loop at 275°C with slurries composed of particles more resistant to degradation than the 800°C-calcined ThO_2 of earlier studies. Examination of the metal surfaces after 114 hr of circulation with a ThO_2 - 8% UO_2 material calcined at 1050°C showed deposits covering most of the stainless steel in the intermediate-velocity section and the nickel in the high-velocity zone; lesser and thinner deposits were seen on the copper in all velocity regions. The data appear to be reproducible. Circulation for an additional 200 hr in the cleaned tube resulted only in a very thin film in the low-velocity section. Circulation of a 1600°C-calcined ThO_2 for 100 hr yielded a thin deposit on the stainless steel in the 5-fps section; no other deposits were noted. At the end of 300 hr of operation, the entire 20-fps region (all nickel and copper plating had been eroded) and about half of the 10-fps section (without surface preference) were covered with a very thin thorium oxide film. The deposition of films by these more degradation-resistant materials seem to follow the caking behavior of 800°C-calcined ThO_2, indicating that the film-forming mechanism is the same as that previously proposed for the 800°C-calcined ThO_2.

15. Slurry Irradiation Studies

A long-term irradiation test of 25-μ Houdry thoria spheres containing 0.5% uranium was begun. Out-of-pile measurements were made of the solubilities of hydrogen and oxygen in slurries. Hydrogen was not appreciably adsorbed by thoria, but at 250°C with slurry containing 1000 g of Th per kg of H_2O, the apparent solubility of oxygen was approximately twice as great as in pure water.

16. Development of Gas-Recombination Catalysts

Gas-recombination rates sufficient to maintain 0.4 and 1.2 w/ml at 280°C and 100 psi H_2 were obtained with palladium concentrations of 60 and 120 ppm, based on thoria, respectively. The catalyst was added as a suspension of Pd on ThO_2 to a ThO_2 - 8% U oxide slurry containing 100 g of Th per kg of H_2O, which was pressurized with excess oxygen (200 psi at 26°C). In the absence of excess oxygen, the rate increased almost a factor of 10.

Modifications were made to the continuous gas production - recombination apparatus to minimize transfer of slurry into the condenser section.

17. Slurry Corrosion

Corrosion-erosion by D_2O slurries of experimental flame-calcined ThO_2, Th-U oxides, and Th-U-Al oxides, as indicated by attack rates of type 347 stainless steel, titanium, Inconel, and Zircaloy-2, was found in toroid screening tests to be about the same as that normally shown by slurries of ThO_2 prepared by regular-production methods. Slurries of 6% U/Th oxide were generally more aggressive than those of pure ThO_2 or of 6% U/Th - 2% Al/Th preparations in an oxygen atmosphere. In tests using deuterium atmosphere, attack by slurries of Th-U-Al oxides was an average factor of 2 greater than with slurries of Th-U oxides.

In a dynamic loop test at 250°C, using an oxygenated slurry of flame-calcined mixed oxide (3.2% U/Th, 1.6 Al/Th) at a concentration of 450 g of Th per kg of H_2O, attack rates of stainless steels, titanium, titanium alloys, Zircaloy-2, and noble metals were 0.1 mpy or less at a velocity of 20 fps. At 40 fps, attack rates ranged from 0.2 to 1.3 mpy. Rates of alloy steels containing 2 and 5% chromium, carbon steel, PH 15-7 Mo stainless steel, Inconel, and INOR-8 ranged from 1 to 6 mpy at 20 fps, from 1 to 11 mpy at 40 fps, and were least affected by changes in slurry flow velocity. The aggressiveness of the flame-calcined material was approximately equal to that of regular-production thoria.

Attack by the slurry of 2.8% U/Th oxide was approximately a factor of 4 greater than that of pure thoria in two loop tests which were made at comparable test conditions: 250°C, ~700 g of Th per kg of D_2O, using oxygenated slurries of 2.8% U/Th oxide and of pure ThO_2 (average diameters of 2.5 and 2.4 μ, respectively). The 1075°C-calcined Th-U oxide was degraded (average diameter, 1.8 μ) during 340 hr of circulation. The pure thoria, calcined at 1600°C, did not degrade. Attack of types 329, 347, 17-7 PH, 15-7 Mo PH, USS Corex, and Croloy-5 stainless steels, Zircaloy-2, titanium, and Ti-13V, 11 Cr, 3 Al alloys ranged from <0.1 to 1 mpy, with the pure ThO_2 slurry flowing at 20 fps. At 40 fps, rates were 0.2 to 1.4 mpy.

Metallographic examination of a section from the suction port of a cast Zircaloy-2 impeller revealed a moderate increase in zirconium hydride concentration over the interior, extending to a depth of approximately 20 mils. The impeller has been in routine service for 2350 hr in oxygenated slurries and 980 hr in hydrogenated slurries.

Irradiation of experiment L6S-151, the first type 347 stainless steel autoclave experiment containing slurry at 280°C in the HB-6 facility of the LITR, was completed. The autoclave, charged with an overpressure of oxygen, contained slurry at a concentration of 1100 g of Th per kg of D_2O, with 4.8 wt % enriched uranium, based on thorium, and 0.017 m Pd added as a recombination

catalyst. This experiment was operated at temperature for 257 hr out-of-pile and 118 hr in-pile. At an assumed flux of 5.6×10^{12} neutrons·cm^{-2}·sec^{-1} in the fully inserted position, the autoclave generated a fission-power density of 7.2 w/ml at 280°C. Over a period of about 200 hr, temperature differences under irradiation between internal and external autoclave thermocouples rose to a maximum of 61°C and was 41°C at the end of the experiment, whereas a difference of 9°C was attributed to normal radiation-heating effects. When the autoclave was opened, the probable cause of this effect was indicated to be an accumulation of slurry found covering the internal thermocouple in the center of the pin-rack assembly. A catalyst-performance index of 10 w/ml at 100 psi D_2 was observed in the first recombination experiment. Values subsequently ranged between 20 and 7.5 w/ml at 100 psi D_2. An over-all corrosion rate of 0.2 mpy was observed for the 1375 hr at 280°C. Incremental rates fell steadily with increased time. A slight increase in corrosion rate was observed under irradiation. Specimen data were consistent with data based on oxygen consumption.

High corrosion rates were observed in two out-of-pile Zircaloy-2 autoclave experiments containing slurry at a concentration of 1200 g of Th per kg of D_2O with 7.4 wt % enriched uranium, based on thorium, and 0.021 m Pd. Both Zircaloy-2 and type 347 stainless steel pins were attacked.

During continued out-of-pile test operation of a prototype 5-gpm in-pile slurry loop, over-all loop performance has been excellent. Some 2500 hr of out-of-pile operation at 280°C have been accumulated in the loop circulating a D_2O slurry of thorium oxide containing 1/2 wt % uranium. Circulating-slurry concentration ranged from 200 to 800 g of Th per kg of D_2O. Some loss of thoria was observed after ~700 hr of operation by deposition in the loop core section where the slurry flow velocity was only 2 to 4 fps. This loss may be associated with the particle-size degradation (from 1.9 to 0.7 μ in average diameter) observed during circulation. Improvement in particle integrity has been indicated in toroid tests when the firing temperature of the thoria was increased from 1225 to 1500°C, and a quantity of 1500°C-calcined material has been prepared for testing in this loop. Also to be tested is a redesigned core section fabricated of bent piping to improve the core flow geometry and increase the flow velocity.

Studies of the kinetics of recombination of D_2 and O_2 at 280°C were made in the loop while circulating slurry containing a palladium catalyst. At a palladium concentration of 180 mg per liter of circulating slurry, catalytic activities ranged from 0.45 (initially) to 0.25 mole of D_2 per liter per hour at a reference partial pressure of 100 psia D_2 during an operating period of 240 hr. Such recombination rates are adequate for the first in-pile slurry loop experiment.

PART V. FUEL MANUFACTURE AND PROCESSING

18. Thorium Oxide Preparation and Production

Further tests with the jet abrasion tester have confirmed that it is possible to differentiate between a material that is easily degraded and one that does not significantly degrade. However, it was not found possible to detect mild degradation.

Mixed oxides containing 3 at. % uranium prepared by the adsorption method can be fired to 1200°C without significant increase in clinker formation if held at 1000°C for 4 hr before increasing to 1200°C. Mixed oxides containing

0.5 and 8% uranium can be fired to 1400°C with similar pretreatment, without significant increase in clinkers. Air-firing caused greater densification of mixed-oxide powders than hydrogen-firing did.

In the preparation of thoria microspheres by the method of forming thoria sols into beads in isopropyl alcohol, the highest densities were obtained when total water in the forming and washing steps was 17%, but washing on a filter caused spheres to adhere to each other.

Coprecipitation of aluminum with thorium oxalate by the usual oxalate precipitation technique was unsuccessful.

PART VI. METALLURGY

19. Metallurgy

The collection of data for the study of the effects of fabrication variables on the anisotropy of mechanical properties and strain in Zircaloy-2 was completed. The last portion of the data is being analyzed and a final report is being prepared. A determination of the reproducibility of the values for yield and tensile strengths has resulted in a value of 500 psi for the accuracy of determination of any individual value. A more realistic value of reproducibility, estimated from an inspection of all the data determined in the study, is believed to be ±1200 psi. Sheet-type tensile specimens have shown yield strengths 12,000 psi lower and tensile strengths 10,000 psi lower than have round specimens made from the same material for three lots of material. The strain and necking behavior of the sheet-type specimens was consistent with the ellipticity of cross section found in the corresponding round specimens.

Quenching temperature and quenching-rate studies for the Zr-15% Nb alloy have shown that the incubation time at 400°C for omega-phase formation from retained beta phase is increased appreciably by lower quenching temperatures and slower quenching rates, unless the quenching rate is so slow that appreciable amounts of omega phase are formed during the quench.

A continuation of a study of Zircaloy-2 hot pressing has shown that a large flare can be formed in the wall of a spherical vessel with only a small amount of thinout. This tends to confirm the feasibility of forming a full-scale pipe-to-core-vessel transition requiring a minimum of welding.

PART VII. ANALYTICAL CHEMISTRY

20. Analytical Chemistry

A nonaqueous titration method was devised for the rapid determination of sulfate in solutions containing cations which interfere in conventional methods for sulfate. The sulfate is precipitated with barium acetate in an acetic acid medium, after which excess barium acetate is titrated potentiometrically.

Free acid in impure solutions of uranyl sulfate was successfully titrated conductometrically. Interference of hydrolyzable cations is avoided by converting them to slightly dissociated fluoride salts or complexes.

An instrument for measuring low concentrations of oxygen in water was constructed and tested, and was installed at the HRT. A reading of 0.035 ppm O_2 in the reactor steam condensate was obtained with the reactor at 3.4 Mw.

CONTENTS

SUMMARY iii

PART I. HOMOGENEOUS REACTOR TEST

1. HRT OPERATIONS 3
   1.1 Reactor Operations 3
      1.1.1 Stability Investigations 3
      1.1.2 Study for Suspended Solids 4
      1.1.3 Operations Analysis 4
      1.1.4 Equipment Problems 7

2. HRT PROCESSING PLANT 9
   2.1 Hydroclone-System Operation in Run 21 9
   2.2 Measurement of Xe^{135} Poison Fraction 9

3. HRT ENGINEERING DEVELOPMENT 11
   3.1 Circulating-Pump Tests Under Adverse Flow Conditions 11
   3.2 Remote Maintenance 13
      3.2.1 Modification of the HRT Core 13
      3.2.2 Dry-Maintenance Facility 13

4. HRT DESIGN 16
   4.1 Condensate Return: Core-to-Blanket System 16
   4.2 Bleed Lines for Steam-System Block Valves 16

5. HRT CONTROLS AND INSTRUMENTATION 19
   5.1 Component Development 19
      5.1.1 Fuel-Feed Flowmeter 19
      5.1.2 Remote Viewing Equipment 19
   5.2 Maintenance and Modification 20
      5.2.1 Radiation Monitors 20
      5.2.2 Steam-System Revisions 20

PART II. REACTOR ANALYSIS AND ENGINEERING DEVELOPMENT

6. REACTOR ANALYSIS 23
   6.1 Two-Dimensional Reactor Calculations 23

7. DEVELOPMENT OF FUEL- AND SLURRY-SYSTEM COMPONENTS 24
   7.1 Centrifugal Pumps 24
      7.1.1 20-cfm Allis-Chalmers Blower 24
      7.1.2 Stator Irradiation Test 24

7.2 Feed Pumps 24
7.2.1 Oxygen Compressor 24
7.2.2 Increased-Capacity Solution Pumps 25
7.2.3 Slurry Feed Pumps 25
7.3 Slurry Low-Pressure System 25
7.4 Slurry Valves 26
7.4.1 Check Valves 26
7.4.2 Letdown Chokes 26
7.4.3 Shutoff Valves 26
7.5 Heat Exchanger Test Facility 26
7.6 Core and Blanket Vessel Development 26
7.6.1 Cylindrical Core with Swirling Flow 26
7.6.2 Cylindrical Core with Straight-Through Flow 27
7.6.3 Slurry Blanket Vessel 27
7.6.4 Reactor-Vessel Design 33
7.6.5 Pressure-Vessel Thermal Stress 33
7.6.6 Core Vessel and Transition Joint 33
7.6.7 Core-Wall Cooling 35

8. DEVELOPMENT OF REACTOR SLURRY SYSTEMS 37
8.1 Circulating-Slurry Experiments 37
8.1.1 200A Loop Operation 37
8.1.2 200B Loop, Run 3B 39
8.1.3 200B Loop, Run 4B 39
8.1.4 50A Loop 40
8.2 Properties of Slurry Settled Beds 41
8.2.1 Dilatancy Tests 41
8.2.2 Flow of Dilatant Plastic Plugs 43
8.3 300-SM Blanket System Development 43

9. INSTRUMENT AND VALVE DEVELOPMENT 46
9.1 Instrument Development 46
9.1.1 Electric-Systems Evaluation 46
9.1.2 Magnetic Flowmeter 46
9.1.3 Flush-Diaphragm Differential-Pressure Transmitter 47
9.2 Valve Development 48
9.2.1 Hammel-Dahl High-Pressure Slurry Control Valve 48
9.2.2 Inspection of Slurry-Mockup-Loop Valves 49

PART III. SOLUTION FUELS

10. REACTIONS IN AQUEOUS SOLUTIONS 55
10.1 Concentration of Peroxide in Uranyl Sulfate Solutions at Incipient Precipitation 55

11. HETEROGENEOUS EQUILIBRIA IN AQUEOUS SYSTEMS 62
11.1 Two-Liquid-Phase Boundary Temperatures for HRT Fuel Solutions and Their Concentrates: Effect of Varying UO_2SO_4:$CuSO_4$:D_2SO_4 Mole Ratios 62
11.2 Observations on Rate of Solution of Heavy Phase 63
11.3 Investigation of the System UO_3-CuO-NiO-SO_3-H_2O at 300°C 64
11.4 The pH of Solutions Containing UO_2SO_4, $CuSO_4$, $NiSO_4$, H_2SO_4, H_2O, and D_2O; Its Use in the Determination of Free Acid in Homogeneous Reactor Fuels 68
11.5 Effect of Pressure in Elevating the Temperature of Two-Liquid-Phase Formation in the System UO_3-SO_3-H_2O(D_2O) 70

11.6 Effect of UO_3/SO_3 Mole Ratio on Immiscibility Temperature of 0.02, 0.05, and 0.20 m Sulfate Solutions 71
11.7 The System UO_3-N_2O_5-H_2O at 25°C and from 135 to 350°C 71
11.8 Two-Liquid-Phase Studies: Composition 74

12. SOLUTION CORROSION 76
12.1 Critical Velocity of Type CD4MCu Steel and of Type 304 Stainless Steel Containing 0.5% Platinum 76

13. RADIATION CORROSION 78
13.1 Supporting Research 78
13.1.1 Sorption of Uranium on Hydrous Zirconium Oxide from UO_2SO_4 Solutions 78

PART IV. SLURRY FUELS

14. ENGINEERING AND PHYSICAL PROPERTIES 85
14.1 Rheology of Suspensions of Spherical ThO_2 Particles 85
14.2 Laminar Heat Transfer Coefficients of Non-Newtonian Suspensions 85
14.3 Thoria Caking Studies 88

15. SLURRY IRRADIATION STUDIES 91
15.1 Slurry Irradiations in the LITR 91
15.2 Gas Solubility in Aqueous Slurries 91

16. DEVELOPMENT OF GAS-RECOMBINATION CATALYSTS 92
16.1 Palladium as a Catalyst 92
16.2 Development of Continuous Gas Production-Recombination Apparatus 93

17. SLURRY CORROSION 94
17.1 Out-of-Pile Tests 94
17.1.1 Introduction 94
17.1.2 Evaluation Tests with Slurries of Flame-Calcined Oxides of Thorium, Thorium-Uranium, and Thorium-Uranium-Aluminum 94
17.1.3 Toroid Screening Tests 94
17.1.4 Pump-Loop Test with Slurry of Flame-Calcined Thorium-Uranium-Aluminum Oxide 95
17.1.5 Loop Tests Comparing Attack by Slurries of Thorium-Uranium Oxide and Pure Thoria 98
17.1.6 Hydriding of Zirconium-Base Alloys 99
17.2 In-Pile Autoclave Slurry Corrosion Studies 102
17.2.1 Introduction 102
17.2.2 Irradiation of Stainless Steel Autoclave Containing Thoria-Urania Slurry 102
17.2.3 Postirradiation Examination 104
17.2.4 Catalyst Activity and Gas Production 105
17.2.5 Correlation of Time and Radiation Effects on the Corrosion of Type 347 Stainless Steel 105
17.2.6 Pin-Specimen Corrosion in Experiment L6S-151S 107
17.2.7 Out-of-Pile Corrosion in Autoclave Experiments 108
17.3 In-Pile Slurry Loop 108
17.3.1 Introduction 108
17.3.2 Slurry Circulation 109
17.3.3 Catalyst Additions 109

17.3.4 Filter Performance 110
17.3.5 Over-all Loop Corrosion 111
17.3.6 Catalysis Studies 111

PART V. FUEL MANUFACTURE AND PROCESSING

18. THORIUM OXIDE PREPARATION AND PRODUCTION 117
18.1 Evaluation of Thoria and Thoria-Urania Powder Preparations for Blanket Slurries 117
18.1.1 Jet Abrasion Testing 117
18.1.2 Studies of Thoria-Urania 117
18.2 Preparation of Thoria for Homogeneous Reactor Blanket 118
18.2.1 Preparation of Thoria Microspheres 118
18.2.2 Preparation of Thoria-Alumina by Coprecipitation 119
18.3 Oxide Preparation Development 119
18.3.1 Flame Denitration 119

PART VI. METALLURGY

19. METALLURGY 127
19.1 Zircaloy-2 Fabrication Study 127
19.2 Zirconium Alloy Development 128
19.3 Forming of Zircaloy-2 128

PART VII. ANALYTICAL CHEMISTRY

20. ANALYTICAL CHEMISTRY 133
20.1 Determination of Total Sulfate in Solutions of Uranyl Sulfate 133
20.2 Determination of Free Acid in Uranyl Sulfate Solutions 134
20.3 Dissolved-Oxygen Analyzer 134

ORGANIZATION CHART 137

Part I

HOMOGENEOUS REACTOR TEST

1. HRT OPERATIONS

S. E. Beall P. N. Haubenreich J. W. Hill, Jr.

H. F. Bauman D. F. Frech H. B. Piper
N. C. Bradley R. H. Guymon J. L. Redford
J. R. Buchanan R. J. Harvey[1] D. M. Richardson
S. R. Buxton J. Hirota H. C. Roller
J. D. Flynn J. O. Kolb W. Terry

1.1 REACTOR OPERATIONS

During the report period, the reactor operated continuously for 83 days and generated approximately 4200 Mwhr(th), bringing the total continuous operating time in run 21 to 105 days and the total heat generation to 5598 Mwhr. Most of the time during this report period was spent studying the problem of fuel instability and means of preventing the instability. In a demonstration of fuel stability, the reactor was operated at 5 Mw for seven days with none of the usual indications of instability (i.e., loss of temperature or power disturbances). Experimental time was also devoted to (1) determination of copper activity as a catalyst for D_2-O_2 recombination in solution and (2) a study for effects of possible suspended solids in the core.

1.1.1 Stability Investigations

(a) Variation of System Pressure.--Studies previously performed and reported[2] have shown that system pressure had a striking effect on the stability of the reactor. There were no indications of instability when the reactor operated at 5 Mw at 1250 psig, but at higher pressures instabilities were evident at lower power levels; at 1750 psig (the highest pressure investigated), the threshold for reactivity loss or power disturbances was only 1.5 Mw.

The great variation in the fuel stability with pressure was thought to be a result of the relationship between the solution boiling temperature and the two-liquid-phase separation point. In order to accumulate data to substantiate this theory, experiments were conducted in which the system pressure was varied while operating at a constant power level. (Holding the power constant was in contrast to the procedure followed in previous stability experiments in which the power was varied while the system pressure was held constant.)

The experiments were conducted at 260°C at power levels of 3.5 and 5.0 Mw (excess-acid level of 0.30 and 0.32 H_2SO_4/SO_4). At 3.5 Mw it was possible to go as high as 1750 psig before a significant loss of temperature was apparent. However, small power disturbances (<500 kw) started occurring at 1650 psig; it was concluded that 1600 psig was the maximum stable pressure at 3.5 Mw for

this acid content. While operating at 5 Mw, no rapid losses of reactivity were found at pressures as high as 1450 psig. Small power disturbances (<300 kw) occurred infrequently (up to one per hour) at 1350 psig and higher pressures; so it was concluded that 1300 psig was the maximum pressure for stable operation at 5 Mw and 260°C.

It was found that the pressure could be raised to take the reactor into an unstable region and then reduced to attain stability again, with no changes in the power level being necessary. The results were consistent with the known relationship of temperature and pressure to heavy-liquid-phase formation.

(b) Increase in Excess-Acid Level.--Since the two-liquid-phase formation temperature was affected by the acidity of the original solution in laboratory experiments (see Sec. 11.1), the stability of the reactor would be expected to vary with acid content. To test this in the reactor, the amount of excess acid in the fuel solution was increased.

Sufficient sulfuric acid (14.3 moles) was added to the fuel solution to raise the excess-acid content (H_2SO_4/SO_4) from 0.25 to 0.35. At the higher acid content the power threshold for fuel instability was elevated by approximately 1 Mw. The results are presented in Fig. 1.1. The correlation of stable power with acid level was difficult because of the wide scatter (±5%) of the data. Furthermore, the excess acid decreased with time, because of corrosion, making it difficult to get all the data needed at the highest acid levels.

On several occasions, temperature increases of 1 to 3°C were observed immediately after raising the power to 5 Mw. Assuming that the increase might be evidence of fuel deposition in a higher-than-average reactivity position, it was decided to take a series of fuel samples at times when the increase existed.

The study was interrupted by a large increase in the concentration of the blanket fuel solution. Since this indicated greater mixing (possibly through another hole in the core wall) between the core and blanket, the reactor was shut down on January 22 for an inspection.

(c) Variation of System Temperature.--The effect of temperature was explored at each pressure investigated. There was little or no effect on reactor stability between 240 and 275°C.

(d) Increase in O_2 Concentration.--The effect of excess oxygen concentration was explored by increasing the O_2 input to the reactor more than twofold above the normal. There was no apparent effect on the pressure threshold for instability at 5 Mw.

1.1.2 Study for Suspended Solids

In an experiment to determine the effects of suspended solids, the blanket and core circulating rates were varied to less than half the normal flow without any indication that suspended solids are present in quantities sufficient to affect reactivity.

1.1.3 Operations Analysis

(a) Internal Recombination.--Experiments were conducted at various temperatures and pressures to measure threshold powers for bubble letdown. The results are presented in Fig. 1.2. The "predicted" curves are based on a

UNCLASSIFIED
ORNL-LR-DWG 46064

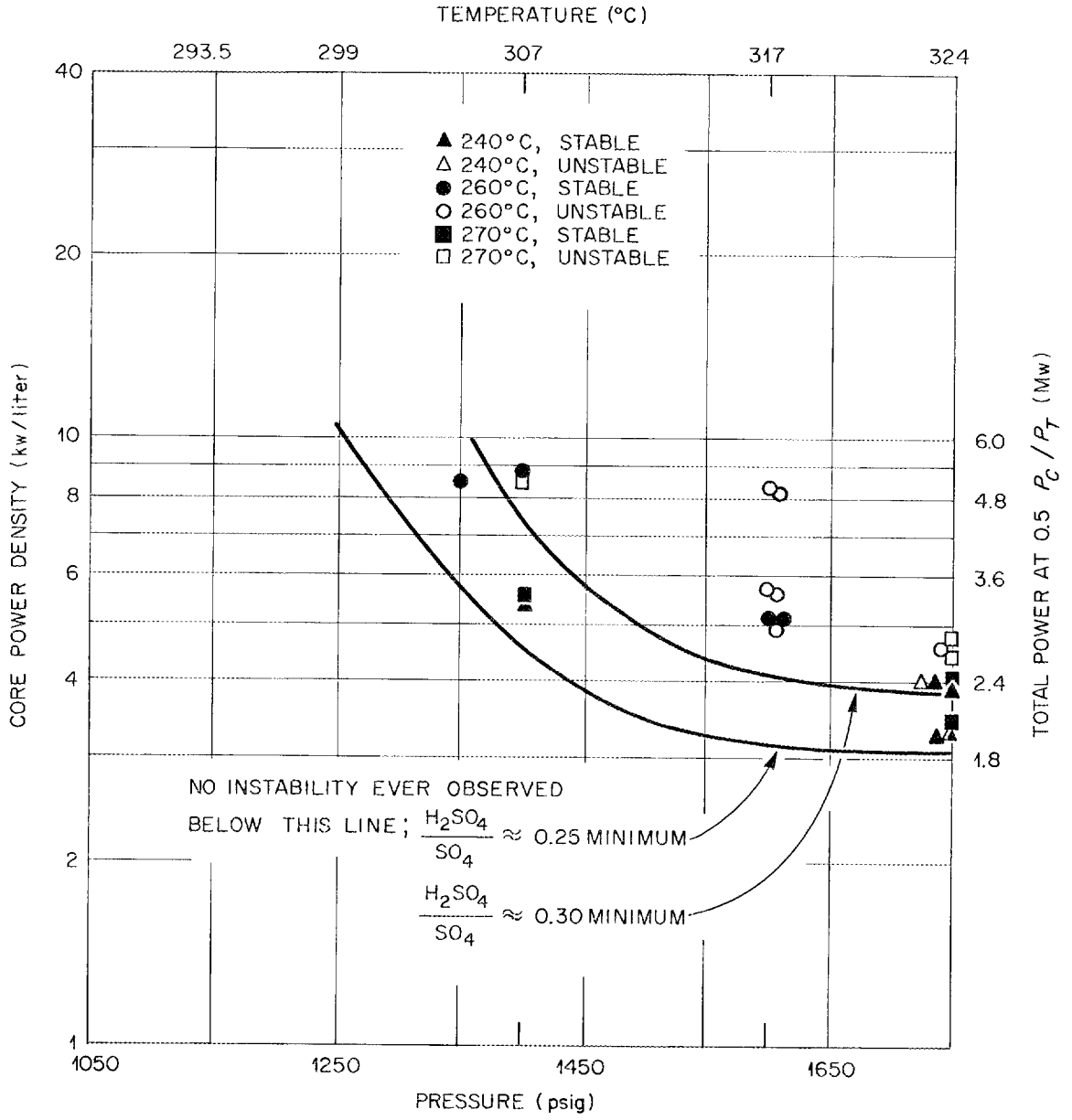

Fig. 1.1. Stability Curves for Two Acid Levels.

specific rate constant for copper 2.5 times that determined in early operation of the HRT and in out-of-pile experiments. The experimental points on Fig. 1.2 were obtained by slowly raising the power at the chosen temperature and pressure until bubble letdown was indicated by the letdown-valve position controller and by an increase in fuel dump-tank pressure. The primary low-pressure catalytic recombiner was completely ineffective and never showed any sign of activity.

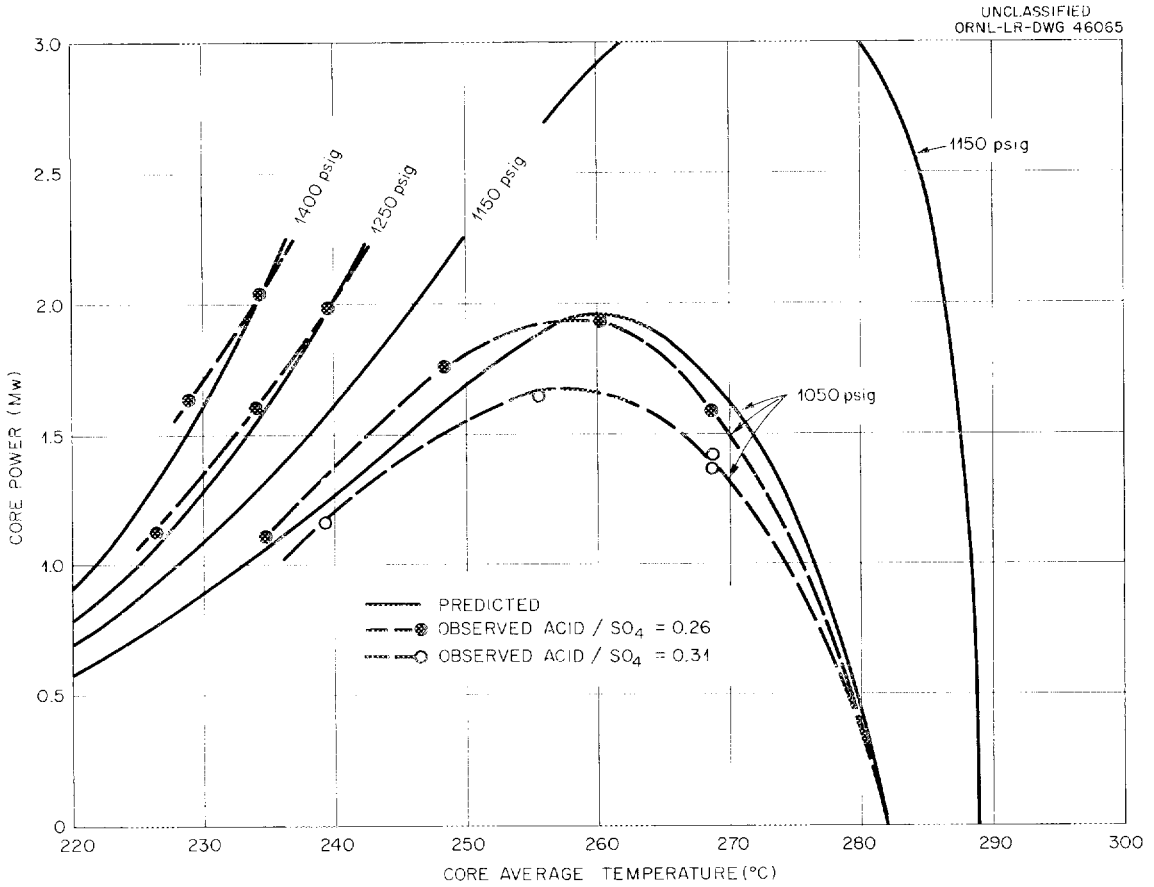

Fig. 1.2. Threshold Powers for Bubble Letdown in Run 21.

These measurements indicate that the catalytic activity of the solution is over twice as great as would be expected from earlier experiments. (Another possible explanation is that the catalyst activity is normal and the G value, or radiolytic yield, only 0.4 of normal.)

The agreement between the predicted and experimental threshold powers indicated that the solution rate constant varied with temperature and copper concentration as expected and was not affected by power level (radiation intensity). Increased acidity lowered the catalyst activity, in qualitative agreement with out-of-pile experiments.

(b) Analysis of Small Power Oscillations.--Further investigations were made into the character of the small oscillations in neutron level which appear whenever the HRT is operated at power.[3] Sensitive, high-speed chart records of neutron level, which had been taken during run 20 under a variety of operating conditions, were analyzed.

A quantitative measure of the "roughness" of the power was obtained by taking many consecutive 0.4-sec intervals and computing the standard deviation of the power. The standard deviation was found to increase with the square of the average power, ranging from 10 kw at 2 Mw to about 50 kw at 5 Mw. There was no significant effect of pressure on roughness, but standard deviations at temperatures around 240°C were slightly less than at 260°C.

The frequency spectrum of the power oscillations was determined for several operating conditions by the auto-correlation technique. At each condition the spectrum exhibited a single strong resonance. The resonant frequency varied with power level, ranging from 0.08 to 0.13 cps. When the reactor was operating with a detectable amount of uranium out of circulation, the power spectrum resonance broadened and shifted to lower frequencies.

The frequency spectrum of the power depends on the spectrum of the input noise and the reactor transfer function, neither of which can be determined separately in the HRT. The resonance in the power spectrum is believed to be influenced mainly by resonance in the transfer function rather than in the noise.

The reactor transfer function depends on the reactor configuration and physical properties of the reactor materials. Transfer functions for the HRT were calculated from a set of equations describing the system. In these equations, a density-reactivity feedback was incorporated. It was possible, by proper choice of values for the compressibility of the core fluid, to obtain transfer functions with characteristics very similar to the observed power spectra. The compressibility required to obtain similarity was about 50 times the compressibility of liquid--or what might reasonably be expected for a fluid containing a small amount of vapor or gas. Increasing the compressibility (or amount of gas) shifts the resonance to lower frequencies.

Analysis of the power oscillations will be extended to a greater number of cases to obtain further insight into the conditions in the reactor.

1.1.4 Equipment Problems

In general, equipment performance has been exceptionally good during the period. Difficulties encountered since run 21 started were:

(a) Feedwater System.--During the shutdown preceding run 21, the stroke on the blanket heat exchanger feedwater control valve (LCV-546) was adjusted during routine testing of the reactor steam system. Early in the run (on October 9), it was found that the C_v of this valve limited the maximum reactor power level to <3.5 Mw. Operation was interrupted for one day to replace the valve plug and increase the C_v almost threefold.

(b) Fuel Feed Pump.--Early in the run (October 22), the diaphragm of the fuel feed pump failed, leaking radioactive liquid into the intermediate system of the pump. The damaged head was isolated by ice plugs without interrupting reactor operation. The second (spare) pumping head (which had been operated previously for 19,000 hr in a pump test rig) has been used since that time without difficulty.

(c) Core Circulating-Pump Circuit.--Core circulation was interrupted for a few hours on October 24 by the burnout of a transformer in the core circulating-pump electrical circuit.

(d) Pressurizer Purge.--Late in November there was a decrease in the pumping rate of the diaphragm pump that purges the fuel pressurizer. The difficulty appeared to be caused by check-valve leakage and was overcome by installing a faster-acting pump drive unit. Since the drive unit is in an accessible area, there was no interruption in reactor operation.

(e) Leak of Steam Valve.--On January 22, reactor steam was observed to be escaping through the packing of a condensate return valve. Since this valve is a part of the secondary containment, it was decided that the reactor should be shut down to permit repair. This coincided with plans to stop power generation so that the change in core-to-blanket mixing rate could be studied.

REFERENCES

1. Japanese Atomic Energy Research Institute.

2. S. E. Beall *et al.*, HRP Prog. Rep. Oct. 31, 1959, ORNL-2879, pp 4,5.

3. J. Hirota, Statistical Analysis of Small Oscillations in the HRT, ORNL CF-60-1-107 (to be issued).

2. HRT PROCESSING PLANT

W. D. Burch O. O. Yarbro

2.1 HYDROCLONE SYSTEM OPERATION IN RUN 21

The multiple-hydroclone system was operated during the initial 86 hr of reactor run 21 (chemical plant run 21-21) and removed 81 g of corrosion-product solids from the reactor system. The solids removal rate (0.95 g/hr) is a factor of 5 below the removal rate observed during a comparable period of run 20. The chemical plant was put on-stream (run 21-22) at the 900th hour of the reactor run after accumulated solids were flushed from the multiclone underflow pot. The purpose of run 21-22 was to measure the removal rate after the circulating solids concentration had reached nominal equilibrium. The solids removal rate of 0.21 g/hr, observed in 324 hr of multiclone operation, is a factor of 2.5 to 3 below the equilibrium rate for the multiclone system indicated by runs 20-15 and 20-16 and is 30% below the equilibrium removal rate observed in reactor runs 16 through 18 for the single-hydroclone system. The reduced removal rate is attributed to some unknown malfunction of the hydroclone system.

The composition of solids removed by the chemical plant during run 21 averaged 50% Zr, 14% Fe, 4.5% Cr, and 2.8% Ti. The ratio of uranium to corrosion-product solids was 0.10 and 0.25 in runs 20-21 and 21-22, respectively. The increased zirconium content of solids removed by the chemical plant indicates additional corrosion of approximately 1 to 3 kg of zirconium through the first 1200 hr of run 21.

During the last 1400 hr of run 21, solids collected in the multiclone were not fed continuously to the chemical plant but were allowed to reach an equilibrium level. (A bypass in the multiclone limits the buildup of solids in normal operation.) After reactor operation ceased, the solids remaining in the multiclone underflow receiver were circulated to the chemical plant hydroclone. Results of the dissolution indicated a removal of 36 g of corrosion products, containing 53% Zr. The ratio of uranium to corrosion products in the solids was 0.08.

2.2 MEASUREMENT OF Xe^{135} POISON FRACTION

The xenon poison fraction was measured directly in one period of operation at 5 Mw. After three days of operation at constant power, a large sample of off-gas was routed to a spare charcoal bed and, after decay of Xe^{133}, the stable isotopes were analyzed by mass-spectrographic techniques for the ratio of Xe^{136} to Xe^{134}. From the known direct fission yield of these two isotopes, the additional Xe^{136} resulting from neutron capture by Xe^{135} could be measured.

By use of Katcoff's yield data,[1] the poisoning was calculated to be 0.96%, with a standard deviation of 0.05%. The absolute accuracy of the calculated poison fraction, which depends on the accuracy of the yield data, may be no better than ±0.15%.

This value compares with an expected poison level of over 2% based on information which indicated that 10% of the iodine and 25% of the xenon in the reactor high-pressure system circulates with the fuel solution.[2] Attempts to estimate the magnitude of xenon poisoning by observing the transient critical temperature following a period of constant high-power operation were inconclusive, but appeared not inconsistent with poisoning of 1%. The only logical explanation of the discrepancy appears to be that the earlier estimates of iodine holdup in the high-pressure system were too high.

REFERENCES

1. S. Katcoff, Nucleonics, 16 (4), 78-85 (1958).

2. W. D. Burch et al., HRP Prog. Rep. Oct. 31, 1959, ORNL-2879, p 10-12.

3. HRT ENGINEERING DEVELOPMENT

I. Spiewak W. R. Gall F. N. Peebles M. I. Lundin

R. Blumberg E. C. Hise P. P. Holz
C. H. Gabbard J. E. Jones, Jr.

3.1 CIRCULATING-PUMP TESTS UNDER ADVERSE FLOW CONDITIONS[1]

The pump torture rig was constructed to investigate the cause and correction of the titanium impeller fires which have occurred in the HRT and in test loops. The Byron-Jackson 50-gpm pump used in the loop was fitted with wear rings of titanium, Zircaloy, and stainless steel, and put through the following test schedule.

1.	Normal operation with oxygenated water at 250°C and 1000 psi	48 hr
2.	Operation with oxygen-saturated water at 250°C and 1000 psi	48 hr
3.	Cavitation run at 250°C and 577 psi (5 to 10% decrease in pump power)	48 hr
4.	Operation with the loop half-full of water at 250°C and 1250-psi oxygen pressure	48 hr
5.	Operation as an oxygen blower at 250°C and 1250 psi	48 hr

A set of titanium wear rings with 0.040-in. (0.020 in. is normal) wear-ring clearance and no contact was run through the test schedule with no damage. A set of stainless steel wear rings with 0.010-in. clearance and rubbing contact was run through parts 1, 4, and 5 with no damage.

A set of Zircaloy wear rings with 0.010-in. clearance and rubbing contact ignited at the conclusion of the second run through the test schedule. Ignition occurred during the cool-down cycle after completing the test schedule. The loop had cooled to 72°C and the oxygen pressure had dropped to 797 psia when the wear rings ignited. Figure 3.1 shows the fresh scoring on the Zircaloy wear rings after the first run. The same rings were used in the second run with slightly heavier contact provided by increased bearing clearance. Figure 3.2 shows the impeller and diffuser after all the Zircaloy and a sizable quantity of stainless steel had been burned.

Testing of titanium wear rings with 0.010-in. clearance is in progress.

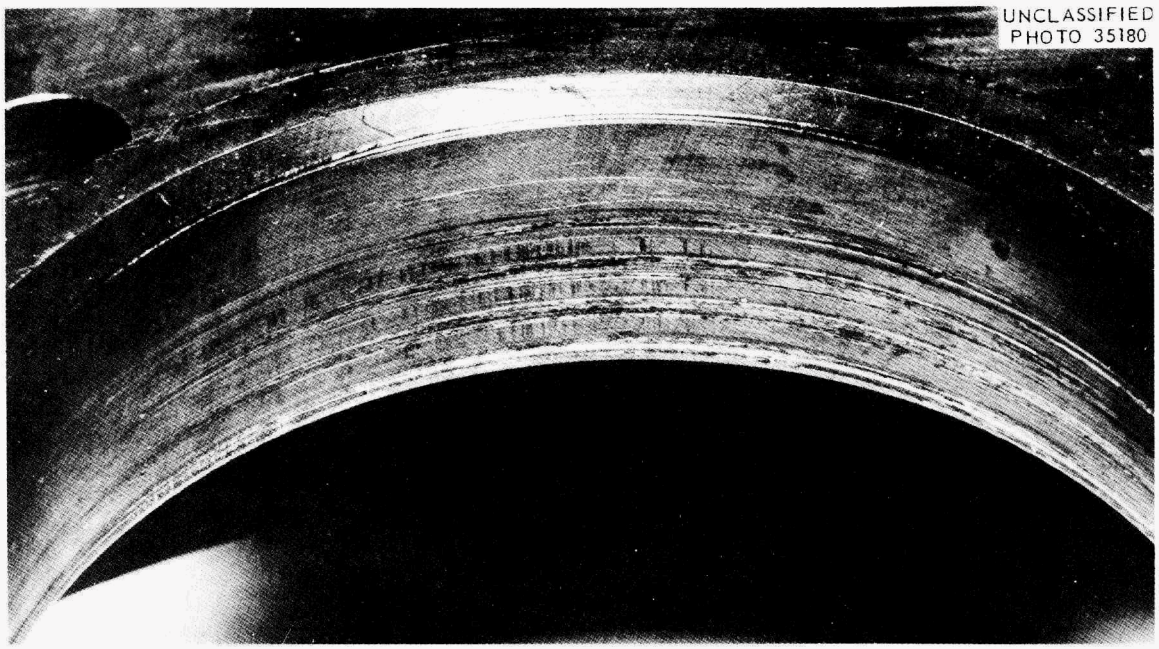

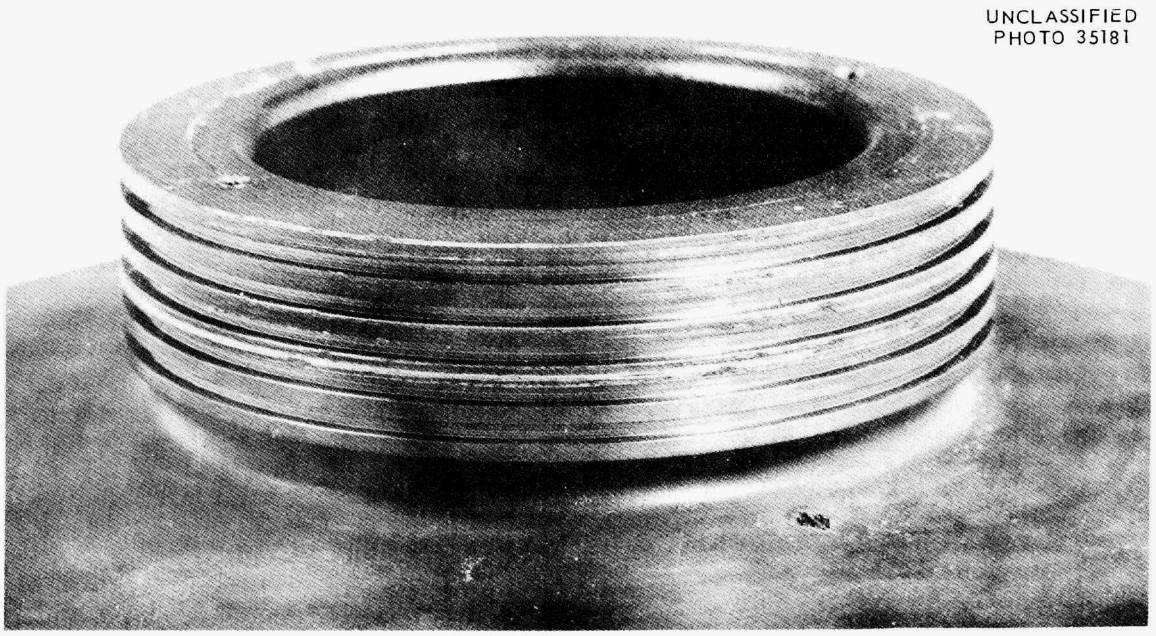

Fig. 3.1. Zircaloy Wear Rings Scored During Test with Rubbing Contact.

UNCLASSIFIED
PHOTO 35237

Fig. 3.2. Pump Impeller and Diffuser After Ignition of Zircaloy Wear Rings.

3.2 REMOTE MAINTENANCE

3.2.1 Modification of the HRT Core[1]

A motion picture was completed showing the detailed operation of each HRT core-modification tool, both on a bench and in the core-maintenance mockup. Developmental reports and detailed operating procedures for each tool were issued.[2]

A universal periscope manipulator for use with the various optical core-inspection devices was designed, constructed, and tested. It provides gear-driven elevation and smooth rotation of periscopes in viewing position.

3.2.2 Dry-Maintenance Facility

A simplified shielding assembly for use in HRT maintenance was designed in cooperation with the Design Section. This assembly (see Fig. 3.3), based on a design reported previously,[3,4] is a temporary replacement for a roof plug and should permit many operations to be performed without flooding the reactor cell with water.

The assembly has four basic components: slide, modules, frame, and track.

1. The slide is 10 ft 10 in. long by 2 ft 8 in. wide and consists of three layers of 3-1/2-in.-thick plate for a total thickness of 10-1/2 in. of steel. A circular cutout near one end accommodates an eccentric plug, several of which are provided for different tool openings.

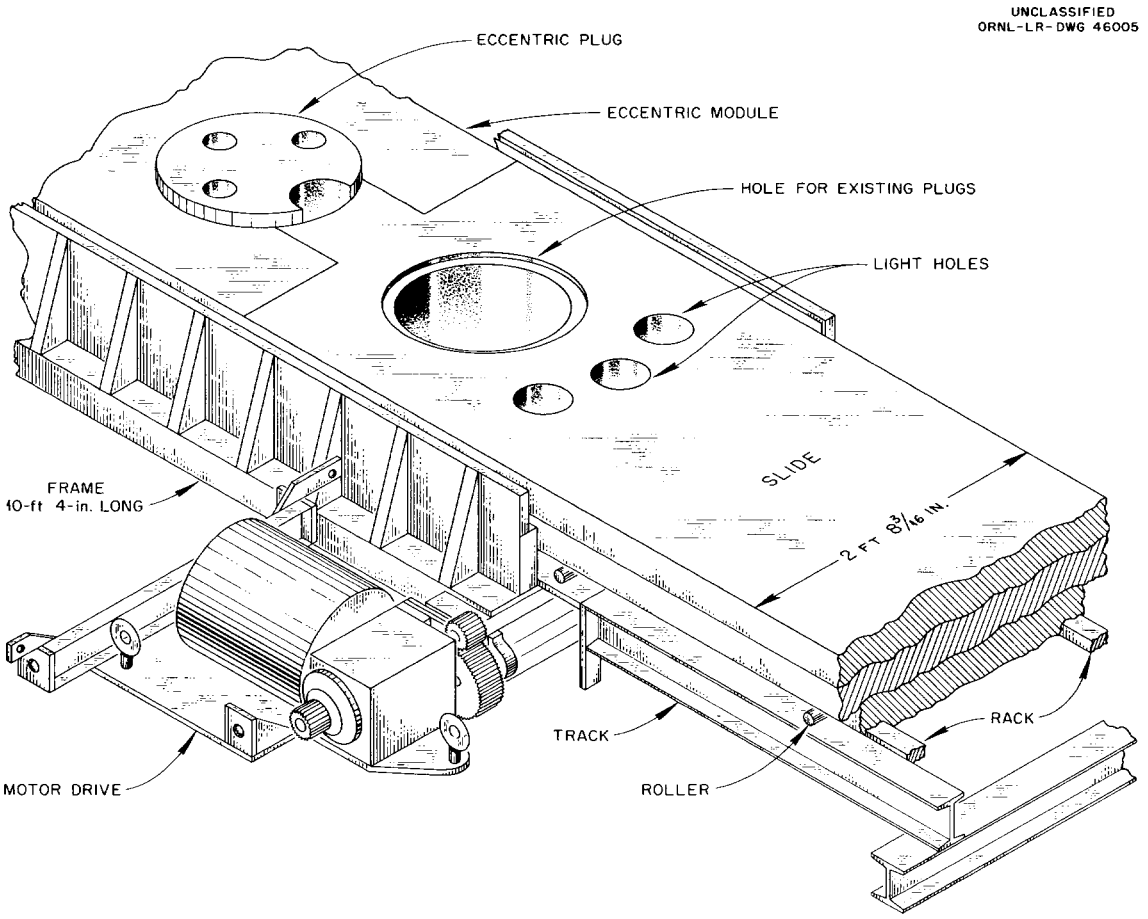

Fig. 3.3. HRT Dry-Maintenance Shield.

2. The modules are additional short sections of slide which can be added to the main slide to allow positioning of tool holes in the slide above the desired work area. One module will contain a rotating plug to allow two-coordinate-positioning of the tool holes.

3. The frame is a support for the slide. After it is installed over a lower roof plug, the slide is removed to one side, the roof plug is removed, and the slide is returned to position over the opening to provide shielding for personnel. A three-quarter-horsepower motor - gear-box combination mounted on the frame moves the slide through a rack and pinion arrangement. The rate of travel is about 1.33 fpm.

4. The track is an extension which can be mounted at either end of the frame and on which the slide and modules move on roller supports.

As many as eleven 150-w lighting fixtures may be mounted in the plugs provided in the slide and modules for illumination of the work area. The work holes are designed to accommodate tools now available.

REFERENCES

1. I. Spiewak et al., HRP Prog. Rep. Oct. 31, 1959, ORNL-2879, p 31-32.

2. J. S. Culver, HRT Core and Blanket Viewing Equipment, ORNL-2886 (in press).

P. P. Holz, Some Miscellaneous Maintenance Tools Used to Manipulate Loose Objects in the HRT Core, ORNL CF-59-11-123 (Nov. 17, 1959)(in press).

R. Blumberg, Design and Development of Tools to Cut Loose the Diffuser Screens and Resize the Access Flange in the HRT Core Vessel, ORNL CF-59-11-124 (Nov. 18, 1959)(in press).

B. D. Draper, Feasibility Tests - Electrolytic Dissolution of Perforated Zircaloy-2 Screens, ORNL CF-59-11-125 (Nov. 24, 1959)(in press).

B. D. Draper and E. C. Hise, Remote Maintenance Procedure Report, ORNL CF-59-11-128 (Nov. 26, 1959)(in press).

P. P. Holz, Miniature TV Camera Manipulator, ORNL CF-59-11-129 (Nov. 26, 1959) (in press).

P. P. Holz, Underwater Electric Arc Cutting Manipulator for HRT Screen Removal, ORNL CF-59-11-130 (Nov. 26, 1959)(in press).

3. W. R. Gall et al., HRP Quar. Prog. Rep. July 31, 1958, ORNL-2561, p 47-48.

4. Vitro Engineering Company Dry Maintenance Study for the HRT (Mar. 12, 1958).

4. HRT DESIGN

W. R. Gall M. I. Lundin

C. A. Burchsted
J. E. Jones
R. C. Robertson

4.1 CONDENSATE RETURN: CORE-TO-BLANKET SYSTEM

Since the formation of a hole in the wall of the HRT core tank (April 1958), the blanket region of the reactor has been kept diluted with a 6-lb/min purge of condensate which is transferred continuously from the fuel condensate tanks to the blanket feed pump. Unfortunately, any fuel solution which reaches the blanket dump tanks by sampling or leakage through valves remains in the dump tanks and must be emptied in batches every day or two.

A design was prepared for a new line (line 1081) to divert condensate flow from the present blanket transfer valve (HCV-434) to the top of the blanket dump tanks (see Fig. 4.1). It will permit the blanket feed pumps to pump continuously from the dump tanks and thus prevent an accumulation of fuel there.

4.2 BLEED LINES FOR STEAM-SYSTEM BLOCK VALVES

In the event of a leak from the tube side to the shell side of a main heat exchanger, radioactive steam could escape the biological shielding if the two sets of steam valves (block and throttling) located downstream of the steam drums do not shut off flow completely.[1] These valves, in the lines to the turbine and heat-dump coolers, all close if the radiation monitors detect activity in the steam-drum pit and initiate a dump of the reactor. New lines (see Fig. 4.2) were added to bleed the space between the block and steam-control valves. Each line is fitted with an air-operated valve which will open on detection of radiation in the steam-drum pit and, in the event of leakage of the main block valves, will thus vent the leakage steam to the reactor cell.

REFERENCE

1. E. H. Gift, Determination of Maximum Permissible Leakage from the HRT Process Steam System, ORNL CF-59-1-143 (Jan. 30, 1959).

UNCLASSIFIED
ORNL—LR—DWG 46006

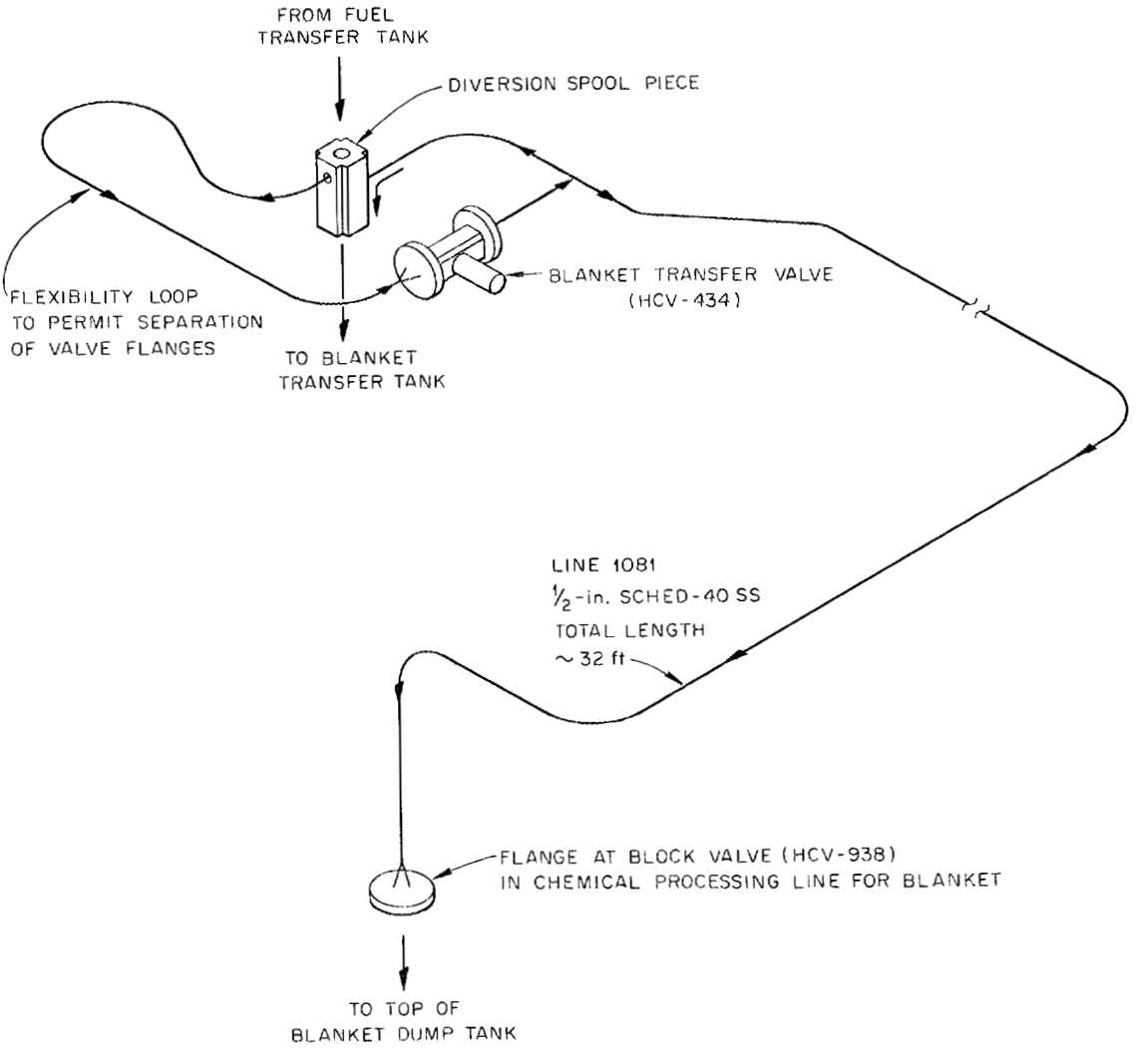

Fig. 4.1. Line 1081 for Transferring Fuel-System Condensate to Top of Blanket Dump Tanks.

UNCLASSIFIED
ORNL-LR-DWG 46007

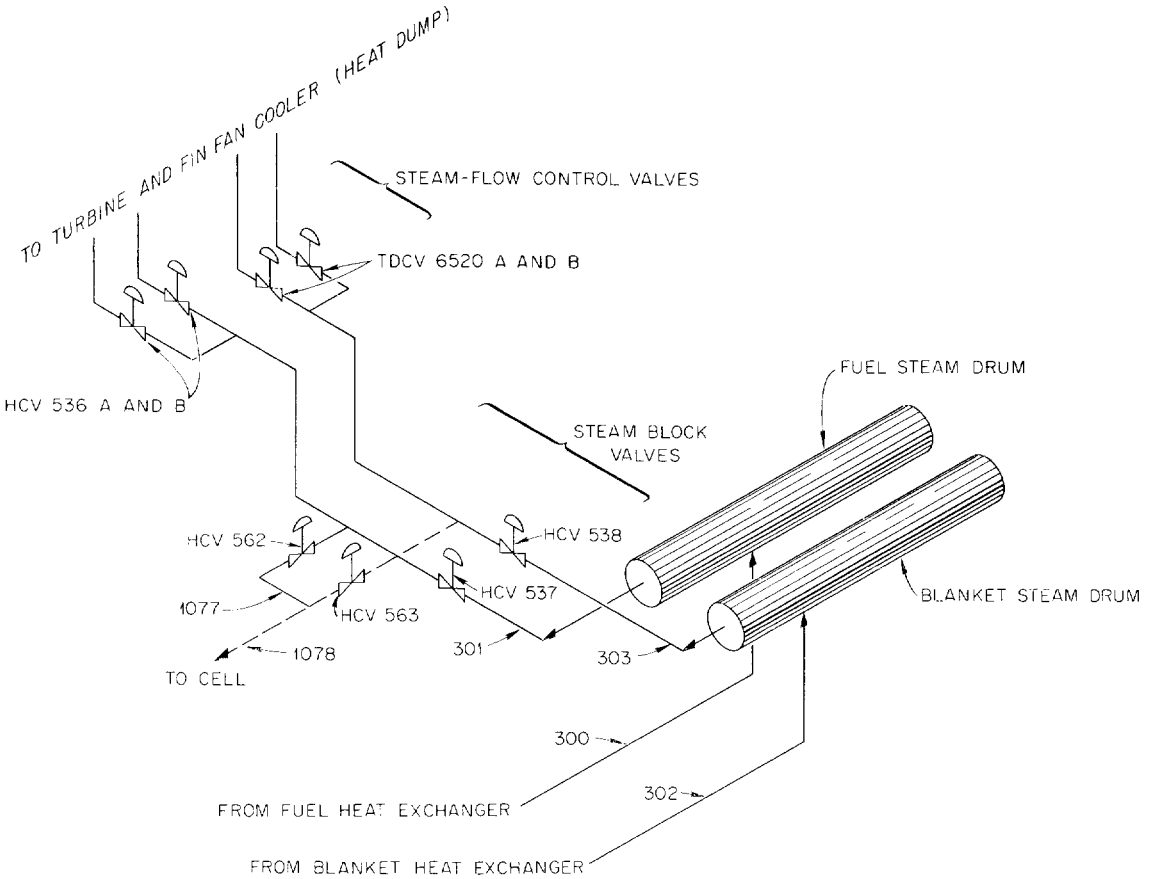

Fig. 4.2. Schematic of Installation of Steam-System Bleed Lines.

5. HRT CONTROLS AND INSTRUMENTATION

R. L. Moore

A. M. Billings J. R. Brown
P. G. Herndon

5.1 COMPONENT DEVELOPMENT

5.1.1 Fuel-Feed Flowmeter

Shop tests of the Laub Electrocaloric (heat balance) flowmeter revealed that the fluctuations in indicated flow rate, observed during operation of this instrument in the HRT mockup,[1] were inherent characteristics of the instrument and were not due to flow pulsation. These fluctuations were determined to be oscillations within the feedback loop resulting from a large distance-velocity lag which is present at low flow rates. These oscillations could be eliminated by increasing the damping of the instrument; however, the instrument would have a response time of 3 to 5 min for a range of 0.1 to 0.5 gpm. Faster response at low flows could be obtained by redesign of the flow sensing element; however, this would involve a reduction in the inside diameter of the pipe and a resultant increase in pressure drop across the element.

Investigation of the Laub Electrocaloric flowmeter has been discontinued because considerable design, development, and testing would be required before it could be considered acceptable for use in the measurement of the HRT fuel-feed flow, and because magnetic-type flowmeters appear to offer greater promise of successful development.

As reported in Sec. 9.1.2, the feasibility of constructing an aluminum-oxide-lined flowmeter for use in ThO_2 slurry at 300°C is being investigated. This program will be extended to include 100°C, 500-psi, UO_2SO_4 applications, such as the HRT fuel-feed flow measurement.

5.1.2 Remote Viewing Equipment

Radiation tests of the Dage 2-in.-dia television camera[2] were repeated[3] by using a Wollensak 1-in. f/2.5 nonbrowning lens. The camera was exposed to 3.9×10^5 r/hr of gamma radiation produced by Co^{60} slugs in the canal at the ORNL Graphite Reactor. The only effect observed was a gradual loss of sensitivity which was compensated by adjustment of the target control. The duration of the test was 248.5 hr, and the total integrated dosage was 9.6×10^7 r. At the end of the test the target control had been advanced to its maximum position, and there was slight loss in resolution of the picture.

Inspection of the camera, after removal and decontamination, showed that the loss of sensitivity was due primarily to browning of the Vidicon tube and the lamp bulbs. Comparison tests of the lens indicated that the light transmission of the lens had been reduced by only 6%. Further tests showed that 14% of the loss of sensitivity was due to browning of the lamp bulbs which supplied illumination for the test pattern. The remaining 80% loss in sensitivity was apparently due to loss of Vidicon sensitivity; replacement of the Vidicon restored the original sensitivity of the equipment. The loss of Vidicon sensitivity is believed to have been caused by browning of the glass on the Vidicon face plate, and the tube has been shipped to the Dage Television factory for study. Two additional Vidicon tubes have been exposed to 10^8 r of gamma radiation. These tubes, which were pretested, will be returned to Dage Television for testing.

5.2 MAINTENANCE AND MODIFICATION

5.2.1 Radiation Monitors

Two Eberline model RM-2 radiation monitors were installed in the 7500 Area to give better coverage of the radiation monitoring for personnel hazards. One unit is located near the waste evaporator, and the other between the chemistry laboratory and the reactor steam condenser. There are audible and visual alarms in each area.

5.2.2 Steam-System Revisions

Field revisions were made to the HRT control system to permit operation of the turbine with reactor steam. This portion of the system had been inoperative since the start of one-region operation. A new pressure controller was installed, and minor revisions to the electrical control circuitry were made.

REFERENCES

1. R. L. Moore *et al.*, HRP Quar. Prog. Rep. Oct. 31, 1959, ORNL-2879, p 39.

2. D. S. Toomb *et al.*, HRP Quar. Prog. Rep. July 31, 1958, ORNL-2561, p 50.

3. D. S. Toomb et al., HRP Quar. Prog. Rep. Apr. 30, 1959, ORNL-2743, p 47.

Part II

REACTOR ANALYSIS AND ENGINEERING DEVELOPMENT

6. REACTOR ANALYSIS

P. R. Kasten

M. L. Tobias T. B. Fowler

6.1 TWO-DIMENSIONAL REACTOR CALCULATIONS

An IBM-704 code (Equipoise) for the solution of two-group, two-dimensional, neutron-diffusion equations in cylindrical geometry was constructed using FORTRAN. In its present form, the code can treat problems involving a maximum of 625 mesh points (including boundary points). Material placement may be completely arbitrary. The iterative procedure used is simpler than others currently in use. A combination of the "extrapolated Liebmann" method[1] and the "Aitken-δ^2" process[2] is used to speed convergence. Machine running times and the required number of iterations have been equal to or often less than those required by similar programs. A typical 200-point case converged to the critical eigenvalue (pointwise convergence) in 4.5 min and required 50 sweeps through the mesh. Machine times are roughly proportional to the number of mesh points used. This code facilitates the writing of programs which utilize two-dimensional calculations as subroutines.

REFERENCES

1. S. P. Frankel, Mathematical Tables and Other Aids to Computation, vol. IV, p 65-75, National Research Council, Washington, D. C., 1950.

2. A. S. Householder, Principles of Numerical Analysis, p 126-28, McGraw-Hill, New York, 1953.

7. DEVELOPMENT OF FUEL- AND SLURRY-SYSTEM COMPONENTS

I. Spiewak F. N. Peebles

C. H. Gabbard C. G. Lawson H. R. Payne
B. A. Hannaford J. C. Moyers M. Richardson
E. C. Hise R. P. Wichner

7.1 CENTRIFUGAL PUMPS

7.1.1 20-cfm Allis-Chalmers Blower

A test to evaluate the 20-cfm canned-motor blower for pumping a steam-gas mixture at 1500 psi was terminated by an electrical failure of the stator,[1] after 10,744 hr of blower operation.

The blower was disassembled to investigate the failure. One of the stator slots had apparently shorted to ground, burning through the motor cooling coil and initiating a water leak into the stator. The cause of the electrical short is undetermined. Although the blower is repairable, the repair will not be undertaken at this time.

7.1.2 Stator Irradiation Test

The insulation-test stator, irradiated in a Co^{60} source to determine the life expectancy of a typical canned motor, failed after approximately 5.4×10^9 rads. Although the measured resistance to ground is 150,000 ohms, the location and nature of the failure is uncertain. Further tests are planned to determine if the failure is actually within the stator and if the failure was caused by leakage of moisture into the stator.

It is concluded from the test that pump motors in aqueous homogeneous reactor service have the capability of service life well in excess of ten years, assuming proper functioning of the shaft seal.

7.2 FEED PUMPS

7.2.1 Oxygen Compressor

Testing of a three-stage diaphragm compressor, designed to recycle radioactive oxygen, was continued. The unit was shut down after a total of 756 hr of operation, due to a third-stage diaphragm failure. The failure was caused by fragments of the drive-line filter, which had ruptured. The filter and diaphragm were replaced, and operation was resumed. The compressor was again shut

down after 192 hr, following another third-stage diaphragm failure. Failure again occurred at a small dent. A detailed study of possible corrective measures will be made prior to the reassembly of the unit.

7.2.2 Increased-Capacity Solution Pumps

Endurance testing of feed-pump heads (10-3/4-in. double diaphragm and 12-in. single diaphragm) was interrupted due to thorium oxide contamination of the test loop as a result of a slurry spill from some nearby equipment. The loop was cleaned and operation resumed. The two heads have now operated for totals of 12,611 and 7,991 hr, respectively.

7.2.3 Slurry Feed Pumps

Successful injection of thoria slurries into a 1500-psi system over a period of 6200 hr was reported previously.[2] Following examination of the duplex diaphragm pump, the remote-leg head was reassembled with a new diaphragm and the single-contour head with its original diaphragm. The feed pumps have since operated for 1700 hr, bringing the total to 7900 hr.

A report of slurry feed-pump development was prepared.[3]

7.3 SLURRY LOW-PRESSURE SYSTEM

Pumping of small flows of slurry has been difficult because of the tendency to solids to drop out in low-velocity lines; therefore, simple low-pressure system was set up to test various methods of coupling the feed tank and the pump.[4]

The slurry low-pressure system was operated first with a simple inclined 4-ft-long pump suction line. It was determined that 800°C-fired thoria slurry of at least a specific gravity of 2.0 and at a temperature of 110°C could be pumped readily from the flat-bottom storage tank. It appeared that heating alone was not providing adequate slurry suspension in the tank, so a tangential steam jet was added near the bottom of the tank.

The suction line was then changed to what is considered the minimum convenient suction line for the 300-SM system (see Sec. 8.3). This consists of about 2 ft of pipe inclined upward from the bottom center of the tank at a 45° angle out through the wall, a 5-ft cooler section, 1 ft of flexible pipe, a purge connection, a valve, and the suction check-valve yoke, totaling approximately 10 ft of 1/2-in. pipe. The suction check valves are placed approximately 4 ft above the bottom of the tank. Operation of this unit indicated that a feed pump so coupled to a supply tank can empty the tank of a slurry of specific gravity of at least 2.0 at temperatures up to 110°C.

Positive suction head was required for the pump to function, and was provided in this system by heating the slurry. Satisfactory operation of the system required purging the suction line with condensate before and after each feeding operation.

The flat-bottom tank, which was used because it was available, is not recommended because of the obvious difficulty of draining solids completely. However, the suction line which runs upward from the bottom of the tank and out through the wall was demonstrated in both flat- and conical-bottom tanks to be little subject to plugging and easily cleared when plugged.

7.4 SLURRY VALVES

7.4.1 Check Valves

A set of American Lava Alsimag 614 aluminum oxide check-valve trim has been on test in the slurry feed-pump test loop for 1700 hr. Pump performance gives no indication of valve deterioration.

7.4.2 Letdown Chokes

The 110-ft-long, 0.125-in.-ID restrictor tube has been in service in the slurry feed-pump loop for 7000 hr. Periodic weighings of one section have shown no weight loss.

7.4.3 Shutoff Valves

A 1/2-in., normally closed, high-pressure shutoff valve utilizing Al_2O_3 trim was constructed and was installed between the high- and low-pressure systems of the slurry feed-pump test loop. It is tested by opening against an average system pressure of 1500 psi, releasing about a liter of slurry. It then closes against little pressure differential but with full pump output flowing through it.

The trim is in the form of a 1-in. ball and seat of the type used in feed-pump check valves. The free ball is seated by system pressure and unseated by the bellows-sealed operator stem traveling through the seat opening. The valve has been on test for 1700 hr and has been operated 101 times. A conventional valve with type 17-4 PH stainless steel trim failed after 72 hr and 20 operations in the identical service.

7.5 HEAT EXCHANGER TEST FACILITY

Fabrication of the test heat exchangers was continued at Griscom-Russell Company.

7.6 CORE AND BLANKET VESSEL DEVELOPMENT

7.6.1 Cylindrical Core with Swirling Flow

A method which shows promise for maintaining a core-tank wall at a temperature near the core-inlet temperature involves the stabilizing influence of swirling motion within a cylindrical vessel to keep the cooler fluid flowing near the wall. The fluid is introduced through swirl-generator vanes at the periphery in the top of the vessel, flows downward along the wall, turns at the bottom of the vessel, and is removed through a central outlet at the top. Dye-injection tests conducted on a 5-in.-dia cylindrical vessel[5] employing this principle showed that a hemispherical bottom will induce a boundary flow that hugs the entire vessel wall. The tests also showed that there is a radially inward flow from the boundary-flow stream to the interior of the vessel.

A 2-ft-dia, 6-ft-long model of a cylindrical core vessel is being constructed which will be used to obtain hydrodynamic data required to calculate the temperature distribution within the core. These data include the three-dimensional velocity distribution. A sketch of the 2- by 6-ft core model is

shown in Fig. 7.1. The inlet flow, which is swirled 45° by 40 vanes, proceeds down the core wall, makes a 180° turn, and is removed at the top polar outlet pipe. A portion of the fluid (up to 10% of the total flow) may be withdrawn from the bottom bypass if it is required to vent the forced vortex generated along the vessel axis. There are 28 probe stations at which the velocity and flow direction will be measured. Visual observations will be made with tufts of string suspended in the vessel.

If the flow behavior is similar to that observed in the 5-in. model, it may be possible to operate a cylindrical core with swirling flow at power densities greater than 100 kw/liter without cooling the core wall internally.

7.6.2 Cylindrical Core with Straight-Through Flow

Calculations were made to estimate the temperature distribution that would exist in a cylindrical core 4 ft in diameter by 12 ft long operating at 320 Mw (thermal) with a 40°C (104°F) mean temperature rise from inlet to outlet. The flow is straight through, and the velocity and eddy diffusivity distributions used were those that would exist in a 4-ft-dia pipe far downstream from the entrance. The power distribution was the same as would exist with the core containing approximately 2 g of U^{233} as UO_2SO_4 per liter of D_2O and surrounded by a 2-ft-thick ThO_2-D_2O blanket having a concentration of 1000 g of Th per liter and 3 g of U^{233} per kg of Th.

Figure 7.2 shows the axial temperature rise across the core as calculated for two cases: case I includes radial diffusion and axial convection; case II includes only axial convection. The wall boundary condition for both these cases is zero heat flow into the fluid at the wall. The comparison of these cases shows that the effect of diffusion is to increase the temperature rise of the ambient fluid near the core wall at the outlet about 15% above the temperature rise calculated for the case with no diffusion.

Figure 7.3 is a plot showing the heat-removal rates in Btu/ft^2·hr required to establish a wall temperature varying from 250°C (482°F) at the inlet to 260°C (500°F) at the outlet. The heat is conducted across a 1/4-in.-thick wall of Zircaloy and absorbed by water flowing in a coolant channel between the core and blanket. Curve I represents the heat flux due to gamma heating of the core wall, curve II represents the heat flux removed from the core fluid, and curve III represents the total heat flux. Figure 7.4 shows the radial temperature drop across the Zircaloy wall vs the distance from the inlet along the core wall; the temperature drop plotted is that required to maintain the heat flux distribution shown in Fig. 7.3. The thermal stress resulting from the maximum radial temperature drop is about 5000 psi.

These calculations suggest that the straight-through cylindrical-core concept is feasible for a core operating at 100 kw/liter (total power/core volume) if core-wall cooling is provided. The high cooling rates required to maintain the core wall at less than 260°C (500°F) can be reduced by increasing the axial velocity of the fluids near the wall. Additional calculations will be made to investigate this possibility.

7.6.3 Slurry Blanket Vessel

Preliminary tests of models were carried out to establish the feasibility of a blanket-vessel concept for a circulating slurry blanket of a two-region 380-Mw (thermal) breeder reactor.[6] The blanket is to be a cylindrical annulus

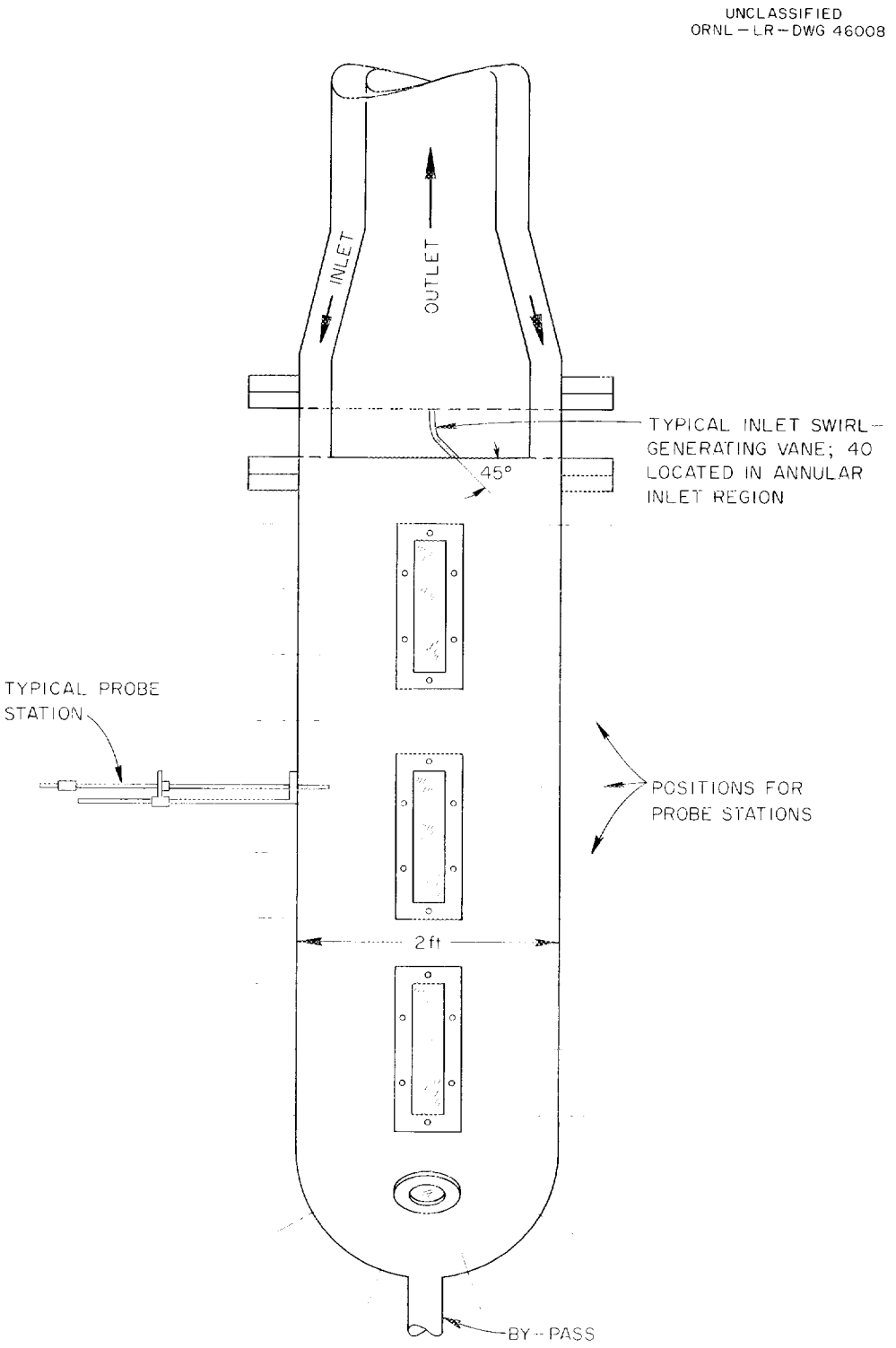

Fig. 7.1. Cylindrical Core Model for Swirling Re-entrant Flow.

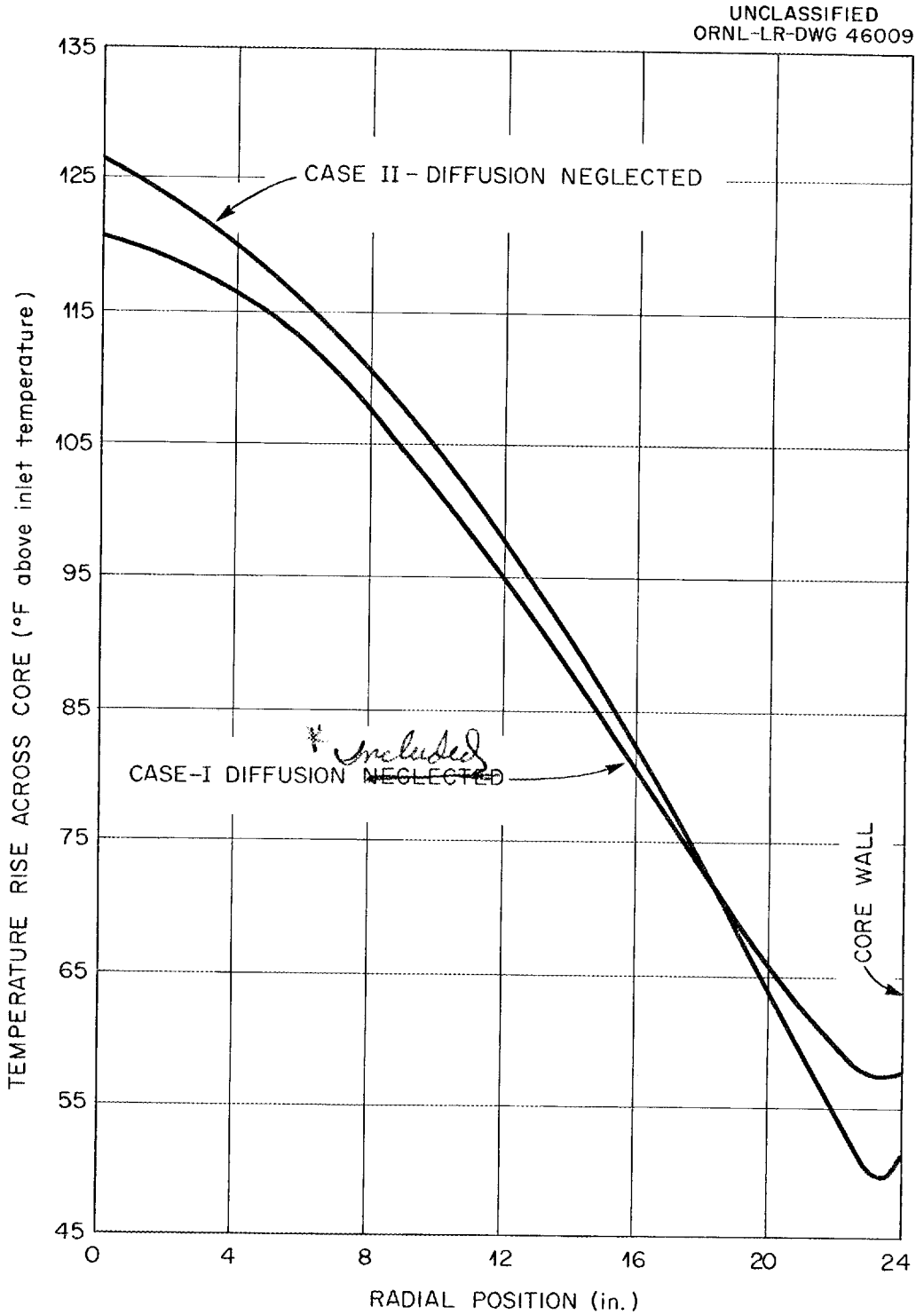

Fig. 7.2. Temperature Distribution at Core Outlet, 320-Mw (Thermal) Straight-Through Core.

* See note

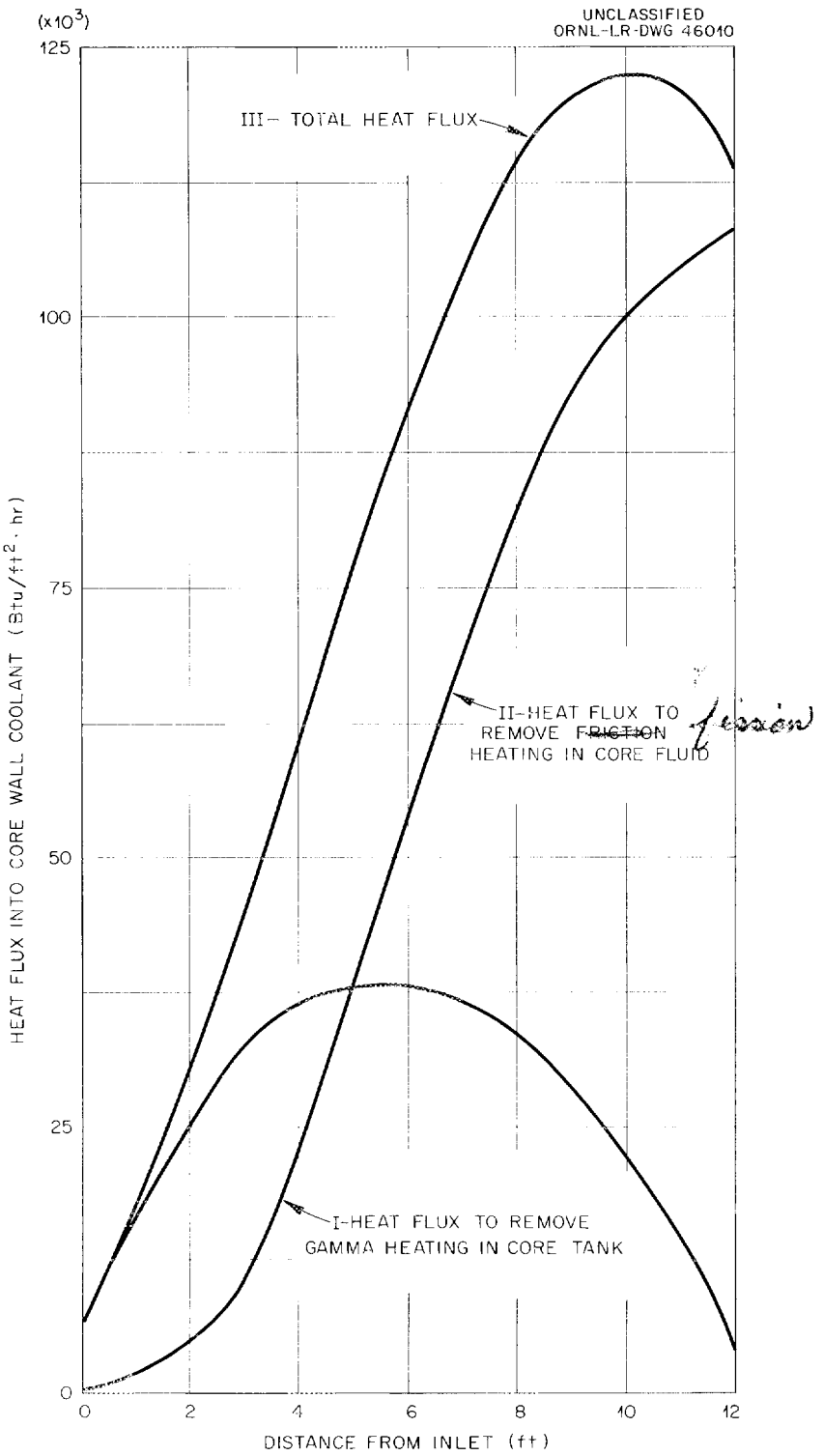

Fig. 7.3. Cooling Requirements to Maintain Interior Core Wall Between 250 and 260°C, 320-Mw (Thermal) Straight-Through Core.

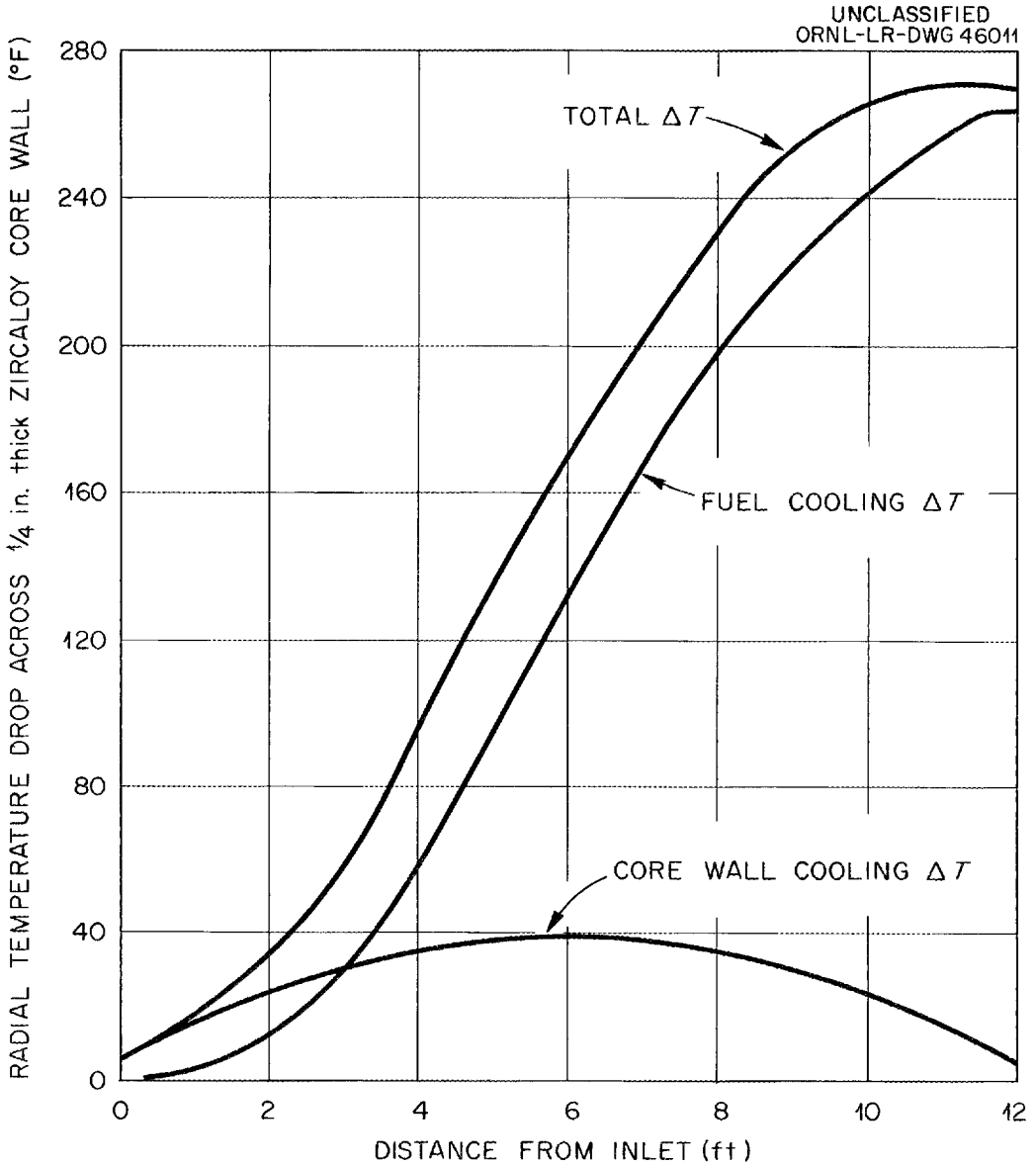

Fig. 7.4. Required Zircaloy Temperature Drop to Maintain Interior Core Wall Between 250 and 260°C, 320-Mw (Thermal) Straight-Through Core.

2 ft thick by 16 ft long surrounding a cylindrical core 4 ft in diameter by 12 ft long. The inlet and outlet slurry nozzles are concentric and at the bottom of the blanket vessel. The slurry, at a concentration of 1000 g of Th per liter of slurry, flows into the vessel at a rate of 15,000 gpm. The inlet slurry flows through an annular jet pump and then through a 6-in.-thick region within the shroud which surrounds the core vessel. The Zircaloy shroud provides for ordered, high-velocity slurry flow in the vicinity of the core wall, and the jet pump amplifies the primary slurry flow by inducing flow from the outer region of the blanket. Sufficient slurry recirculation is expected to give a total internal flow rate of 2-1/2 to 3 times the primary slurry throughput of 15,000 gpm. Figure 7.5 shows schematically the blanket vessel and flow concept.

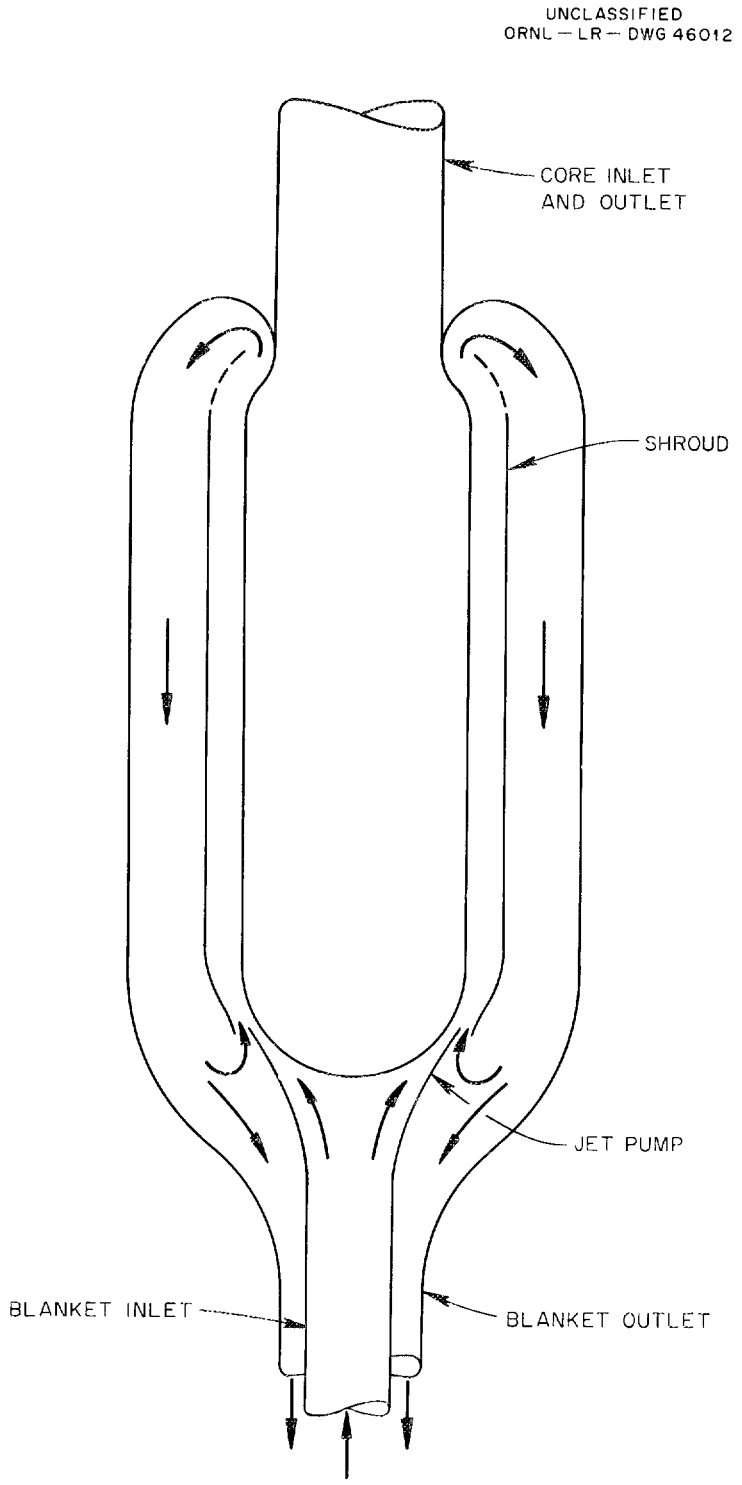

Fig. 7.5. Sketch Showing Proposed Flow Concept for Slurry Blanket.

Several two-dimensional models were built and tested, each incorporating some modification of the jet-pump and shroud configuration. The tests were qualitative and consisted mainly of locating and attempting to eliminate stagnation regions, through the use of flow visualization techniques. Based on the best design from these models, a geometrically scaled, 25-gpm, three-dimensional plastic model of the 8- by 16-ft blanket vessel was constructed. Tests will be carried out to determine the blanket flow behavior, velocity distribution, and extent of turbulence within the blanket region.

7.6.4 Reactor-Vessel Design

The preliminary mechanical design was completed for the pressure vessel and core for a 380-Mw (thermal) two-region breeder reactor having a slurry blanket and solution core. The general arrangement is shown in Fig. 7.6. The 4- by 12-ft cylindrical core is surrounded by a 2-ft-thick slurry blanket. Core-wall cooling, which may be necessary to maintain the inner core-wall surface below approximately 260°C (500°F), is provided by circulating a cooled stream of D_2O through an annular gap between the double core walls. The core is surrounded by a shroud which forms a 6-in.-thick annular passage for the upflowing slurry. The incoming slurry, by acting as the driving fluid through a jet-pump arrangement at the bottom of the shroud, induces a flow through the shroud which consists of two parts recirculated slurry and one part inlet slurry. This threefold amplification of inlet-slurry flow rate will aid in maintaining a uniform slurry concentration in the blanket vessel.

The core is of the annular-inlet, polar-outlet type with swirling flow similar to that described in Sec. 7.6.1. The incoming fuel is distributed evenly in the annular inlet by a double-volute distributor. The blanket, a modified polar-inlet, annular-outlet type, is provided with a single-volute discharge collector to provide an even flow distribution in the outlet, thereby reducing any tendency for channeling.

The core tank and shroud are replaceable as a unit. A transition joint which can be remotely disassembled and reassembled is provided at the top of the core. A slip joint is provided between the slurry inlet pipe and the jet-pump nozzle to permit withdrawal of the core tank assembly from the lower portion of the pressure vessel and to allow differential thermal expansion during operation. Clamp-ring joints are provided in the coolant inlet line and the core drain line.

7.6.5 Pressure-Vessel Thermal Stress

Calculations were made to determine the thermal stress due to nuclear heating in the pressure-vessel wall. It was found that a thermal shield is not required to keep the stress below the allowable limit. Table 7.1 summarizes the results for pressure vessels having wall thicknesses of 5.5 to 10 in.

The table indicates that a 6.5-in. or greater wall thickness is acceptable. Thermal stresses in actual practice can be reduced substantially below those calculated here by permitting some heat loss from the vessel.

7.6.6 Core Vessel and Transition Joint

The two 1/4-in.-thick walls of the core vessel are separated by longitudinal or spiral ribs which form 1/8-in.-wide coolant passages. These ribs, which are integral with the inner wall and bonded to the outer wall, strengthen the vessel, maintain the concentricity, and direct the coolant flow.

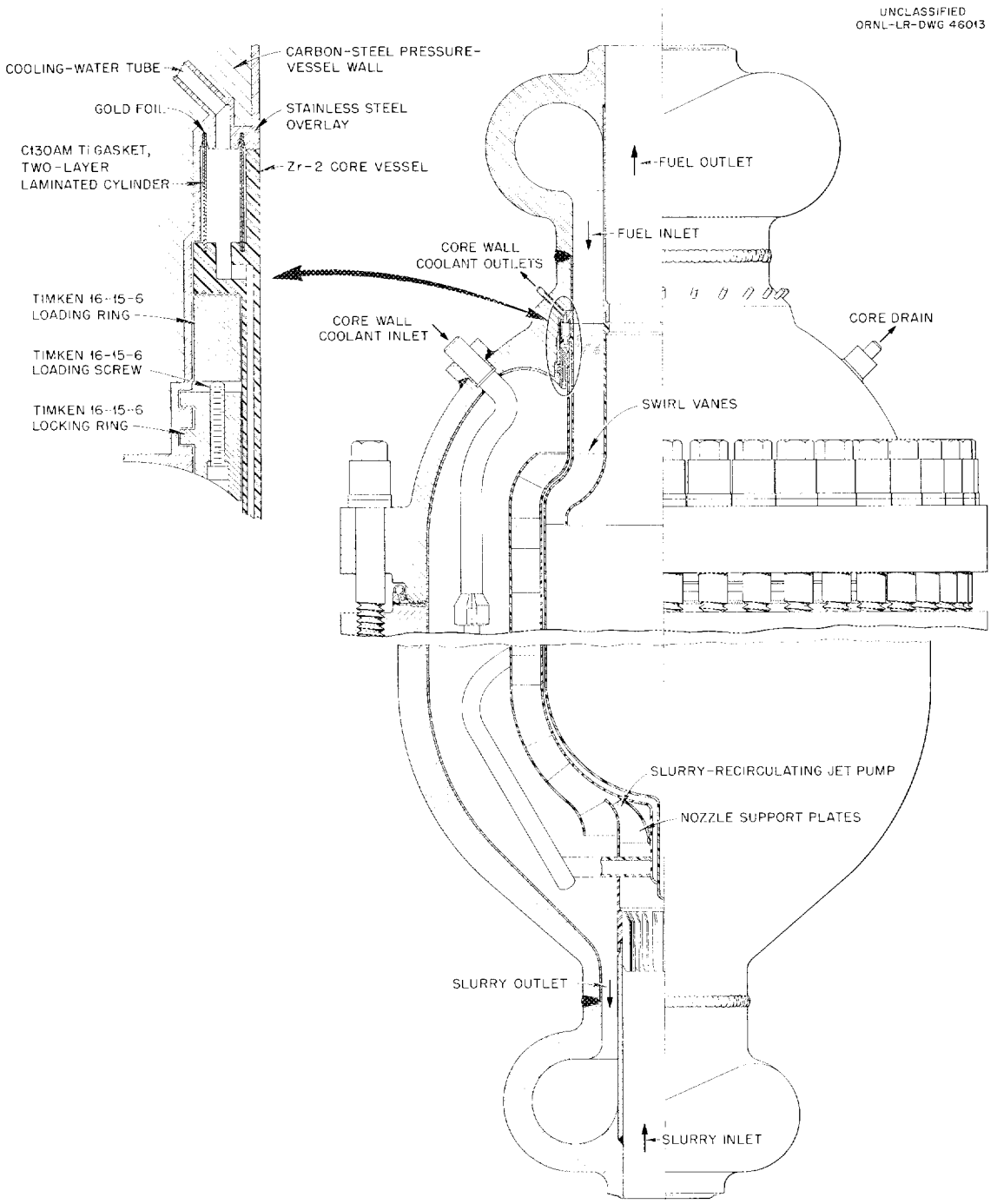

Fig. 7.6. Pressure Vessel and Core for 380-Mw (Thermal) Two-Region Breeder Reactor.

Table 7.1 Summary of Pressure-Vessel Stresses

Vessel thickness, in.	5.5	6.5	7.5	8.5	10
Pressure stress, psi[a]	19,640	16,810	14,730	13,160	11,370
Allowable thermal stress, psi[b]	10,360	13,190	15,270	16,840	18,630
Calculated thermal stress with vessel insulated, psi	11,120	12,470	13,630	14,531	16,714
Outside surface cooling required to reduce stress to allowable limit, $Btu/ft^2 \cdot hr$	300	0	0	0	0

[a]In accordance with Par. UG-27, Sec. VIII, ASME Boiler and Pressure Vessel Code, with a design pressure of 2000 psi.

[b]Allowing pressure stress plus thermal stress to equal 1.5 times the allowable design stress as permitted by ASME Boiler and Pressure Vessel Code Interpretation Case 1273N, par. (2)(allowable design stress of 20,000 psi, as for SA 302, Grade B).

The ribs, sized and spaced so that the stresses in them and in the shells near them are relatively small, give the vessel approximately the same strength against collapsing from an external pressure as that of a 5/8-in.-thick solid shell. The zirconium-alloy vessel, constructed with longitudinal ribs having a cross section of 0.125 by 0.140 in. and spaced 10° apart, will withstand a collapsing pressure differential of 50 psi. The allowable pressure differential for a 5/8-in.-thick solid-wall vessel at 500°F, calculated using ASME Boiler and Pressure Vessel Code-type charts and safety factors based on Zircaloy-2 properties,[7] is 33 psi. Spiraling the ribs will substantially increase the strength of the double-wall vessel.

The transition joint between the core vessel and the pressure-vessel head utilizes two concentric, laminated, cylindrical gaskets of high-strength titanium alloy. The core-wall coolant leaving the core vessel passes through the annulus between the cylindrical gaskets to the coolant outlet manifold. A pressure ring and loading screws provide the gasket sealing load. The loading screws are held by a ring having interrupted lugs around its circumference which interlock with lugs in the pressure-vessel head. Gold foil is used between the sealing surfaces of the joint.

7.6.7 Core-Wall Cooling

Axial temperature distributions were calculated for the inner core-wall surface, the fuel in the 4-in.-thick annulus adjacent to the wall and through which the incoming fuel is assumed to flow, and the internal coolant. The results are shown in Fig. 7.7. A coolant flow of 300 gpm, with an inlet temperature of 183°C (361°F) and with entry at the bottom of the core-tank wall, was found to maintain the fuel-side wall temperature equal to or less than 261°C (502°F) and to give a coolant outlet temperature equal to the fuel inlet temperature of 250°C (482°F). It is necessary to limit the temperature difference between the fuel inlet and the coolant outlet in order to prevent high thermal stresses in the transition joint. The calculations considered the effects of heat transfer across the core wall, the recirculation of hot fuel

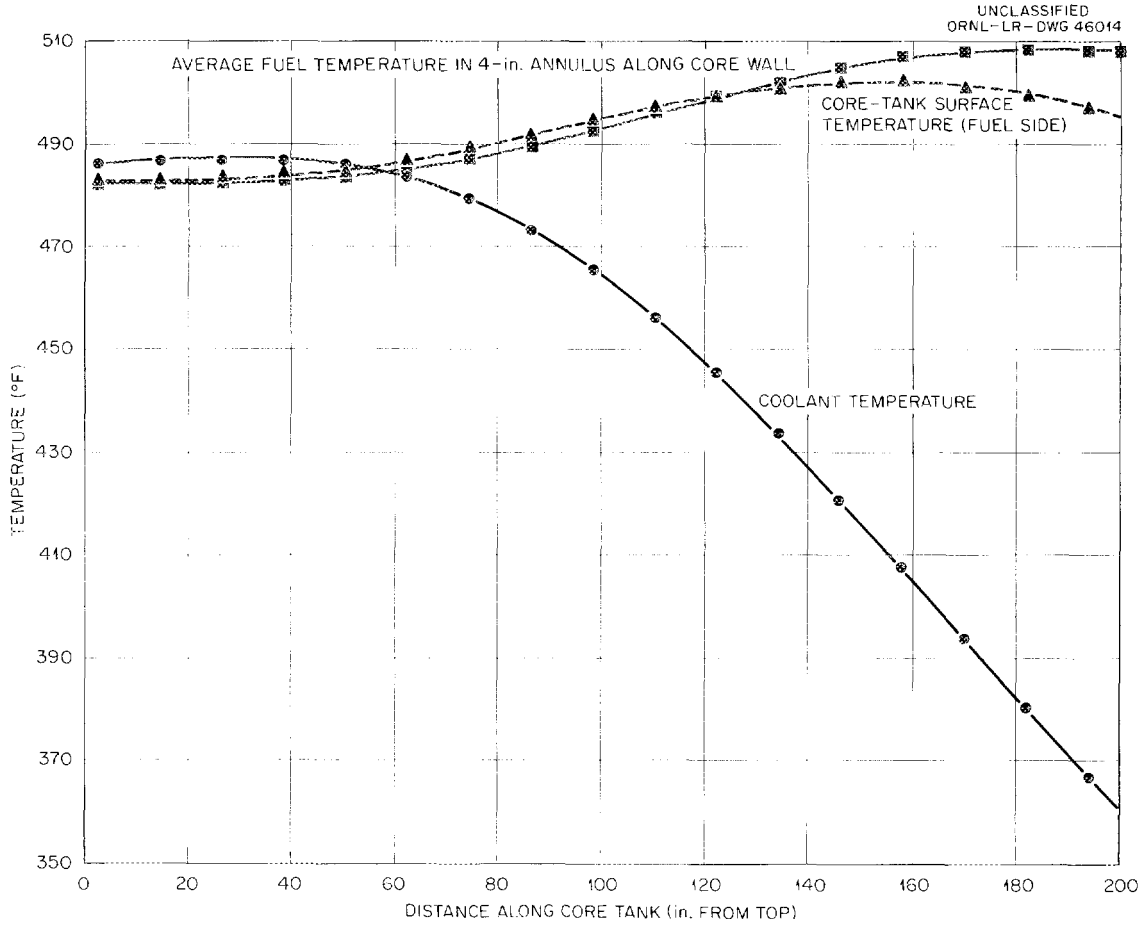

Fig. 7.7. Calculated Temperatures of Fuel, Interior Core Wall, and Internal Coolant for 380-Mw (Thermal) Reactor; Core with Swirling Re-entrant Flow.

into the annular region from the center of the core, and the heat generation in the fuel, core walls, and coolant.

REFERENCES

1. I. Spiewak et al., HRP Prog. Rep. Oct. 31, 1959, ORNL-2879, p 51.

2. Ibid., p 53-55.

3. E. C. Hise, Slurry Feed Pump Development, ORNL CF-60-1-90, Jan. 27, 1960 (in press).

4. I. Spiewak et al., HRP Prog. Rep. Oct. 31, 1959, ORNL-2879, p 55.

5. Ibid., p 57-61.

6. R. B. Briggs, Thermal Breeder Reactor Program - Aqueous Homogeneous Reactors, ORNL CF-59-7-129.

7. R. D. Cheverton, Allowable External Pressures for Zircaloy-2 Cylindrical and Spherical Vessels, ORNL CF-57-11-56 (Nov. 12, 1957).

8. DEVELOPMENT OF REACTOR SLURRY SYSTEMS

I. Spiewak F. N. Peebles

D. M. Eissenberg L. F. Parsly
P. H. Harley A. N. Smith

8.1 CIRCULATING-SLURRY EXPERIMENTS

The 200A, 200B, and 50A slurry loops are operated to investigate the high-temperature engineering properties of thoria slurries, and to provide a basis for improving the specifications for oxide production and for slurry-handling components. Important characteristics being studied include rheology, long-term oxide stability, attack rate on components, heat transfer coefficients, and settling.

8.1.1 200A Loop Operation

Run 21A, currently in progress in the 200A loop, was designed to investigate the homogeneity of a thoria slurry flowing in a horizontal 3-in. pipe at high temperature. Secondary objectives of the run are tests of an Ohmart gamma-ray densitometer for continuous indication of slurry density, and of various sample configurations. The oxide being circulated is an 800°C-fired, long-digested material having a mean particle size of 1.7 μ.

Indications of inhomogeneity are obtained by measuring the relative transmission, at various conditions of flow, concentration, and temperature, of a collimated beam of gamma rays passed horizontally through the loop pipe.[1] By use of an elevator, the vertical position of the beam is varied and the pipe is scanned from top to bottom. The attenuated-ray intensity is indicated by a decimal scaler and recorder. This equipment is shown in Fig. 8.1. In run 21A, a 160-millicurie Co^{60} source is used as a gamma supply, and the elevator was calibrated to permit a reading of the average count rate at selected, reproducible positions.

Pipe scans are being obtained at concentrations of 300, 600, 800, and 1000 g of Th per liter at linear velocities of 2.7 to 12.5 fps and at 240, 260, and 280°C. The data will be analyzed quantitatively after the scanning equipment has been calibrated satisfactorily with water.

Operation of the Ohmart gamma-ray densitometer appears to be satisfactory. This instrument consists of a 5-curie Cs^{137} source and an Ohmart null-type detector cell coupled with a Beckman micromicroammeter and a Brown recorder. The instrument is being calibrated with reference to sample concentrations during the run.

UNCLASSIFIED
ORNL-LR-DWG 24994A

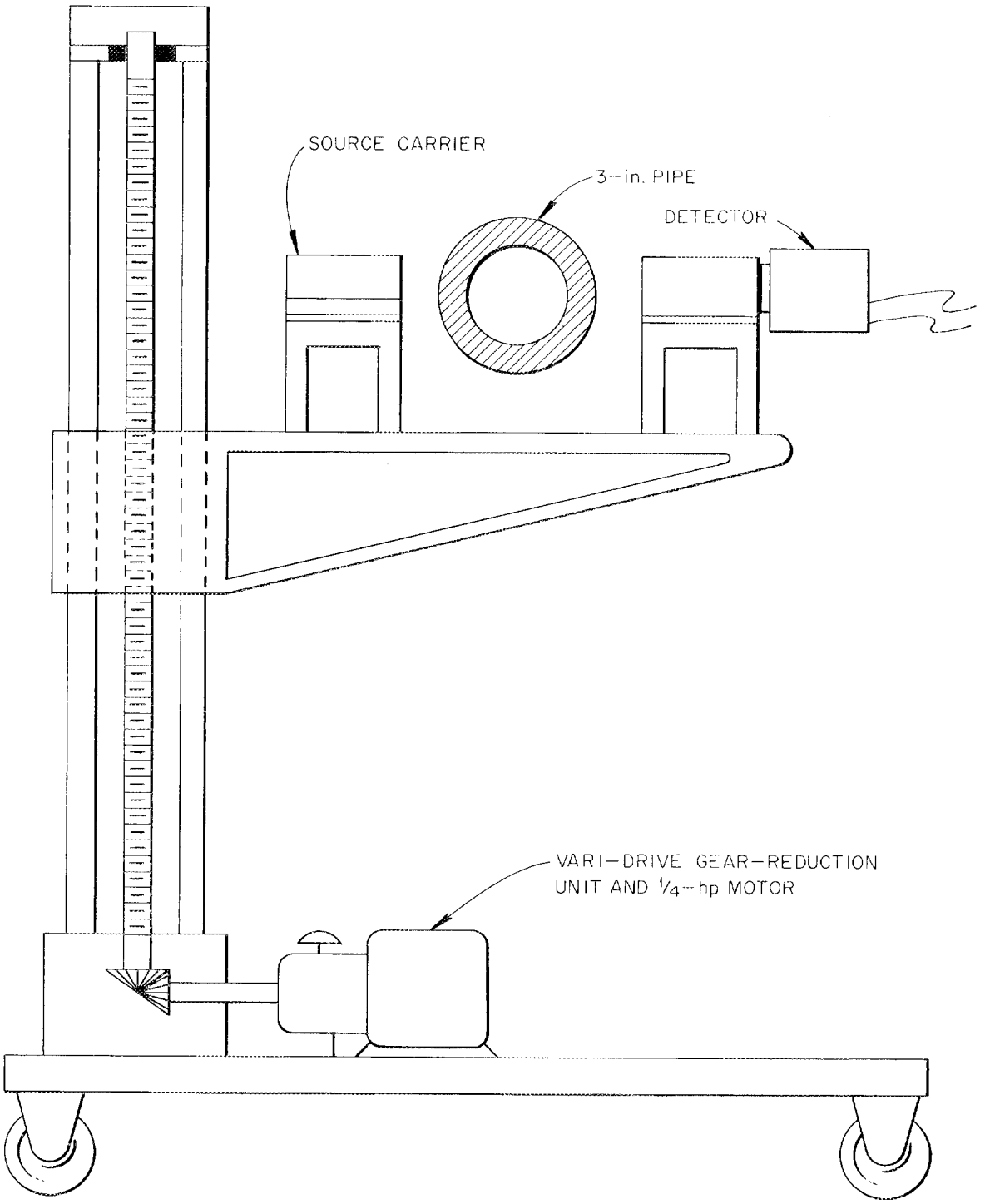

Fig. 8.1. Gamma-Ray Attenuation Equipment Used to Determine Slurry Concentration in 3-in. Pipe During Run 21A.

8.1.2 200B Loop, Run 3B

Run 3B, for the purpose of measuring the high-temperature heat transfer and rheological behavior of a mixed U-Th oxide containing 8% uranium, was started in the 200B loop during the previous quarter.[2] Following the buildup of a soft cake on the heat transfer surface, the loop was shut down, the cake was examined, and the loop was then reassembled. Attempts to restart the loop were at first unsuccessful because of the formation of a dense settled bed which plugged the lower portion of a 16-ft vertical run of 3-in. pipe (Fig. 8.2). A differential hydraulic pressure of 1600 psi was required to move the bed, but the bed merely found a more stable position. The plugged portion of the loop piping was dismantled, and the dense bed was physically removed. The density of the sludge was 3.9 g/cc. Examination revealed it to be dilatant.

The loop was reassembled, the slurry was replaced, and run 3B was continued. The heat-transfer-disk data did not indicate the presence of a cake or film during the following 500 hr. The run was terminated after a total of 1410 hr of operation, and the slurry was removed without further occurrence of plugging.

It was concluded from the run that the mixed oxide containing 8% uranium, fired to 1050°C, was not satisfactory from the standpoint of plugging. Its tendency to form a film on the heat-transfer disk was also undesirable.

8.1.3 200B Loop, Run 4B

As a result of the caking and plugging experience with the run-3B slurry, it was desired to demonstrate that similar misfortunes would not occur with a properly prepared pure thoria. Accordingly, run 4B was scheduled as a duplicate of 3B except with a 1600°C-fired thoria having an average particle size of 1.7 μ.

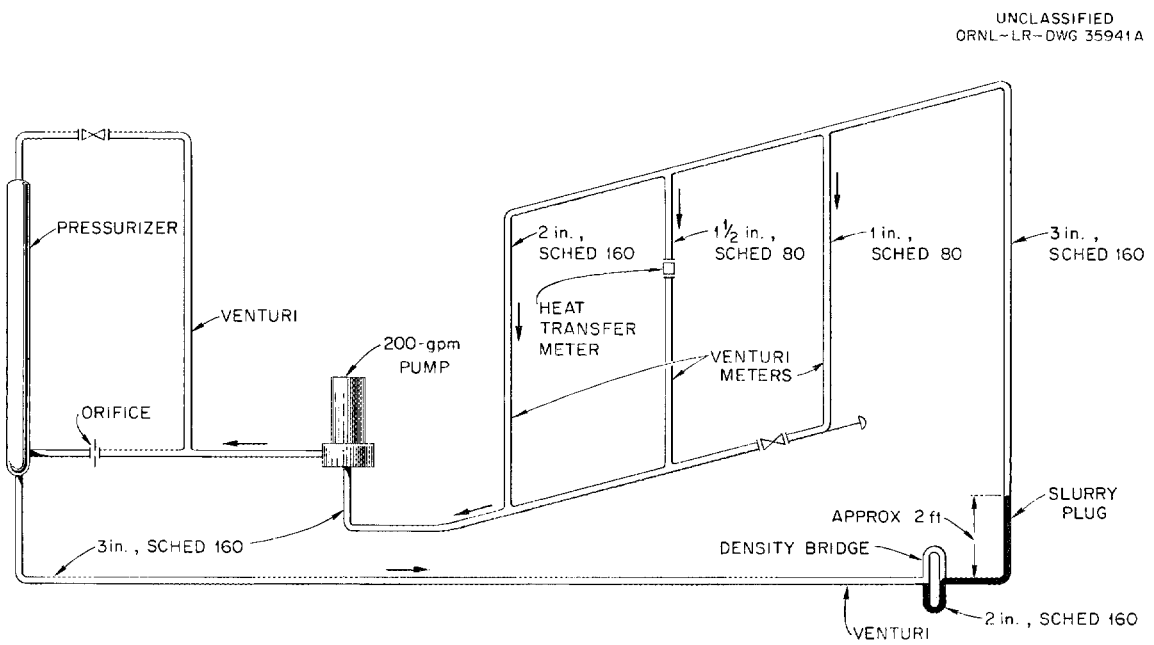

Fig. 8.2. Flowsheet of the 200B Loop Showing Location of Slurry Plug After Run 3B.

After 190 hr of slurry circulation at 275°C, the loop was permitted to cool and settle. No cake had formed on the heat transfer surface. After several days, the slurry settled-bed height in the vertical 3-in. leg indicated a settled-bed concentration of 2000 g of ThO_2 per liter. During the next two weeks, while the heat meter was being renovated and the piping was subjected to the vibration which accompanies maintenance work, the slurry in the 3-in. vertical leg flowed into the horizontal piping under its own weight. This settled bed was quickly resuspended when the pump was started.

Following this test, the loop has been operated at 275°C with a concentration of 820 g of ThO_2 per liter, and heat transfer coefficients and high-temperature rheological properties are being measured.

8.1.4 50A Loop

Construction and shakedown of the 50A loop (Fig. 8.3) were completed during the quarter. In this loop, 15-hp Byron-Jackson canned-motor pump is used to circulate fluid through the 1-1/2-in. sched-80 piping at about 12 fps. The loop enables observation of slurry behavior with a 10-liter charge.

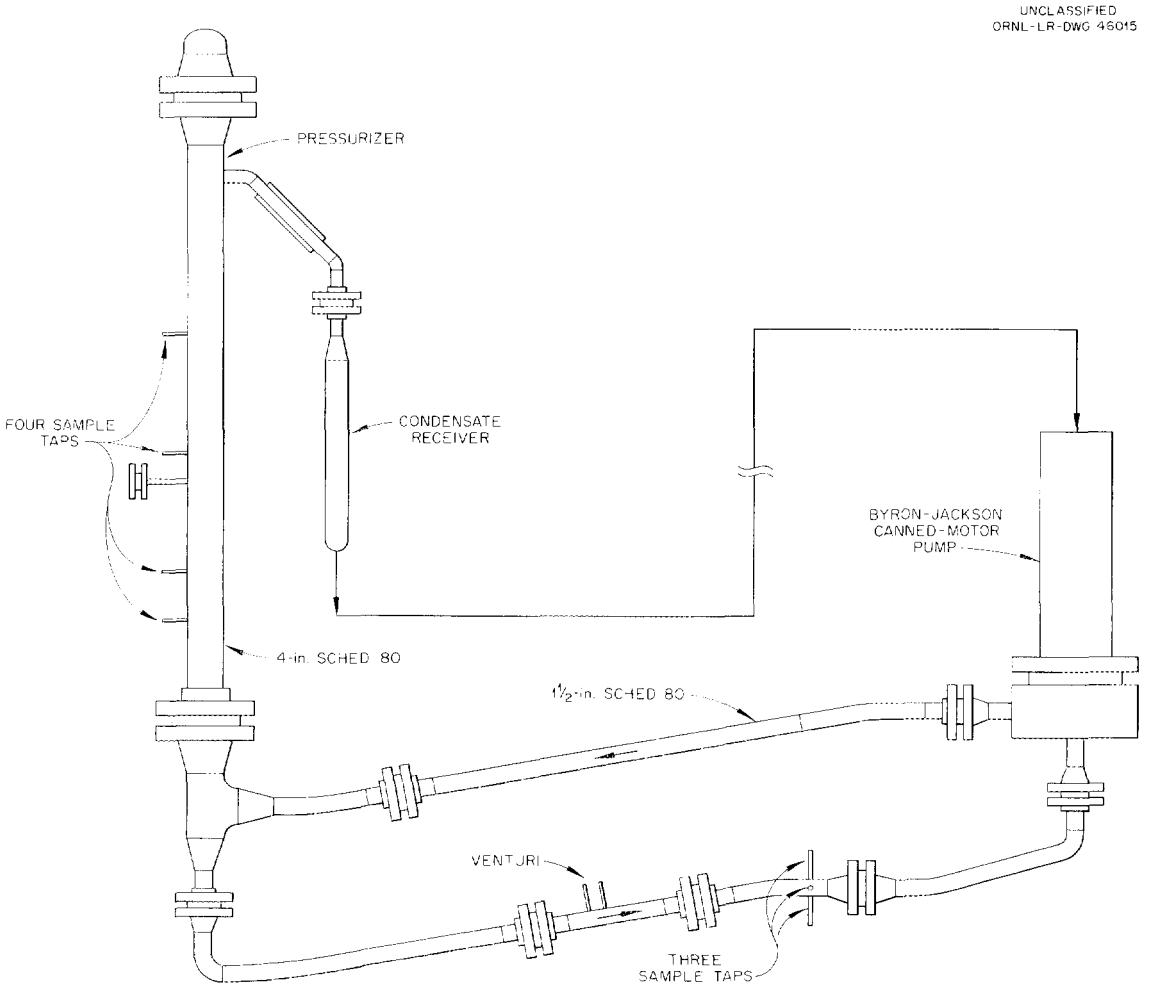

Fig. 8.3. 50A Slurry Loop.

Run 50A-1 is being made to measure the properties of this slurry during pumping under both oxidizing and reducing conditions. The loop was charged with a 1600°C-fired thoria having an average particle size of 3.6 μ, to a book concentration of 1000 g of ThO_2 per liter. During the first 300 hr of the run, mechanical loop performance was excellent, and an average loop-corrosion rate of 2.4 mpy was observed.

8.2 PROPERTIES OF SLURRY SETTLED BEDS

8.2.1 Dilatancy Tests

As a result of the plug which formed in the 200B-loop piping following operations with U-Th mixed oxide (see Sec. 8.1.2), laboratory experiments were performed to investigate the problem and to determine whether there are methods for preventing such occurrences.

Examination of the 200B sludge showed that it had characteristics typical of dilatant materials (i.e., materials which show increased viscosity as shear stress is increased). For example, it resisted the sudden shearing action of a spatula and appeared to dry adjacent to a point where pressure was applied. At the same time, the material possessed a yield value high enough to prevent flow at low shear stress. Thus the plug material could be characterized as a dilatant plastic.

In suspensions of several types of materials it has been found that the appearance of dilatancy is restricted to volume fraction solids of 0.38 to 0.45, and also, dilatancy appears most pronounced when the particles are in the size range of 1.5 to 5 μ (refs. 3,4). It was possible to reproduce the dilatant behavior of the 8% U mixed oxide in the laboratory by concentrating a suspension of the material to the appropriate high volume fraction solids. Centrifugation, chemical dispersion and settling, and partial drying on damp blotter paper all produced dilatant plastic masses of this slurry of density 3.9 g/cc.

The volume fraction solids at this density can only be estimated, since the particle density is unknown. However, a reasonable solid specific gravity of 7.5 to 8.0 would yield a volume fraction solids of 0.375 to 0.40, which is in the range designated previously.

Samples of 15 slurries, representing a wide range of types, were concentrated by three methods: centrifugation, dispersion, and partial drying. The resulting ultimate concentrations are shown in Table 8.1. The compacted materials were examined and compared.

It was found that two types of classifications could be made by inserting a 1/4-in. glass rod into the compacted mass in the centrifuge cup. Certain sludges permitted easier penetration of the glass rod than others. Certain sludges, after penetration by the glass rod, resisted the removal of the glass rod more than others.

It was also found that two types of classifications could be made by examining the compacted masses on damp blotter paper: some slurry masses showed characteristic dilatancy (loss of surface water upon stressing); some slurry masses drained water faster than others.

The tabulation of slurries (Table 8.1) includes the results of the above testing, of necessity qualitative. The following conclusions appear justified:

1. Dilatancy is a very common property of dense thoria sediments.

Table 8.1 Dilatancy Tests

Slurry Designation	Comments	Ultimate Conc. (g oxide/liter)	Firing Temp. (°C)	Dilatant by Spatula Test	Speed of Drying	Resistance to Penetration of Rod	Resistance to Removal of Rod
DT-25	Unpumped	2380	800	Yes	Medium	High	Yes
DT-25	Pumped	2950	800	Yes	Slow	High	Yes
LO-7	Unpumped (micronized)	3180	800	Yes	Medium	High	Yes
LO-7	Unpumped (micronized)	4270	1600	Yes	Medium	Medium	Yes
DT-37	Unpumped	1980	800	Yes	Medium	High	Yes
LCC-1108	Unpumped	2230	650	Yes	Medium	Low	Yes
DT-2,3	Unpumped	3920	1600	Yes	Slow	High	Yes
BS-21-5L	Pumped	3550	1600	Yes	Medium	High	Yes
BS-22-11L	Pumped	4497	1600	No	Very slow	Low	Yes
BS-22-90L	Pumped	4955	1600	No	Very slow	Low	Yes
S113	Pumped	4650	1600	No	Very slow	Low	Yes
ES-6-2L	Pumped	3720	1600	Yes	Slow	Medium	Yes
Flame-fired mixed oxide	Unpumped	5260		Yes	Slow	Low	Yes
MO41,43,44 (8% U)	Pumped	3200	1050	Yes	Fast	High	No
MO-57 (8% U)	Unpumped	2950	1050	Yes	Medium	High	No

2. Lack of dilatancy is associated with retention of water, which may be due to a hydrophilic particle surface or to a broad particle-size distribution.

3. The 8% U mixed oxide, which formed the plug in the 200B loop, was the most dilatant material tested. Pumped 1600°C-fired thoria slurries showed little or no dilatancy.

8.2.2 Flow of Dilatant Plastic Plugs

The following equation was derived in order to estimate the influence of geometry on the resistance to flow of dilatant plastic plugs:

$$P = \frac{\tau_y}{c} \left(e^{4cL/D} - 1 \right),$$

where P = critical pressure differential; τ_y = yield value of the plug, L = length of plug, D = diameter of plug, and c = static coefficient of friction between the plug and the pipe wall.

Plugs of the 8% U mixed-oxide slurry removed from the 200B loop (see Sec. 8.1.2) were formed in 1/4-in. tubing at a concentration of 3000 g of ThO_2 per liter. The validity of the equation was demonstrated, and τ_y of 13 lb/ft^2 and a coefficient of friction of 0.17 were obtained.

It is inferred from these experiments that if the plug in the 200B loop had been of 6 L/D rather than 12, it would have flowed with as little as 40 psi differential, rather than the 1600 psi observed.

8.3 300-SM BLANKET-SYSTEM DEVELOPMENT

The 300-SM system is a slurry-circulating facility simulating the slurry core or blanket system of a 5-Mw reactor. Run SM-8, the initial high-pressure, high-temperature run with a mixed-oxide slurry containing 8% U/Th, was continued from the previous quarter.[4]

The program of establishing the limits of good slurry suspension in the 30-in.-dia spherical core vessel as a function of temperature, flow rate, and slurry concentration[4] was completed with a series of measurements at 225 to 300°C at a concentration level of 800 g of Th-U per liter. Suspension was good for all flow rates in the range 130 to 380 gpm up to 300°C.

A complete vessel sampling was carried out at 380 gpm and 300°C. Point concentrations ranged from 91.7 to 101.6% of the circulating concentration, and analysis of variance on the observations indicated that the differences observed were significant at better than the 99% confidence level.

After completion of the circulating-concentration studies, a dilution run was carried out in which water was pumped up from the low-pressure system and slurry was withdrawn through the letdown system. By using a water injection rate of 0.25 gpm, the concentration was reduced from 800 to less than 0.1 g of Th-U per liter in 42 hr. During the early part of the dilution run, a leak developed in a gasketed joint in the upper letdown valve, necessitating an emergency dump.

Following completion of run SM-8, the system was shut down to incorporate some major revisions and improvements. Alterations to the high-pressure system included installation of a modified pressurizer inlet (see Fig. 8.4) to reduce slurry holdup in the pressurizer and of a gamma-ray transmission scanner to enable locating the slurry-water interface, addition of a heat exchanger containing eighteen 3/4-in.-OD by 0.083-in.-wall straight tubes between the pressurizer and pressure vessel, and changes to minimize the number of potential leaks from the high-pressure system. The latter involved replacement of tube fittings with welded joints in the sample lines, removal of slurry traps from instrument lines, replacement of two packed valves with bellows-sealed valves, and modification of several control valves to use ring-joint gaskets instead of flat gaskets for seat-to-body seals. The trim of all system valves isolating the high-pressure system from the low-pressure systems was changed to materials that are more wear resistant.

The alterations to the low-pressure system included direct coupling of the slurry feed pump to the slurry tank. This will eliminate the centrifugal pump used earlier to supply suction head.

Many components were examined during disassembly of the system. The dump choke had lost 1.7 g of stainless steel and was still in good condition after four dumps. The Inconel letdown heat exchanger coil was radiographed, and indications of pits up to half-way through the tube wall were found at the inlet end; these were confirmed by visual examination. The total active service life for the letdown heat exchanger was less than 100 hr. A type 347 stainless steel replacement was installed.

UNCLASSIFIED
ORNL — LR — DWG 46016

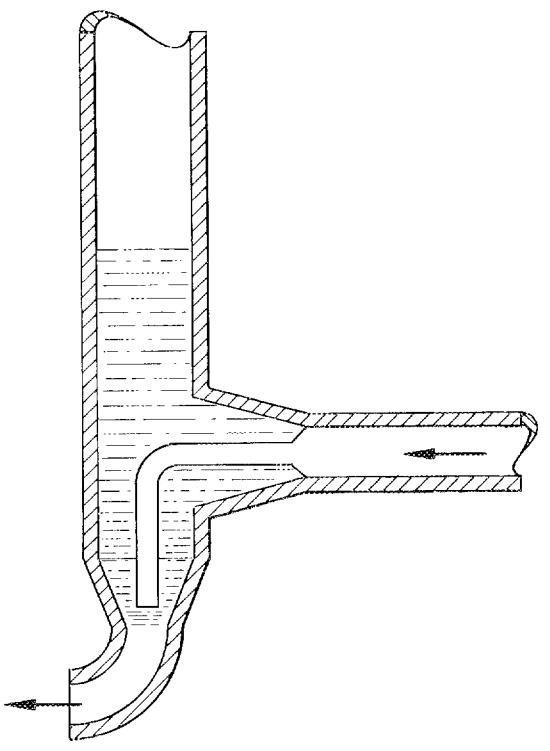

Fig. 8.4. 300-SM Loop Modified Slurry Pressurizer Inlet.

The lower letdown valve, a Hammel-Dahl valve with spline-type metering trim, leaked badly due to erosion of the poppet. The control valves in the suction lines from the dump tank and wash-water tank leaked, but appeared to have been damaged by metal chips rather than by slurry. The other block valves in the low-pressure slurry lines were leak-tight.

REFERENCES

1. M. Richardson and A. S. Kitzes, Elevation of Gamma-Ray Attenuation Techniques for Measuring the Density and Homogeneity of Thorium Oxide Slurries Circulating at 300°C, ORNL CF-57-10-61 (Oct. 10, 1957).

2. I. Spiewak et al., HRP Prog. Rep. Oct. 31, 1959, ORNL-2879, p 65.

3. H. L. Roeder, Rheology of Suspensions, p 36, H. J. Davis, Amsterdam, 1939.

4. A. B. Metzner and M. Whitlock, Trans. Soc. Rheol., II, 239-254 (1958).

5. I. Spiewak et al., HRP Prog. Rep. Oct. 31, 1959, ORNL-2879, p 68-73.

9. INSTRUMENT AND VALVE DEVELOPMENT

R. L. Moore

A. M. Billings D. G. Davis
H. D. Wills

9.1 INSTRUMENT DEVELOPMENT

9.1.1 Electric-Systems Evaluation

Testing of components of the Foxboro Electronic Consotrol instrument system is continuing. In addition to the component tests reported previously,[1] tests were performed on a Foxboro model M/62 universal controller. The controller utilizes transistor circuitry and is available with proportional, derivative, and reset actions. Input and output signals are direct currents having a range of 10 to 50 ma. Frequency-response tests of the controller indicated that the controller gain is down 3 db at 10 cps, with derivative off. Other tests indicated that line-voltage effects and long term control drifts are negligible.

Additional components of the Foxboro ECI system, which are on hand or on order and are scheduled for test, include a model T/693 EMF-to-current converter, a model 63 alarm unit, and a model T/613A differential-pressure transmitter.

Representative components of the Taylor Instrument Companies 700-series electronic system and the Minneapolis-Honeywell Instrument Company Teleset Electronik system were ordered. These components and those of the Swartwout Instrument Company Autronic systems, which are on hand, will be tested to obtain data for use in the selection of instrumentation for future reactor systems.

9.1.2 Magnetic Flowmeter

As part of a continuing effort to obtain a reactor-grade magnetic flowmeter for use in systems having UO_2SO_4 solution at 100°C or ThO_2 slurry at 300°C as the process fluid, four coupons of Al_2O_3 (Coors Porcelain Company) were tested in high-temperature oxygenated water with the following results:

Coupon No.	% Al_2O_3	Temp. (°C)	Corrosion Rate (mpy)
AV30-1	98	100	0.3
AV30-2	98	300	13.7
B890-1	93-95	100	2.2
B890-2	93-95	300	6.1

Porosity tests showed not more than a 0.01% increase in weight after being exposed to water at room temperature and at 100°C.

These tests are presently being repeated. Additional tests in UO_2SO_4 at 100°C and in flowing ThO_2 slurry at 300°C will be made following the water tests.

Foxboro Instrument Company is investigating the feasibility of lining their 1-in. magnetic flowmeter with Al_2O_3 and of providing an acceptable seal for the electrode penetration of the pipe wall.

9.1.3 Flush-Diaphragm Differential-Pressure Transmitter

A prototype differential-pressure transmitter of the type described in an earlier report[2] was received and tested. This transmitter, shown in Fig. 9.1, was constructed on a best-effort basis by the Foxboro Instrument Company.

UNCLASSIFIED
PHOTO 33840

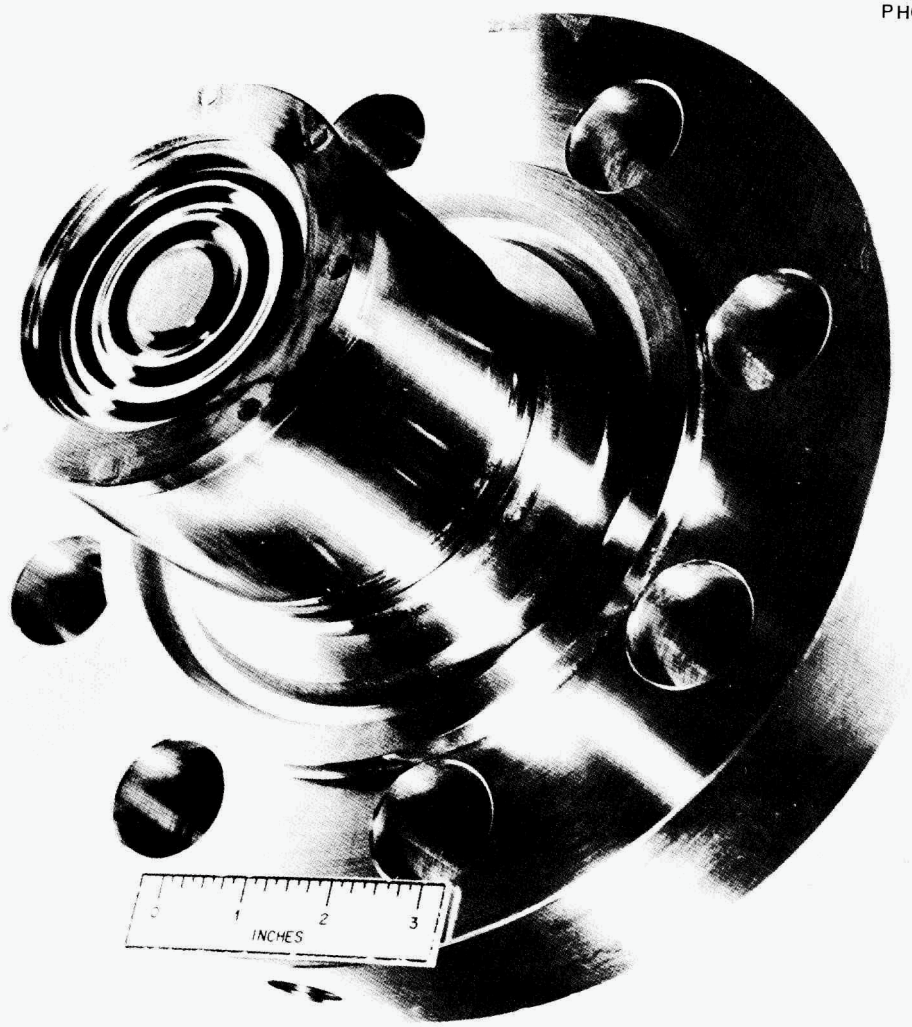

Fig. 9.1. Flush-Diaphragm Differential-Pressure Transmitter.

Test results indicated that the transmitter was linear within 1/2% of full scale and had a hysteresis of 1% of full scale when mounted in the horizontal position. Hysteresis was negligible in the vertical position. The zero shift due to pressure was 2% of full scale at 2000 psi; zero shift due to temperature was negligible at 100°C. During these tests, the range of the instrument was set at 100-0-100 in. of H_2O.

The transmitter was accidentally damaged during the elevated-temperature tests, and the results of tests above 100°C were inconclusive. The instrument is being repaired and after repairs are completed, tests will be performed to determine the effects of temperature on zero and span over the temperature range from 100 to 300°C.

9.2 VALVE DEVELOPMENT

9.2.1 Hammel-Dahl High-Pressure Slurry Control Valve

The stem-sealing bellows of the flushed-bellows Hammel-Dahl valve[3,4] in the 30-gpm loop failed, and the valve was taken apart and inspected. Loop operating schedules did not permit removal of the valve body from the process line to photograph the valve; however, visual inspection revealed considerable pitting in the seating area. The pits appeared to be uniformly sized and were spaced around the periphery of the seating area.

The tip of the valve plug, shown in Fig. 9.2, exhibited a highly polished appearance, with the seating region in good condition. Erosion of the guide region of the plug shank, although rather extensive, appeared uniform.

Since a spare stem-sealing bellows was not available for this valve, the leaky bellows assembly was re-used. Maintaining loop purge-water pressure between the packing gland and the cracked bellows assembly permits use of the valve without leakage to the outside.

UNCLASSIFIED
PHOTO 35236

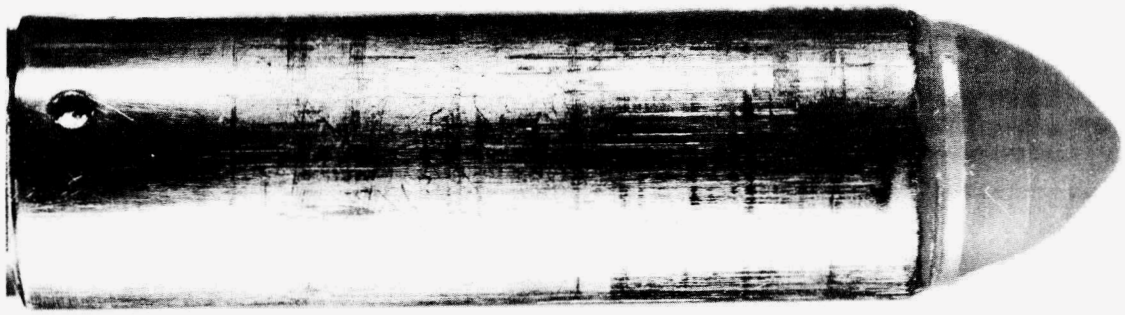

Fig. 9.2. Plug from Hammel-Dahl Valve No. 220 After Test.

The stem-sealing bellows involved is made by Flexonics, Incorporated, and rated at 450 psig at 500°F. The failure is believed attributable to an inability to keep the differential pressure across the bellows wall below 450 psi.

At the time of failure the valve had accumulated 4695 hr of service with a test-loop pressure of 1600 psig at a temperature of 280°C. The service time includes approximately 65 hr with water circulating in the loop.

The 4630 hr of slurry service can be broken down as follows:

Trim Service (hr)	Valve-Plug Position
4180	100% opened
200	30-40% closed
250	65% closed

During test-loop operation, slurry concentration was maintained between 400 and 500 g of ThO_2 per kg of H_2O, while flow through the valve varied from 10 to 30 gpm, with the pressure drop across the valve varying from 25 to 40 psi.

The Zircaloy-2 plug and seat used in this valve have performed better than any materials combination yet tried in this type of application, that is, high temperature, low differential pressure across the valve.[5]

9.2.2 Inspection of Slurry-Mockup-Loop Valves

As part of the scheduled modifications to the 300-SM system, all valves isolating the high-pressure system from the low-pressure system plus several other more critical valves were removed from the loop for leak testing and modification as required.[6]

Of six isolation valves, two were found leaking. HCV-1281, the lower letdown valve, with a Stellite No. 6 plug and a Stellite No. 12 seat, was found to have a high leak rate and severe damage to the plug seating region. The plug and seat, after removal, are shown in Fig. 9.3. Leakage to the

UNCLASSIFIED
PHOTO 35324

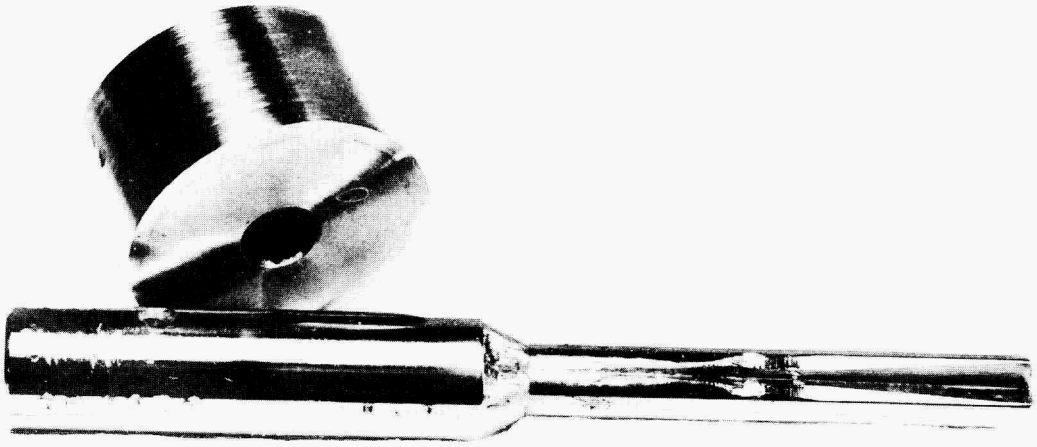

Fig. 9.3. Plug and Seat from Valve HCV-1281 After Service in Slurry Mockup Loop.

low-pressure system through HCV-1281 was prevented by HCV-1271, the upper let-down valve, in which a Zircaloy-2 plug and an Armco 17-4 PH stainless steel seat was used. Upon removal, HCV-1271, which had been installed for three months, was leaktight for 10 min with 2000-psig water applied under the seat. Figure 9.4 shows essentially no wear on either the Zircaloy-2 plug or the Armco 17-4 PH seat.

The other leaky valve, HCV-1141, was one of the three dump valves. This valve utilized Armco 17-4 PH stainless steel for both plug and seat and was found to leak 4 cc/min when 2000-psig water was applied under the valve seat for 10 min.

Three of the Annin Company split-body valves used in critical applications are being modified to accept a standard ring gasket between the body sections. These modifications are illustrated in Fig. 9.5.

UNCLASSIFIED
PHOTO 35326

Fig. 9.4. Plug and Seat from Valve HCV-1271 After Service in Slurry Mockup Loop.

UNCLASSIFIED
ORNL-LR-DWG 46017

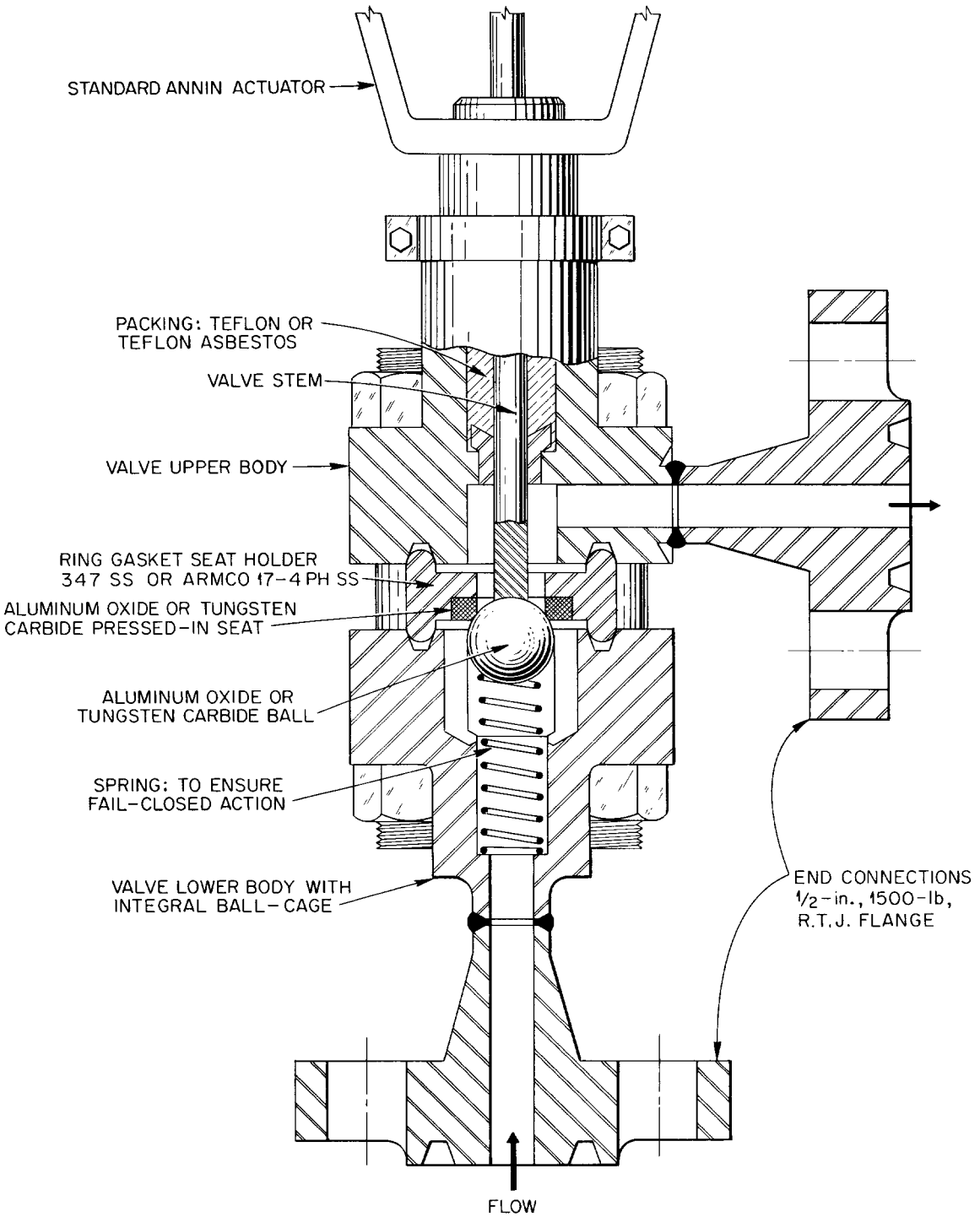

Fig. 9.5. Modified Annin Split-Body Valve.

Trim material for these valves will be as follows:

Valve No.	Function	Plug	Seat
HCV-1171	Dump valve	Conventional on-off plug fabricated of Zircaloy-2	Armco 17-4 PH, machined integrally with the ring gasket
HCV-1211	Feed-pump discharge block	Aluminum oxide ball, spring-loaded-closed	Aluminum oxide, pressed-fit with type 347 stainless steel ring gasket
HCV-1221	Feed-pump discharge by pass	Aluminum oxide ball, spring-loaded-closed	Aluminum oxide, pressed-fit with type 347 stainless steel ring gasket

REFERENCES

1. R. L. Moore et al., HRP Prog. Rep. Oct. 31, 1959, ORNL-2879, p 74-84.

2. D. S. Toomb et al., HRP Quar. Prog. Rep. Oct. 31, 1958, ORNL-2654, p 102.

3. D. S. Toomb et al., HRP Quar. Prog. Rep. July 31, 1958, ORNL-2561, p 143, Fig. 11.13.

4. D. S. Toomb et al., HRP Quar. Prog. Rep. Oct. 31, 1958, ORNL-2654, p 111.

5. D. S. Toomb et al., HRP Quar. Prog. Rep. July 31, 1958, ORNL-2561, p 138.

6. R. L. Moore, Proposed I&C Section Development, Design, and Service Engineering Program for December 1959, HRP-59-213, p 3, Dec. 8, 1959.

Part III

SOLUTION FUELS

10. REACTIONS IN AQUEOUS SOLUTIONS

M. J. Kelly

D. R. Cuneo M. D. Silverman H. H. Stone
L. O. Gilpatrick G. M. Watson

10.1 CONCENTRATION OF PEROXIDE IN URANYL SULFATE SOLUTIONS AT INCIPIENT PRECIPITATION

The effects of changes in acidity, uranium concentration, and temperature on the concentrations of uranium peroxide in simulated homogeneous reactor fuel solutions were explored by two methods. In the first, the consequences following upon an initial addition of excess H_2O_2 were determined, while in the second, uranium peroxide was added initially. The details of the experiments have already been reported and the results discussed.[1]

While the mechanisms of the reactions in this system are not completely understood, the following set of equations is presented for purposes of the discussion.[2,3]

$$UO_4(s) \underset{r_{-1}}{\overset{r_1}{\rightleftharpoons}} UO_4(d) \qquad (1)$$

$$UO_4(d) + 2H^+ \underset{r_{-2}}{\overset{r_2}{\rightleftharpoons}} UO_2^{++} + H_2O_2 \qquad (2)$$

$$H_2O_2 \xrightarrow{r_3} H_2O + 1/2\ O_2 \qquad (3)$$

$$UO_4(d) \xrightarrow{r_4} UO_3(d) + 1/2\ O_2 \qquad (4)$$

$$UO_3(d) + 2H^+ \xrightarrow{(fast)} UO_2^{++} + H_2O.$$

The notations (s) and (d) signify solid or dissolved species, and the symbols r_n and r_{-n} represent the forward and reverse rates of the indicated process. Solid uranium peroxide existing under the experimental conditions is denoted as $UO_4(s)$; no attempt is made to express the number of molecules of water of hydration involved, and the question of the formula or uranium peroxide $[UO_4(s)\cdot(H_2O)_x$ or $UO_3\cdot H_2O_2\cdot(H_2O)_{(x-1)}]$ is ignored.[4]

Equations (1) and (2) represent reversible processes, while (3) and (4) show possible modes of decomposition which are not necessarily unique; they probably occur simultaneously and to a varying degree, depending upon concentration, catalysis, and temperature. Since the decomposition reactions affect the equilibrium processes, which in turn are sources of reactants for the decomposition steps, it is not possible in this system to isolate any one of the listed reactions; the entire set must be studied simultaneously.

Simplification can be attained in the numerical treatment of the system involving solid uranium peroxide in contact with a solution of uranyl ions if the reversible processes (1) and (2) can be made to approach equilibrium through the proper choice of experimental conditions; this can be achieved if the rates r_1, r_{-1}, r_2, and r_{-2} are considerably greater than r_3 and r_4 combined. If these conditions are attained, a nearly saturated solution of uranium peroxide will prevail in the system in spite of the decomposition reactions. To a first approximation this will fix the concentration of dissolved uranium peroxide and bring about the desired simplification in the numerical treatment. The total concentration of H_2O_2 in solution can then be stated in terms of the concentration of H^+ and of UO_2^{++}, the solubility of UO_4, and an equilibrium quotient K_c, assuming that K_c remains sensibly constant during the measurements. Therefore, for equilibrium conditions, the experimental measurements provide the basis for arriving at an order of magnitude for the ratio $UO_4(d)/K_c$, where $UO_4(d)$ is the solubility of uranium peroxide.

In the first method of study, excess H_2O_2 was added to a solution of known acidity in a rapidly stirred autoclave at a constant temperature; subsequently, filtered samples of solution were removed at definite intervals and were analyzed for total uranium, total peroxide, and hydrogen ion concentration. The total uranium concentration was observed to pass through a minimum value immediately upon the addition of H_2O_2; thereafter it increased with time until it reached approximately its original value. The total peroxide content gradually decreased with time after reaching an initial maximum value, while the acidity rose rapidly to a maximum value and then gradually fell to about its initial value.

The general pattern of a typical experiment of this type is shown in Fig. 10.1, which illustrates the course of the reaction after the initial changes. Experiments similar to that shown in Fig. 10.1 were carried out at several temperatures. It was noted in experiments of this type that a rather abrupt change in the observed rate of the process took place at the same time that the total uranium reached its constant concentration in the experiment. Since the rate of decomposition of peroxide in unsaturated uranyl sulfate solutions is well established as first order with respect to total peroxide,[2,3,5] it appears reasonable to assume that the total peroxide concentration at the time when the discontinuity occurs in both curves is that which is present as the last traces of solid uranium peroxide dissolve. Conversely, the peroxide concentration thus determined should approximate that which would exist at the point of incipient precipitation from a solution whose composition corresponds to that of the liquid phase present at the observed point of discontinuity.

In the second method of study of this system, solid uranium peroxide was suddenly released in a stirred solution containing acid (but no uranium) and held at constant temperature. Filtered samples were taken and analyzed as in the precipitation studies. The concentration of total uranium increased very rapidly until it reached the value of the crossover point noted in Fig. 10.1; subsequently, the experiments were identical.

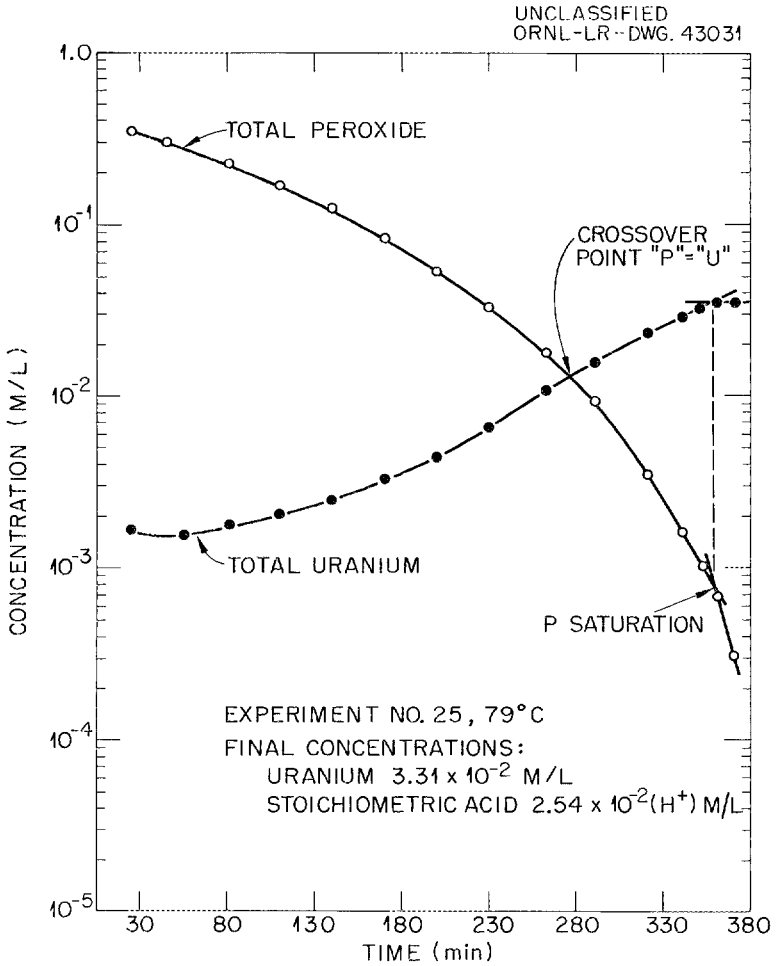

Fig. 10.1. Concentrations of Total Peroxide and Total Uranium vs Time in a Typical Experiment. Run 25; 79°C. Final concentrations: uranium, 3.31×10^{-2} mole/liter; stoichiometric acid, 2.54×10^{-2} (H^+) mole/liter.

Figure 10.2 illustrates the course of a typical experiment of this type. When solid uranium peroxide is added to an acidic solution initially containing UO_2^{++}, a similar rapid initial increase in both uranium and peroxide is observed; in this case the "crossover" point is not reached, but concentrations are established which satisfy the equilibrium. The previous discussion of the significance of the peroxide concentration at the point where the uranium concentration reaches its final constant value also holds for this type of experiment.

The rapidity of the initial concentration changes in both methods of study indicates that the rate of precipitation or dissolution of solid uranium peroxide is much faster than the rate of decomposition under the conditions used.

To establish the mobility of the equilibrium of Eq. (2), sudden changes were made in the solution composition by adding UO_2^{++} or H^+. Figure 10.3 shows the results of adding H^+ at the crossover point; there was immediate dissolution of additional uranium peroxide to reestablish the equilibrium as seen by the equal

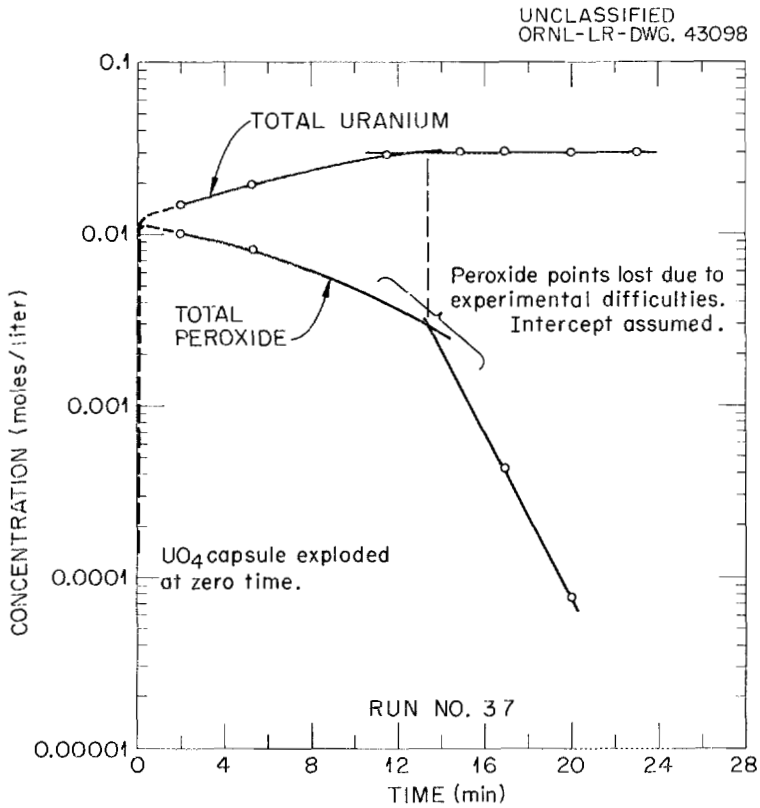

Fig. 10.2. Rate of Solution of Solid UO_4 in Acid Solution. Run 37.

change in the concentration of both total uranium and total peroxide. Figure 10.4 shows that when UO_2^{++} was added to a system there was again an essentially instantaneous shift in the equilibrium in the expected direction. From this experimental evidence it seems likely that solutions such as these are, indeed, always near equilibrium and that it may be assumed that

$$K_c = \frac{UO_4(d)[H^+]^2}{[UO_2^{++}]\ [H_2O_2]} \quad . \qquad (6)$$

In order to treat the data numerically, stoichiometric concentrations were used for calculation.

Since

$$P_{(saturation)} = UO_4(d) + H_2O_2,$$

and

$$[H_2O_2] = \frac{UO_4(d)}{K_c}\ \frac{[H^+]^2}{[UO_2^{++}]} \quad ,$$

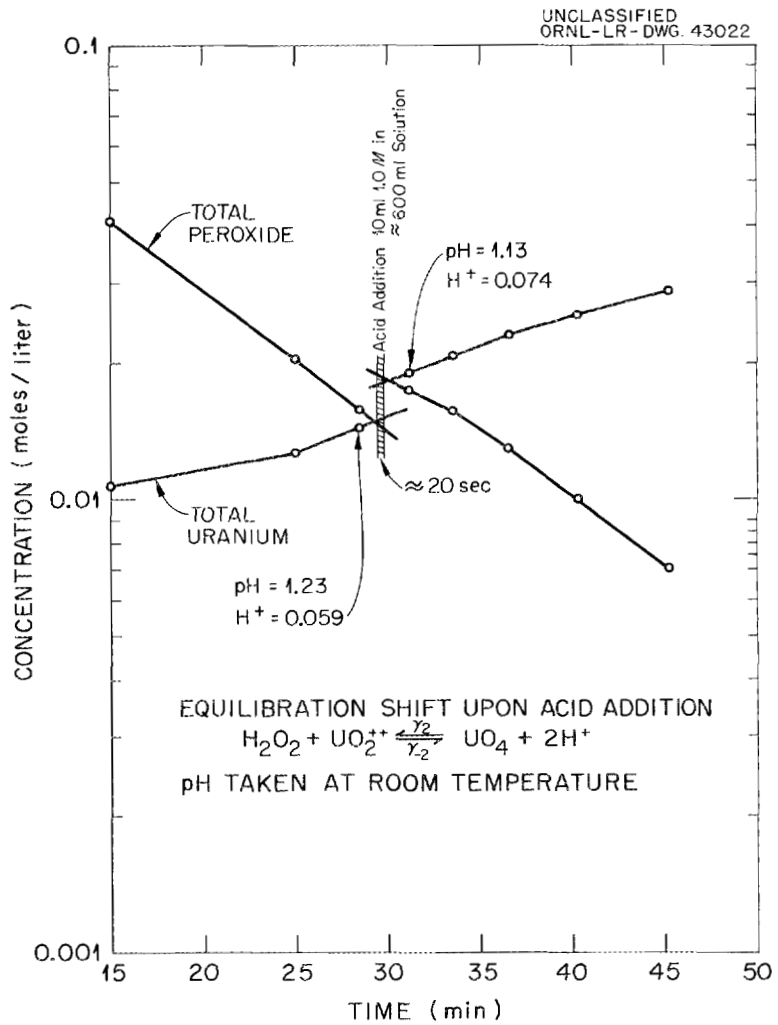

Fig. 10.3. Equilibration Shift Upon Acid Addition: $H_2O_2 + UO_2^{++} \underset{r_{-2}}{\overset{r_2}{\rightleftharpoons}} UO_4 + 2H^+$. pH taken at room temperature; run 35; 93°C.

then

$$P_{(\text{saturation})} = UO_4(d) + \frac{UO_4(d)}{K_c} \frac{[H^+]^2}{[UO_2^{++}]} , \qquad (7)$$

where $[H^+]$ and $[UO_2^{++}]$ concentrations are measured parameters for a given solution and P is the total peroxide in the solution. The solubility of uranium peroxide is known to be about 1×10^{-4} *M* in a solution of uranyl sulfate with no excess acid at 78°C; this same order of magnitude was assumed in making these calculations. The first term in Eq. (7) may be neglected in most cases.

The value of the ratio $UO_4(d)/K_c$ was calculated from the experimental data and the equilibrium expression. The average of the calculated values of the ratio $UO_4(d)/K_c$ for all experiments performed is 3.6×10^{-2}. This ratio appeared to be independent of temperature over the interval 79-114°C. In order to test

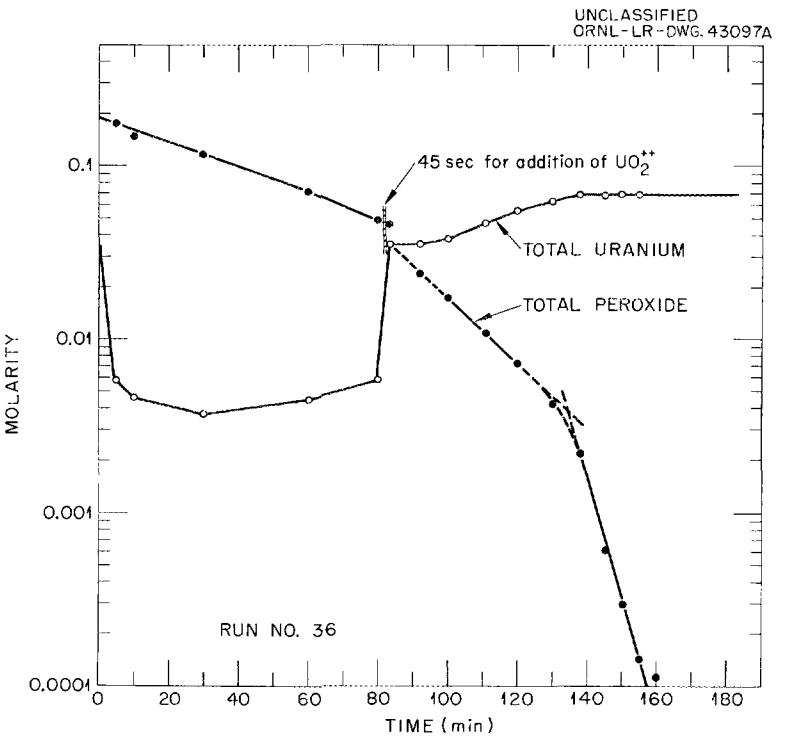

Fig. 10.4. Effect of Addition of UO_2^{++} on Equilibrium. Initial concentrations doubled by addition.

the self-consistency of the data, this average value was used to calculate the concentration of peroxide at incipient precipitation for all the experiments. The calculated values were found to agree satisfactorily with the experimental data, notwithstanding changes in environmental conditions in which concentrations of uranium were varied by a factor of 2, stoichiometric H^+ by a factor of 4, and the temperature by 35°C.

The results of the present investigation can be represented by the following relation:

$$P_{(\text{saturation})} = \left(1.0 + 360 \frac{[H^+]^2}{[UO_2^{++}]}\right) \times 10^{-4}\ M \qquad (8)$$

as a function of the stoichiometric free-acid concentration and the uranyl ion concentration (taken as equal to the molarity of uranium in solution).

An equation for calculating the power density (W_{max}) of a homogeneous reactor at the point of incipient precipitation of uranium peroxide is given elsewhere.[6] If Eq. (8) is introduced into this expression and a value of G_{H_2} of 1.6 is used, the maximum allowable power density is given by:

$$W_{max} = \left(1.05 + 378 \frac{[H^+]^2}{[UO_2^{++}]}\right) k_{obs}, \qquad (9)$$

where W is given in watts per cubic centimeter and k_{obs} is the observed[2,3,5] first-order rate constant for the decomposition of peroxide expressed in min^{-1}. Since the reference equation for W_{max} (ref. 6) was based on a single assumed value for $P_{(saturation)}$, it was strictly valid only for a solution in which $P_{(saturation)}$ had that value. Equation (9) permits values of W_{max} to be calculated for solutions of many different acidities and uranium concentrations. The most obvious limitation of Eqs. (8) and (9) is the assumption that the ratio $(UO_4(d))/K_c$ is independent of temperature. For the narrow temperature range investigated, this ratio did appear to be independent of temperature, within experimental variations.

REFERENCES

1. L. O. Gilpatrick et al., The Concentration of Peroxide in Uranyl Sulfate Solutions at Incipient Precipitation, ORNL CF-59-10-121 (Oct. 22, 1959).

2. M. D. Silverman, G. M. Watson, and H. F. McDuffie, Ind. Eng. Chem. 48, 1238 (1956).

3. G. M. Watson, M. D. Silverman, and H. F. McDuffie, Anal. Chem. 28, 1107 (1956).

4. C. Duval, Anal. Chem. Acta 3, 337 (1949).

5. L. O. Gilpatrick and H. F. McDuffie, HRP Quar. Prog. Rep. Apr. 30 and July 31, 1958, ORNL-2561, p 313-316.

6. J. A. Lane, H. G. MacPherson, and F. Maslan, Fluid Fuel Reactors, p 110, Addison-Wesley, Reading, Mass., 1958.

11. HETEROGENEOUS EQUILIBRIA IN AQUEOUS SYSTEMS

W. L. Marshall

J. S. Gill
G. M. Hebert
E. V. Jones
R. E. Moore
J. E. Savolainen
R. Slusher

11.1 TWO-LIQUID-PHASE BOUNDARY TEMPERATURES FOR HRT FUEL SOLUTIONS AND THEIR CONCENTRATES: EFFECT OF VARYING UO_2SO_4:$CuSO_4$:D_2SO_4 MOLE RATIOS

Previous determinations of the temperatures of immiscibility for synthetic HRT fuels and their concentrates indicated a correlation between the minimum temperatures at which liquid-liquid immiscibility could exist for solution concentrates and the maximum pressurizer temperature at which operational stability could be achieved in the reactor.[1-3] The proposal was made that if the pressurizer temperature exceeded the two-liquid-phase boundary minimum temperature, localized boiling within the reactor core might be sufficient to concentrate the fuel solution by factors of 5 to 10 and to produce liquid-liquid immiscibility with a deleterious effect on reactor stability. The effect of free D_2SO_4 on the two-liquid-phase boundary temperatures was determined in those experiments for a synthetic HRT fuel having a UO_2SO_4:$CuSO_4$:$NiSO_4$ mole ratio of 1:0.5:0.25.

The present investigation was conducted to determine, in the presence of a higher $CuSO_4$ concentration, the effect of sulfuric acid concentration on the temperature of appearance of the heavy liquid phase. The temperatures of second-liquid-phase formation in synthetic HRT fuel solutions were obtained for concentrates of solutions having UO_2SO_4:$CuSO_4$:D_2SO_4 molar ratios of 1:1:1, 1:1:1.5, and 1:1:2. $NiSO_4$ has not yet been included as a component in these solutions. Data obtained by observing the temperature of formation of the two liquid phases are plotted as functions of the concentration factor in Fig. 11.1. The concentration factor is the ratio of the molar concentration of a component in the concentrate to the concentration of that component in the original solution. The UO_2SO_4 concentration for each of the three series was approximately 0.025 M at a concentration factor of 1.

The minimum two-liquid-phase temperature for each series of concentrates increased as the ratio of acid to other components increased. It is interesting to note that the minimum point in each series fell close to a constant free-acid concentration of 0.15 M, an observation which may be helpful in predicting minimum two-liquid-phase temperatures for solutions of other compositions.

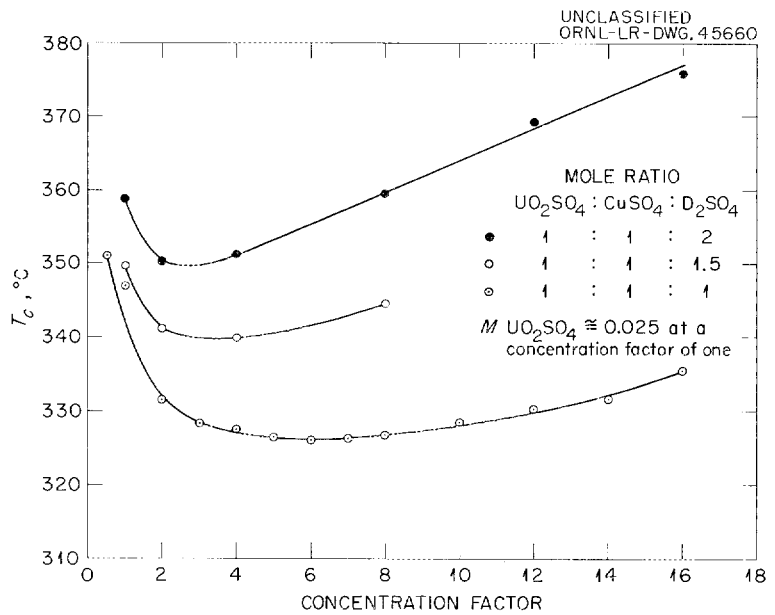

Fig. 11.1. The Temperature of the Appearance of the Second Liquid Phase of Solutions of UO_2SO_4, $CuSO_4$, D_2SO_4, and D_2O as a Function of Concentration Factor.

11.2 OBSERVATIONS ON RATE OF SOLUTION OF HEAVY PHASE

When the temperature of a synthetic HRT fuel solution contained in a silica tube becomes just greater than the two-liquid-phase boundary temperature, the heavy phase is immediately produced throughout the bulk of the solution in the form of very small droplets. No delay in the formation process has ever been observed once the immiscibility temperature has been reached. After formation, the small droplets of heavy phase coalesce to produce larger drops which settle to the bottom. On cooling the system, the heavy phase does not redissolve quickly at temperatures just below the immiscibility temperature unless good mixing is provided. Qualitative laboratory experiments have shown that as the temperature is decreased the heavy phase dissolves faster into the light phase. This effect was noted both when the solution was agitated and when it was not; the rate at which the heavy phase dissolved was, of course, much greater under agitation.

By cooling the synthetic fuel solution without agitation, it was possible to maintain a considerable quantity of the heavy phase in contact with the light phase down to a temperature of about 270°C. However, at this temperature a qualitative change took place; the interface between the phases disappeared, leaving only a concentration gradient where the interface had been. Experiments with UO_2SO_4-H_2O solutions of various concentrations of UO_2SO_4 showed the same effect, but the temperature of disappearance of the interface was not so easily observed as in the case of the synthetic homogeneous reactor fuel solution.

The minimum immiscibility temperature for the system UO_2SO_4-D_2O is 274°C at 1 m UO_2SO_4. The minimum temperature for two-liquid-phase formation in the system formed from $CuSO_4$, UO_2SO_4, and H_2O is slightly below 285°C at 18 wt % UO_2SO_4 and 3 wt % $CuSO_4$. Lower temperatures should occur in acid-deficient portions of the five-component system UO_3-CuO-NiO-SO_3-D_2O.

11.3 INVESTIGATION OF THE SYSTEM UO_3-CuO-NiO-SO_3-H_2O AT 300°C

Considerable solubility information has been obtained for the system UO_3-CuO-NiO-SO_3-H_2O, its D_2O analog, and its included four- and three-component systems at 300°C. In past progress reports,[1,4,5] solubilities at a fixed SO_3 concentration, either 0.08 m or 0.06 m SO_3, were selected from established solubility curves and were presented on orthogonal axes in order to specify the concentrations of three of the components. The basic solubility data at 300°C and a discussion of their significance were given in a recent report.[6]

These basic data are plotted in Fig. 11.2 through 11.8 and show the simultaneous solubilities for the metallic oxide components as a function of SO_3 concentration for the five-component and its included four- and three-component systems. The saturating solid phases in equilibrium with liquid phase or phases are stated in the figures. It is of interest to note the composition regions in which a heavy-liquid phase is a saturating component (Fig. 11.4).

These over-all solubility data provide the basic information for plotting skeletal figures which represent solubility relationships at a fixed SO_3 concentration, as shown by the example in Fig. 11.9. This figure, representing the most recent interpretation of the system, shows a region in which unsaturated solution exists, in addition to showing the saturation boundaries for solution compositions and the specified saturating solid phases. From figures

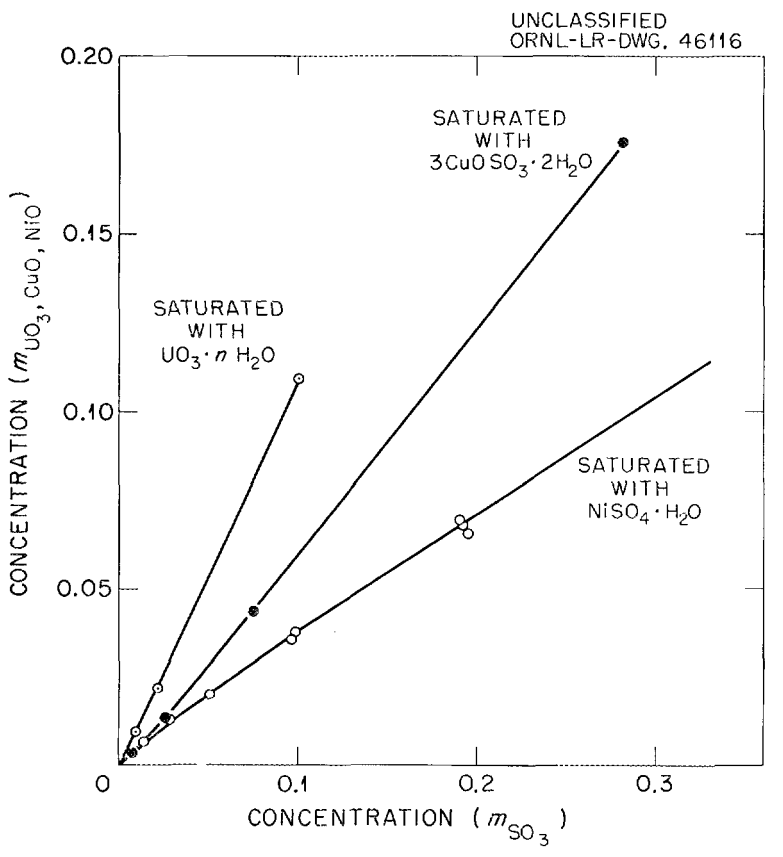

Fig. 11.2. Molal Concentrations of CuO, UO_3, NiO, and SO_3 in Separate Three-Component Systems NiO-SO_3-H_2O at 300°C, Each Saturated with the Specified Solid Phase.

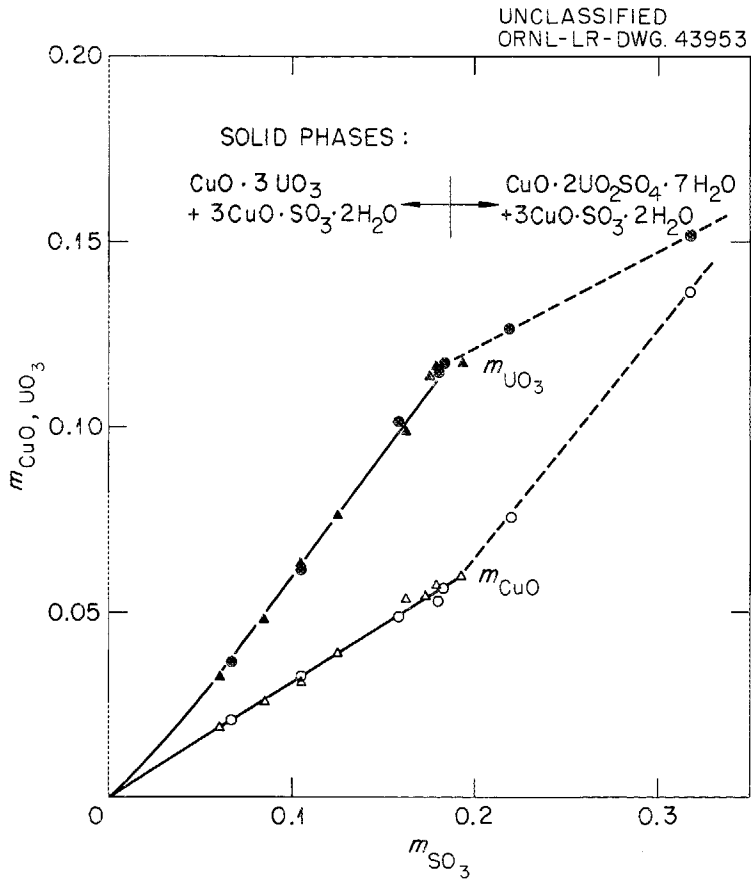

Fig. 11.3. Molal Concentrations of CuO, UO_3, and SO_3 in H_2SO_4-H_2O Solutions at 300°C, Saturated with $3CuO{\cdot}SO_3{\cdot}2H_2O$, $CuO{\cdot}3UO_3$, and $CuO{\cdot}2UO_2SO_4{\cdot}7H_2O$.

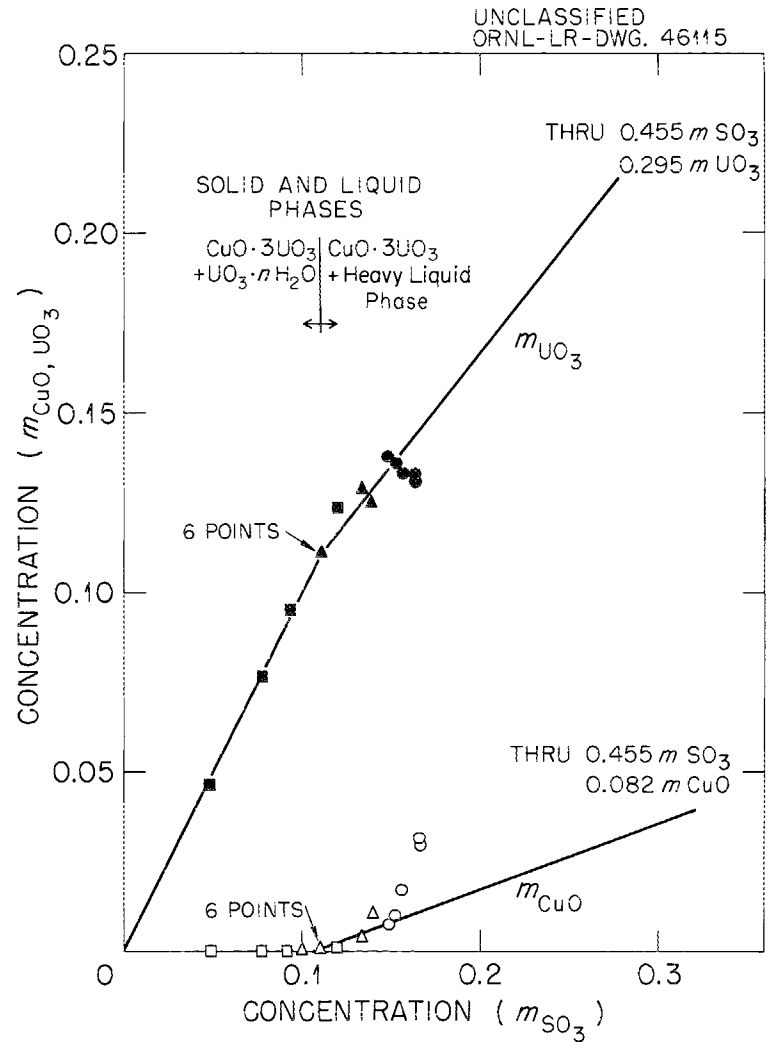

Fig. 11.4. Molal Concentrations of CuO, UO_3 and SO_3 in H_2SO_4-H_2O Solutions at 300°C, Saturated with $CuO{\cdot}3UO_3$, $UO_3{\cdot}nH_2O$, and Heavy-Liquid Phase.

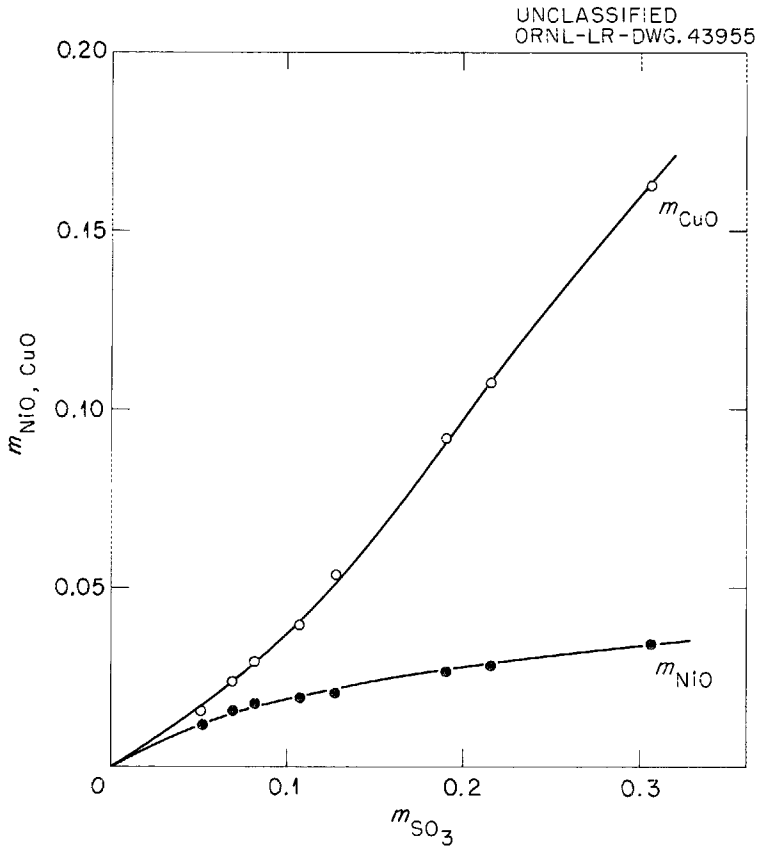

Fig. 11.5. Molal Concentrations of NiO, CuO, and SO_3 in H_2SO_4-H_2O Solutions at 300°C, Saturated with $3CuO \cdot SO_3 \cdot 2H_2O$ and $NiSO_4 \cdot H_2O$.

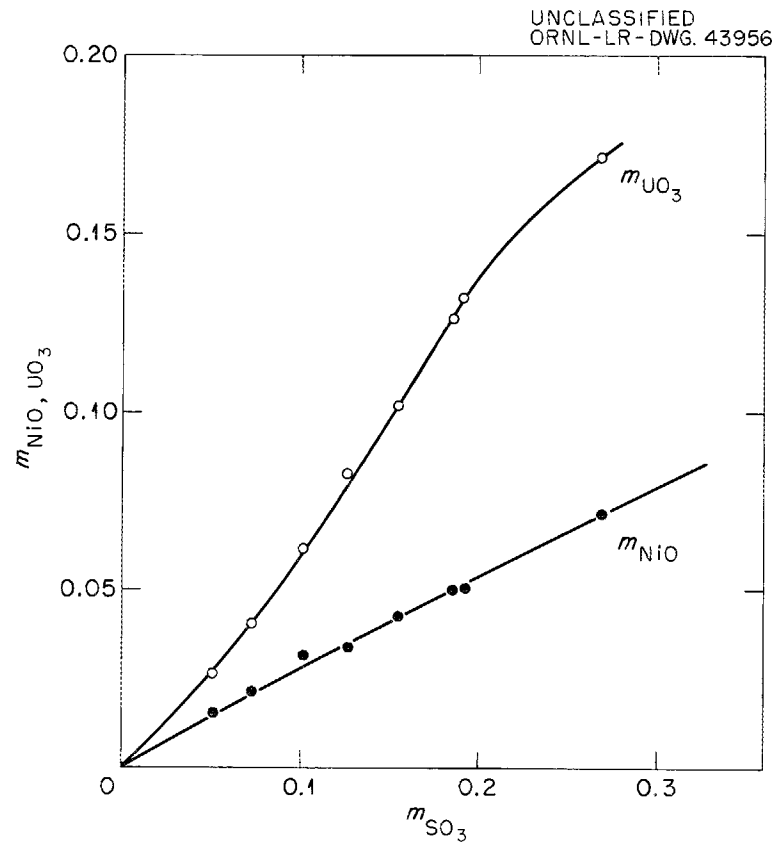

Fig. 11.6. Molal Concentrations of NiO, UO_3, and SO_3 in H_2SO_4-H_2O Solutions at 300°C, Saturated with $UO_3 \cdot UO_2SO_4 \cdot 5H_2O$ and $NiSO_4 \cdot H_2O$.

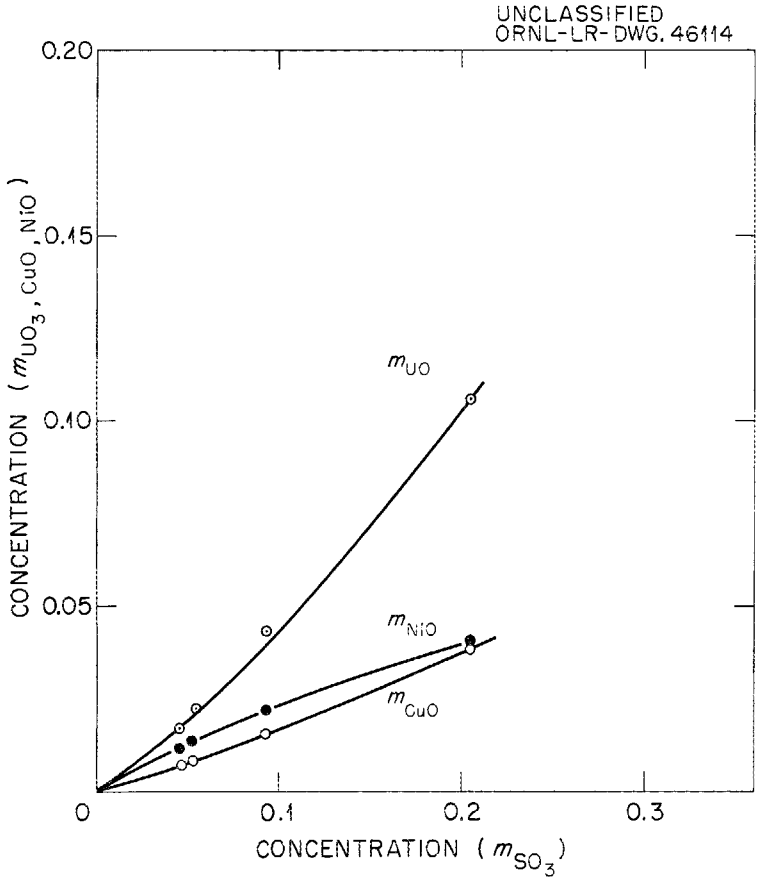

Fig. 11.7. Molal Concentrations of UO_3, CuO, NiO and SO_3 in H_2SO_4-H_2O Solutions at 300°C, Saturated with $UO_3 \cdot UO_2SO_4 \cdot 5H_2O$, $3CuO \cdot SO_3 \cdot 2H_2O$, and $NiSO_4 \cdot H_2O$.

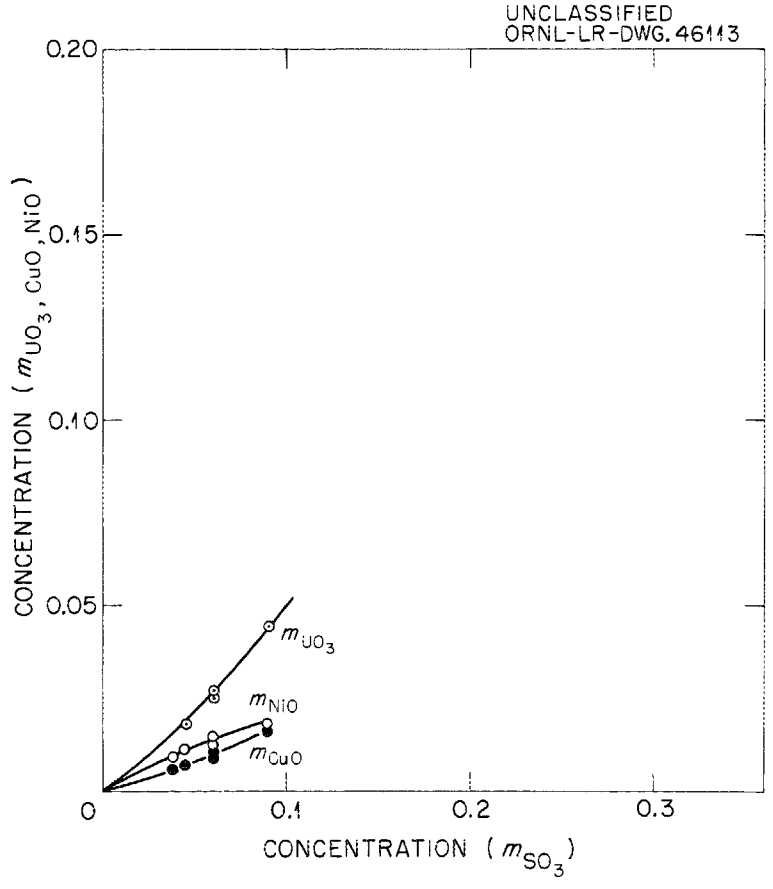

Fig. 11.8. Molal Concentrations of UO_3, CuO, NiO, and SO_3 in D_2SO_4-D_2O Solutions at 300°C, Saturated with $UO_3 \cdot UO_2SO_4 \cdot 5D_2O$, $3CuO \cdot SO_3 \cdot 2D_2O$ and $NiSO_4 \cdot D_2O$.

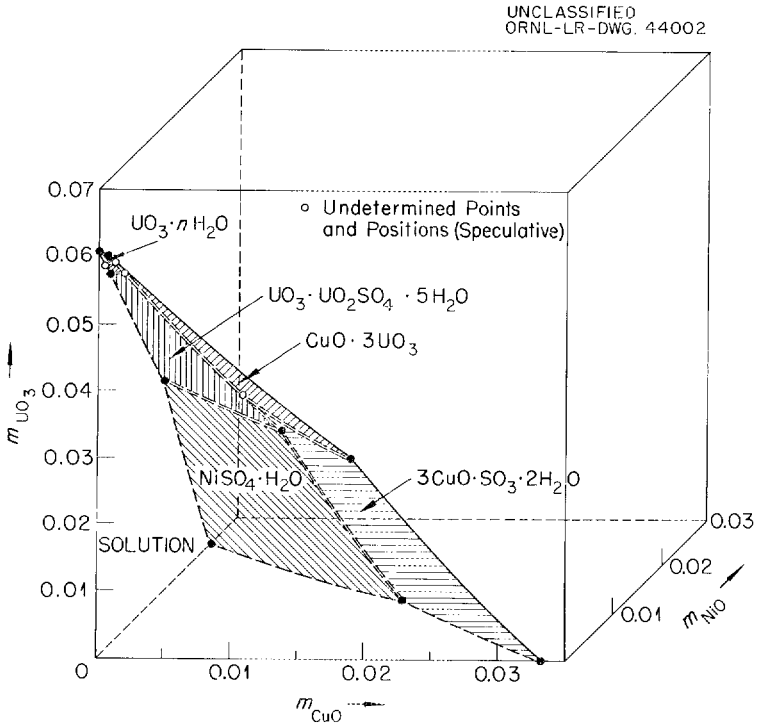

Fig. 11.9. System UO_3-CuO-NiO-SO_3-H_2O at 300°C (SO_3 = 0.06 *m*).

of this type aqueous reactor-fuel compositions may be selected which are at desired distances from regions of saturation. Moreover, if by increasing one of the components, (3.g., Ni, by corrosion) the solution could become saturated, the solid phase which would first appear could be determined from the figure.

11.4 THE pH OF SOLUTIONS CONTAINING UO_2SO_4, $CuSO_4$, $NiSO_4$, H_2SO_4, H_2O, AND D_2O; ITS USE IN THE DETERMINATION OF FREE ACID IN HOMOGENEOUS REACTOR FUELS

The precise measurement of pH of intensely radioactive homogeneous reactor fuel solutions by use of glass electrodes is difficult because of the detrimental effect of radiation on glass. The glass electrode must be replaced frequently, a procedure which may become difficult, since the electrodes and part of the equipment are used in "hot cells". However, if the intensely radioactive solution were diluted considerably with H_2O, it was believed the pH of the resulting solution of lowered radioactivity might perhaps be measured with less difficulty. A brief study was made to determine the pH at 25°C of various dilutions of solutions simulating the HRT fuel composition and of similar solutions containing varying concentrations of the major fuel components.

Hopes for the ultimate usefulness of the method were predicated on the expectation that the pH measurements of diluted fuel solutions would, to a close approximation, give values the same as those for sulfuric acid at the same concentration as that of the free acid in the test solutions, i.e., that the diluted UO_2SO_4, $CuSO_4$, and $NiSO_4$ would have little effect on the pH of the diluted H_2SO_4. Moreover, dilution by H_2O of solutions initially in D_2O would convert the measured solutions to dilute H_2O solutions and substantially eliminate any effect on pH due to D_2O.

The experimental technique was similar to that used for the determination of free nitric acid in uranyl nitrate solutions reported previously.[1] The measured pH's for the solutions diluted 1:10, 1:100, and 1:1000 are listed in Table 11.1 for reference. These values are plotted in Fig. 11.10 vs the known concentration of free acid present in each dilution. It is obvious that the original expectation was justified except for 1:1000 dilutions of solutions which initially had low concentrations. Further development of the method with radioactive solutions and remote operation may now be desirable.

Table 11.1 pH of Solutions of UO_2SO_4, $CuSO_4$, $NiSO_4$, and D_2SO_4 in D_2O Solution After Dilution with H_2O

	pH (25°C)		
	1:10 Dilution	1:100 Dilution	1:1000 Dilution
Solution A - 0.025 M UO_2SO_4, 0.0125 M $CuSO_4$, and 0.006 M $NiSO_4$			
A + 0.01 M D_2SO_4	2.79	3.71	4.73
A + 0.02 M D_2SO_4	2.48	3.45	4.45
A + 0.03 M D_2SO_4	2.33	3.24	4.25
A + 0.04 M D_2SO_4	2.23	3.15	4.15
A + 0.05 M D_2SO_4	2.13	3.03	4.05
Solution B - 0.025 M UO_2SO_4, 0.025 M $CuSO_4$, and 0.006 M $NiSO_4$			
B + 0.01 M D_2SO_4	2.80	3.76	4.65
B + 0.02 M D_2SO_4	2.51	3.38	4.40
B + 0.03 M D_2SO_4	2.35	3.28	4.30
B + 0.04 M D_2SO_4	2.25	3.18	4.18
B + 0.05 M D_2SO_4	2.12	3.08	4.05
Solution C - 0.025 M UO_2SO_4, 0.0125 M $CuSO_4$, and 0.012 M $NiSO_4$			
C + 0.01 M D_2SO_4	2.78	3.73	4.65
C + 0.02 M D_2SO_4	2.50	3.45	4.47
C + 0.03 M D_2SO_4	2.35	3.27	4.28
C + 0.04 M D_2SO_4	2.25	3.18	4.15
C + 0.05 M D_2SO_4	2.13	3.05	4.02
Solution D - 0.05 M UO_2SO_4, 0.0125 M $CuSO_4$, and 0.006 M $NiSO_4$			
D + 0.01 M D_2SO_4	2.75	3.68	4.53
D + 0.02 M D_2SO_4	2.52	3.48	4.40
D + 0.03 M D_2SO_4	2.35	3.30	4.28
D + 0.04 M D_2SO_4	2.24	3.18	4.17
D + 0.05 M D_2SO_4	2.10	3.10	4.06

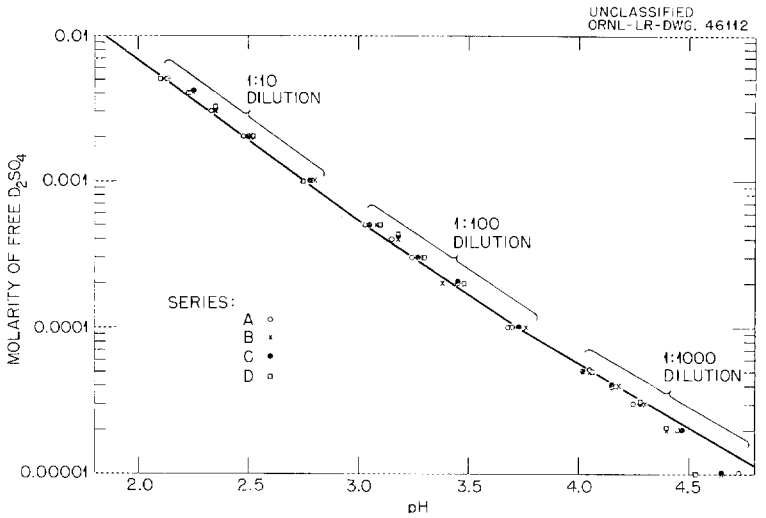

Fig. 11.10. The pH of Dilutions of UO_2SO_4, $CuSO_4$, $NiSO_4$ and D_2SO_4 in D_2O Solution, pH vs Free D_2SO_4 (Dilutions with H_2O).

11.5 EFFECT OF PRESSURE IN ELEVATING THE TEMPERATURE OF TWO-LIQUID-PHASE FORMATION IN THE SYSTEM UO_3-SO_3-H_2O(D_2O)

A comment was made previously[7] on the possible effect of pressure in elevating the temperature of appearance of two liquid phases in the system UO_3-SO_3-N_2O_5-H_2O. Briefly, the appearance of the second liquid phase for one solution was not observed at its expected temperature or even 7°C higher in a sealed tube which became completely full (i.e., no vapor phase present) one degree below the expected temperature. The purpose of the following experiment was to establish approximately the order of magnitude of the temperature-pressure coefficient $\Delta t/\Delta p$ for the formation of the second liquid phase.

The procedure according to the recent suggestions of Morey,[8] consisted in sealing an aqueous solution of UO_2SO_4 in platinum tubing (8 cm long, 0.3 mm in internal diameter) and adding sufficient solution to almost fill the tube before sealing. The filled tube was placed in a vertical position in a pressure vessel connected to a Sprague high-pressure pump. The pressure vessel was filled with water, sealed, and hydraulically pressurized to the desired pressure. It was then placed in a heating block and heated to a temperature above the known two-liquid-phase boundary temperature for the solution when at its saturation vapor pressure. The high pressure was maintained throughout this operation. After a short time had elapsed, during which time a heavy-liquid phase, if formed, would fall to the lower end of the platinum tube, the pressure vessel was pulled from the furnace and cooled rapidly by placing it in a bucket of ice water. The high pressure was removed, the vessel was opened, the partially collapsed platinum tube was removed, frozen, and cut in half; the two segments of liquid were analyzed for uranium. A comparison of the analyses permitted a determination as to whether liquid-liquid immiscibility was eliminated by the applied pressure at the specified temperature.

Table 11.2 indicates that a hydraulic pressure of 15,000 psi at 312°C suppressed the liquid-liquid immiscibility for a 1.02 M UO_2SO_4 solution in H_2O. The pressure-temperature coefficient $\Delta t/\Delta p$ for this solution apparently is greater than 1.9°C per 1000 psi.

Table 11.2. Effect of Pressure in Elevating the Temperature for the Formation of Liquid-Liquid Immiscibility in the System UO_3-SO_3-$H_2O(D_2O)$

Molarity of UO_2SO_4 in Initial Solution	Expected Two-Liquid Phase Temperature at Saturation Vapor Pressure (°C)	Experimental Conditions		Concentration of Uranium in Tube Segments (wt %)	
		Temp. (°C)	Hydraulic Pressure (psi)	Upper	Lower
1.02(in D_2O)	285	312	15,000	10.9	11.4
1.10(in H_2O)	275	346	9,000	9.0	11.6

A heavy-liquid phase was not eliminated by the application of 9000 psi of pressure to a 1.0 M UO_2SO_4 solution in D_2O at 346°C. Upon visual observation of the contents of the upper and lower contents of the platinum tube, it appeared that liquid-liquid immiscibility had, however, been reduced considerably. Under its saturated-vapor pressure at 346°C the heavy-liquid phase would have probably crystallized upon cooling at 25°C. However, the contents in the lower half were still liquid but contained a higher uranium concentration than the upper half. The pressure-temperature coefficient for the second solution composition, therefore, appeared to be less than 8.7°C per 1000 psi.

11.6 EFFECT OF UO_3/SO_3 MOLE RATIO ON IMMISCIBILITY TEMPERATURE OF 0.02, 0.05, and 0.20 m SULFATE SOLUTIONS

The temperature of separation of a second liquid phase for a series of solutions, each 0.10 m in total SO_4^{--}, in which the UO_3/SO_3 mole ratio varied from 0.10 to 1.0 was reported previously.[1] It was shown that an approximately linear curve was obtained when the mole ratio, UO_3/SO_3 was plotted vs the separation temperature. The proposition was made that the over-all mole ratio, UO_3 + CuO + NiO)/SO_3, might also show a relationship with temperature which would be sufficiently close to linear to be useful. At mole ratios, UO_3/SO_3, below 0.18 for solutions 0.10 m in SO_3, UO_2SO_4 was observed to be soluble in the supercritical fluid which appeared above approximately 380°C. This program was continued, and data are now available for three additional series of solutions.

The new data, together with the previous data for solutions 0.10 m in total SO_4^{--}, are plotted in Fig. 11.11. The two-liquid-phase curves are approximately linear. Furthermore, at the low concentrations of UO_2SO_4 for each series of experiments, the component UO_2SO_4 was found to be soluble in the supercritical fluid.

11.7 THE SYSTEM UO_3-N_2O_5-H_2O AT 25°C AND FROM 135 TO 350°C

The investigation of the system UO_3-N_2O_5-H_2O was continued in order to expand the range of study to 25, 325, and 350°C. Details concerning earlier studies of this system from 135 to 300°C and from 0.00025 m to 4 m HNO_3 were

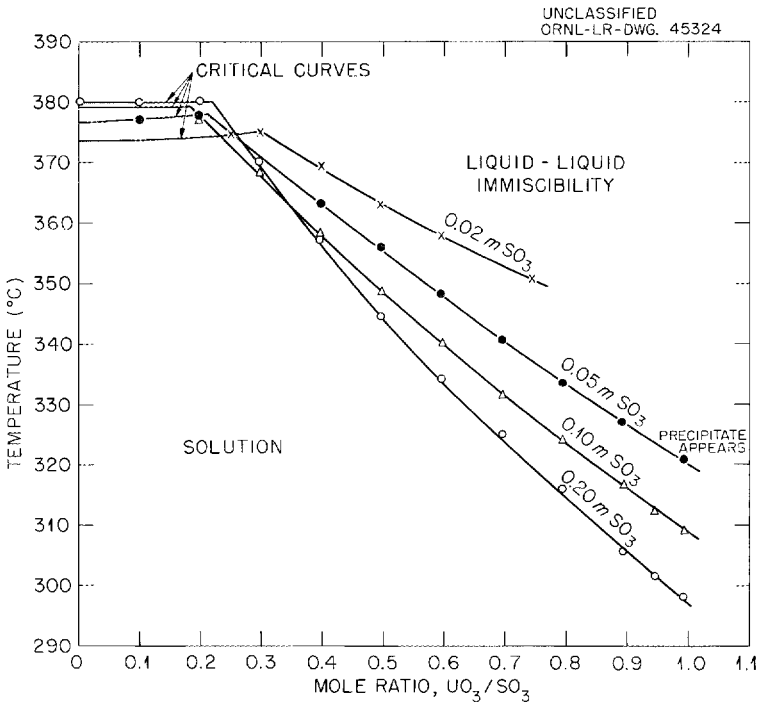

Fig. 11.11. Temperature of Two-Liquid-Phase Formation for the System UO_3-SO_3-H_2O.

presented in the two previous progress reports.[1,5] The over-all motivations for the study were also presented previously.[9,10]

Solubility experiments for this system were completed at 325 and 350°C. The best experimental data to date are shown in Fig. 11.12, which includes data previously reported. Plots of 1/T(°K) vs the logarithm of the mole ratio, UO_3/NO_3, indicated a small discrepancy in 300°C data in the concentration range from 0.05 to 2.0 $\underline{m}$ HNO_3. More recent data at 300°C which did not show this discrepancy are given in Fig. 11.12.

The solubility of $UO_3 \cdot \underline{n}H_2O$ in aqueous solutions of HNO_3 at 25°C was determined in the following manner. Several solutions of HNO_3 of different concentrations were saturated with $UO_3 \cdot \underline{n}H_2O$ by sealing mixtures of solid and liquid in inert containers and rotating the containers in a 25°C constant-temperature bath for one to two weeks. The rotator was stopped, the solid phases were allowed to settle, and the liquid phases were sampled and analyzed by methods described previously. The solid phase saturating each solution was found to be $UO_3 \cdot H_2O$ by x-ray diffraction identification.

The data at 25°C are also included in Fig. 11.12. It is apparent that $d(\underline{m}_{UO_3}/\underline{m}_{NO_3})/d(HNO_3)$ is negative, whereas this value is positive at temperatures between 150 and 350°C in the same concentration range. The saturated solutions at 25°C have pH's in the 4.0 to 5.0 range, where CO_2 could, if present in sufficient quantity, exert a noticeable effect on the solubilities. Since no precautions were taken to remove the CO_2 from the 25-cc air space in each container after filling with solution but before sealing, it is possible, though unlikely, that CO_2 may have affected the saturation mole ratios at 25°C.

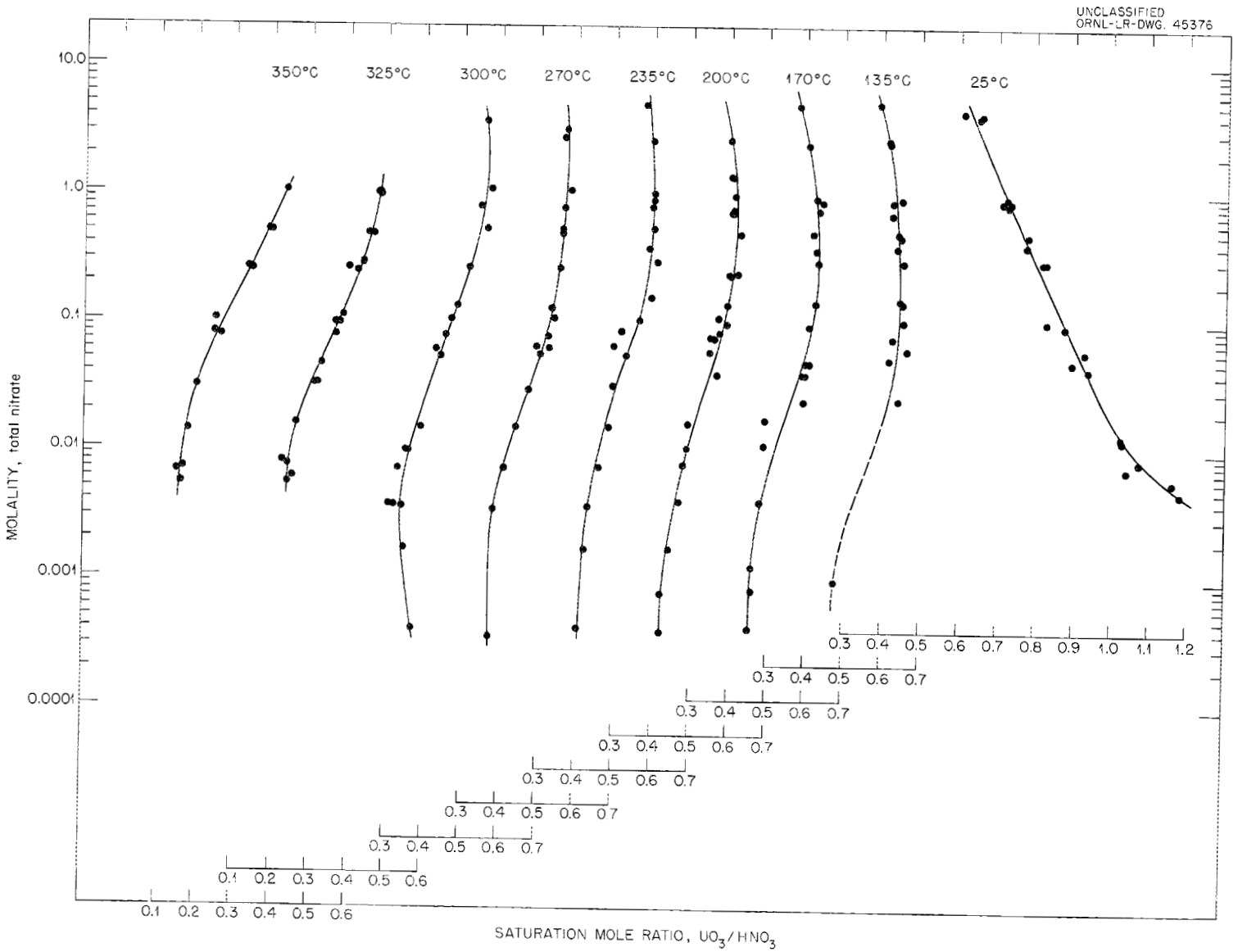

Fig. 11.12. The Solubility of $UO_3 \cdot nH_2O$ in HNO_3-H_2O Solutions, 25 to 350°C.

11.8 TWO-LIQUID-PHASE STUDIES: COMPOSITION*

The study of the formation of two liquid phases in uranyl sulfate solution was continued[11] by using a titanium loop equipped with a titanium hydroclone and underflow pot for collecting the heavy phase. The underflow pot was modified by welding a 1/4-in. nipple on the bottom and attaching to the nipple with a Parker fitting a 1/4-in. tube 3 in. long, crimped and welded at one end. The 1/4-in. tube served as the sampler for collecting heavy phase by merely freezing off the 1/4-in. nipple after the heavy phase had settled into the tube under the appropriate conditions.

A solution of 0.034 M UO_2SO_4, 0.0194 M $CuSO_4$, 0.0097 M $NiSO_4$, and 0.0275 M D_2SO_4 in D_2O (measured at 25°C) similar to the composition of the core solution in HRT run 21, was circulated at 325°C until samples of the circulating stream indicated no further separation of heavy phase (the second-liquid-phase temperature for this solution is about 320°C). The compositions of the light and heavy phases isolated at that time are given in Table 11.3. Also given are the molar ratios of the various constituents.

Table 11.3. Composition of Light and Heavy Phases Formed from a Dilute Uranyl Sulfate Solution at 325°C

	Original (M)	Light Phase (M)	Heavy Phase (M)	
U	0.0340	0.0315	4.56	
Cu	0.0194	0.0183	1.53	
Ni	0.0097	0.0084	0.413	
SO_4	0.0907	0.0864	6.52	
Acid	0.0275	0.0265	<0.01	
U/SO_4	0.375	0.365	0.700	(0.750)*
Cu/SO_4	0.214	0.212	0.235	(0.250)*
Ni/SO_4	0.107	0.0967	0.0634	
$Acid/SO_4$	0.304	0.307	0.0	
U/Cu	1.75	1.72	2.98	
U/Ni	3.52	3.77	11.0	
Volume heavy phase/volume light phase			0.00062	

*Neglecting sulfate associated with nickel as $NiSO_4$.

Of interest is the fact that the U/Cu ratio in the heavy phase was almost exactly 3:1. Furthermore, if one subtracts an amount of sulfate equivalent to the nickel from the total sulfate in the heavy phase and then takes the U/SO_4 and Cu/SO_4 ratio to the remaining sulfate, the results are exactly 0.750 and 0.250, respectively. Thus, in this case the ratio of $U:Cu:SO_4$ in the heavy phase was 3:1:4, with some nickel sulfate dissolved or dispersed in it.

Unfortunately, the presence of uranium and copper in a 3:1 ratio in the heavy liquid phase complicates greatly the attempt to differentiate between

*This section contributed by J. C. Griess, H. C. Savage, S. E. Bolt, and R. S. Greeley, REED.

two of the mechanisms proposed for the power-dependent loss of uranium in the HRT, viz., by formation of a second liquid phase or by precipitation of the compound $3UO_3 \cdot CuO$ (ref. 12). The presence of sulfate in a 3:4 ratio with uranium is interesting and is perhaps due to HSO_4^- rather than OH^- in the ion postulated by Marshall et al.,[13] $U_3O_8(OH)_4^{--}$.

REFERENCES

1. W. L. Marshall et al., HRP Prog. Rep. Oct. 31, 1959, ORNL-2879, p 99-125.

2. W. L. Marshall, J. S. Gill, and R. E. Moore, Two-Liquid-Phase Temperature Limits in the Homogeneous Reactor Fuel Solution and its Concentrates; Comments on Solid-Liquid Equilibria, ORNL CF-59-8-41.

3. R. E. Moore and W. L. Marshall, Effect of Excess Acid on Two-Liquid-Phase Temperature Limits for the Homogeneous Reactor Fuel Solution and Its Concentrates, ORNL CF-59-11-27.

4. W. L. Marshall et al., HRP Quar. Prog. Rep. Jan. 31, 1959, ORNL-2696, p 205-214.

5. W. L. Marshall et al., HRP Prog. Reps. Apr. 30 and July 31, 1959, ORNL-2743, p 227-238.

6. W. L. Marshall and J. S. Gill, Investigation of the System UO_3-CuO-NiO-SO_3-H_2O at 300°C, ORNL CF-59-12-60, Rev. 1 (1959).

7. C. J. Barton, G. M. Hebert, and W. L. Marshall, Liquid-Liquid Immiscibility Above 300°C in the System UO_3-SO_3-N_2O_5-H_2O, ORNL CF-59-11-64 (1959).

8. G. W. Morey, U. S. Geological Survey, Washington, D. C.

9. W. L. Marshall, Consideration of the $UO_2(NO_3)_2$-HNO_3-$H_2O(D_2O)$ as a High-Temperature Homogeneous Reactor Fuel, ORNL CF-59-5-100.

10. W. L. Marshall, Further Consideration of UO_3-HNO_3-H_2O as a Homogeneous Reactor Fuel; Investigation of Solution Stability of Solutions Suitable for HRT Operation, ORNL CF-59-8-27.

11. J. C. Griess et al., HRP Prog. Rep. Oct. 31, 1959, ORNL-2879, p 100-102.

12. HRP Monthly Information Meeting, Jan. 7, 1960.

13. W. L. Marshall et al., HRP Quar. Prog. Rep. April 30, 1959, ORNL-2743, p 229.

12. SOLUTION CORROSION

J. C. Griess H. C. Savage

S. E. Bolt R. S. Greeley

12.1 CRITICAL VELOCITY OF TYPE CD4MCu STEEL AND OF TYPE 304 STAINLESS STEEL CONTAINING 0.5% PLATINUM

It has been shown previously[1] that type CD4MCu steel has favorable mechanical and fabrication properties, is more resistant to stress-corrosion cracking, galling, and crevice attack than type 347 stainless steel, and is as resistant to corrosion in uranyl sulfate solution as type 347. Also, it has been found[2] that the addition of 0.5% platinum to type 304 stainless steel improves its corrosion resistance to uranyl sulfate and uranyl nitrate solutions. Since the corrosion studies on both these alloys had been conducted either at low (10-20 fps) or at high (45-70 fps) velocities, it was of interest to determine the critical velocity of each alloy relative to that of type 347 stainless steel. Two runs were made by using 0.04 *m* UO_2SO_4, 0.025 *m* D_2SO_4, and 0.02 *m* $CuSO_4$ in D_2O at 250°C for 200 hr. In the first, CD4MCu coupons made from cast material were compared with type 347 cast and wrought material. In the second, type 304 + 0.5% Pt coupons made from wrought material were compared with type 304 and type 347 wrought materials. In both cases in-pile-loop type coupon holders were used.

The cast CD4MCu weight losses were essentially the same as the cast type 347 weight losses at each velocity, and were somewhat greater than the wrought type 347 weight losses at 10 to 30 fps and somewhat less at 30 to 70 fps. The critical velocities appeared to be about the same for all three materials, 10 to 20 fps. This value of the critical velocity cannot be considered highly reliable because of the large velocity gradient over each coupon and the short duration of the runs.

The weight losses of the platinum-containing alloy at all velocities were less than those of the type 304 or 347. The critical velocity was definitely slightly higher, about 15 to 25 fps in this particular test.

The CD4MCu and the type 304 + 0.5% Pt should be tested further in relation to anticipated applications in the homogeneous reactor program.

REFERENCES

1. D. N. Hess *et al.*, *Corrosion Resistance of CD4MCu Stainless Steel in Reactor-Related Environments*, ORNL CF-59-11-114 (Nov. 30, 1959).

2. J. C. Griess *et al.*, *HRP Quar. Prog. Rep. Apr. 30, 1959*, ORNL-2743, p 112; J. C. Griess *et al.*, *HRP Prog. Rep. Oct. 31, 1959*, ORNL-2879, p 126-127.

13. RADIATION CORROSION

J. C. Banter G. H. Jenks
S. E. Bolt S. H. Wheeler

13.1 SUPPORTING RESEARCH

13.1.1 Sorption of Uranium on Hydrous Zirconium Oxide from UO_2SO_4 Solutions

Batch-type experiments similar to those of Heston[1] were performed to study further the sorption of uranium on hydrous zirconium oxide from UO_2SO_4 solutions at 250°C. Heston's technique was refined to allow the use of larger samples of solution and oxide and to allow the separation of the solution and oxide while still at temperature.

Eleven runs were made in which 0.5 g of oxide and 5 ml of the UO_2SO_4 solution of interest were sealed in Pyrex capsules having one end conically tapered. The Pyrex capsules were then placed in an autoclave with a small amount of water and heated at 250°C for specified lengths of time. While still hot, the whole autoclave was centrifuged to draw the oxide into the restricted portion of the capsule. The capsule was then opened and the supernatant was drawn off for analysis. The oxide was sent for surface-area determination or was used for x-ray or electron diffraction studies of the changes incurred. An all-titanium autoclave, which eliminated the use of Pyrex capsules but retained the feature of allowing separation at temperature, was used in four other similar experiments.

Solutions in the range of 1 to 30 g/liter for uranium and 0.02 *m* in H_2SO_4 were used. In three runs, only water was used in the capsules with the oxide; in one run, with the titanium autoclave, only 0.02 *m* H_2SO_4 was used as the solution. All runs except three were at 250°C for 4 hr. Two of the water runs were at temperature for 1 hr and 6 hr; one UO_2SO_4 run was at temperature for only 1 hr.

Results showed that uranium was sorbed in amounts which varied from 35 to 115 mg per gram of oxide from solutions having a uranium concentration in the range of 1.5 to 28.6 g/liter. A comparison of the present results with the earlier work of Heston is given by the linear plots of the data in Fig. 13.1. The molar ratio of sorbed uranium to sorbed sulfate was found to be essentially constant at 1.25 + 0.05 for 11 of 13 runs, and the variation of the ratio from this value in at least one of the other two runs may be attributed to a rather small analytical error. This is contrary to previous results,[2] based on much less reproducible data, which indicated that more sulfate than uranium was sorbed, on a molar basis.

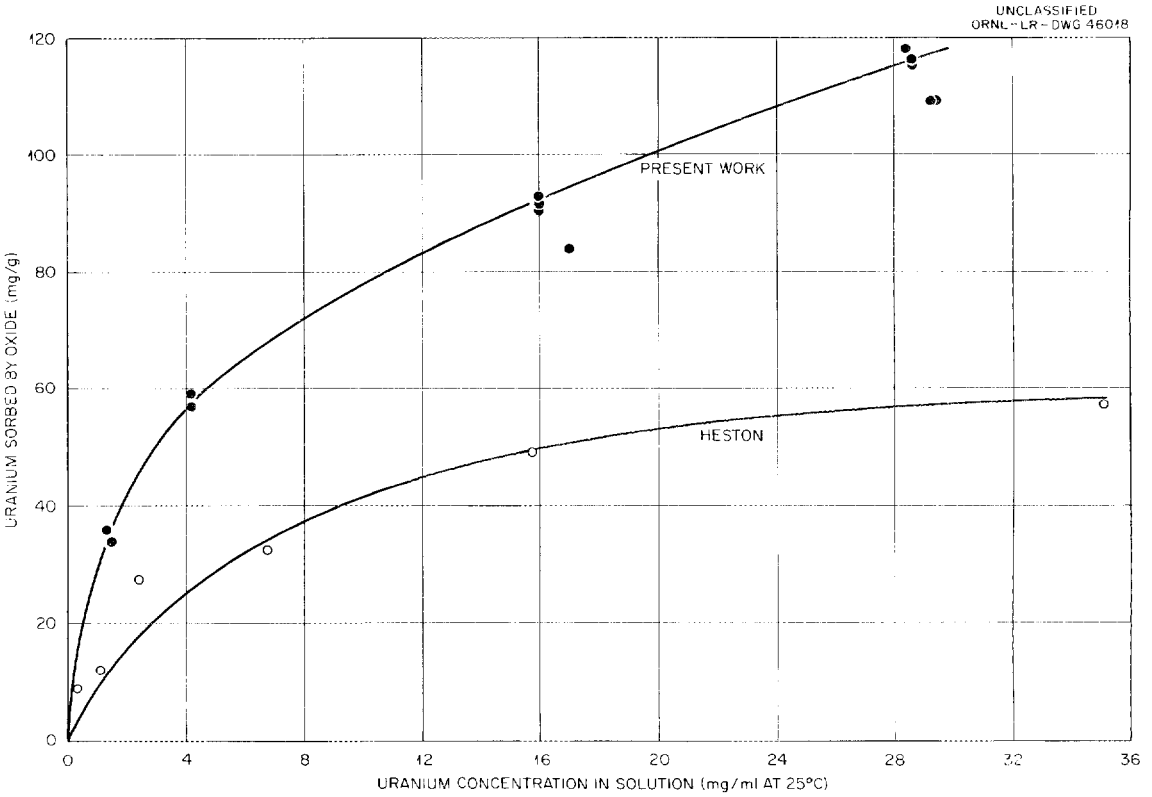

Fig. 13.1. Linear Plot of Data for Sorption of Uranium on Hydrous ZrO_2 at 250°C.

Ion balances on the analyses performed on the supernatants taken from the autoclaves after each run showed that there was a deficiency of cations in the amount of about 0.01 *m* if it was assumed that hydrogen and uranyl ions were the only cations present. Spectrographic analysis of the oxide has shown that it contains calcium and magnesium as impurities in concentrations of 1000 and 800 ppm, respectively. If these impurities were dissolved during the course of a run, they could account for the apparent deficiency of cations. Silicon, which is also present in the concentration of 1000 ppm, is probably not soluble and would not affect the balance. Certain other impurities in the oxide, some of which should also be insoluble, are present in such small amounts that they should have a negligible effect on the ion balance if dissolved.

The oxide surface area (determined by gas adsorption) decreased in all runs from an initial value of 221 m^2/g to values as low as 70 m^2/g. Three runs in water and one with 0.02 *m* H_2SO_4 as the solution indicated that the surface area dropped to about 70 m^2/g after 4 hr at 250°C and remained at that value upon heating for an additional 2 hr. The surface-area determinations of the oxide samples after the runs with UO_2SO_4 indicated a dependence of the area on the uranium concentration. Final areas ranged from 72 m^2/g at a uranium concentration of about 1.5 g/liter to a maximum of 122 m^2/g at 16 g/liter, then fell off again to 95 m^2/g as the uranium concentration was increased further to 28.6 g/liter. No correlation between the final surface area and the amount of uranium sorbed was evident.

X-ray diffraction studies of the oxide indicate that the original oxide, air-fired at 100°C, is amorphous, but is crystallized to the monoclinic form during the course of an experiment. There is also evidence that small amounts of the oxide may have crystallized in the cubic form. Average diameters of the monoclinic crystallites are in the range 60 to 100 Å. No electron diffraction results are available as yet.

In general, all experimental results were quite reproducible and well within experimental error. Earlier objections to the use of Pyrex capsules were based on the possibility of their being etched by the UO_2SO_4 solutions. The results in the titanium autoclave runs indicate that comparable results were obtained with the two materials and that etching of the Pyrex is not a complicating factor in these 250°C exposures.

The results of one run, which was at room temperature for a time comparable to that used by Heston, indicated greater sorption of uranium than was indicated by his data. Since the oxides used in each case were essentially the same, as far as could be determined, one explanation for the difference in results could be that the separation of the oxide while at temperature prohibited the desorption of uranium, as may have occurred in Heston's work. The constancy of the U/SO_4^{--} ratio indicates that there may be some relation between sorbed uranium and sorbed sulfate. The fact that decrease of the oxide surface area was less in the presence of UO_2SO_4 was unexpected. In particular, it is surprising to note that the area decrease was smallest at a uranium concentration of about 16 g/liter, an intermediate concentration of those studied.

It was found that the uranium sorption data can be represented by an equation of the type $U_A = kc^n$ in which U_A is the amount of uranium sorbed in milligrams per gram of oxide, c is the solution concentration in milligrams per milliliter, and k and n are constants having the values 30.6 and 0.397, respectively. This equation is a form of the Freundlich isotherm. A plot of the data based on weighted averages and this equation is shown in Fig. 13.2. It is interesting to note that this equation indicates that the ratio of the amount of uranium sorbed from a 40-g/liter solution to that sorbed from a 10-g/liter solution is about 1.7. Theoretical considerations of the in-pile loop corrosion results for Zircaloy-2 indicate that this ratio should be about 2.0 to best explain the difference in corrosion rates in the two solutions. These two values are at least in reasonable agreement.

Most of these data have been accumulated only recently, and further analysis of them is planned. However, their excellent reproducibility warrants the use of the sorption data as a base line to study the effects of other variables (e.g., temperature and additives to the solution, such as acid and copper), which may radically change the amount or nature of the sorption.

REFERENCES

1. G. H. Jenks et al., HRP Quar. Prog. Rep. Oct. 31, 1958, ORNL-2654, p 179-183.

2. G. H. Jenks et al., HRP Quar. Prog. Rep. Oct. 31, 1959, ORNL-2879, p 148-149.

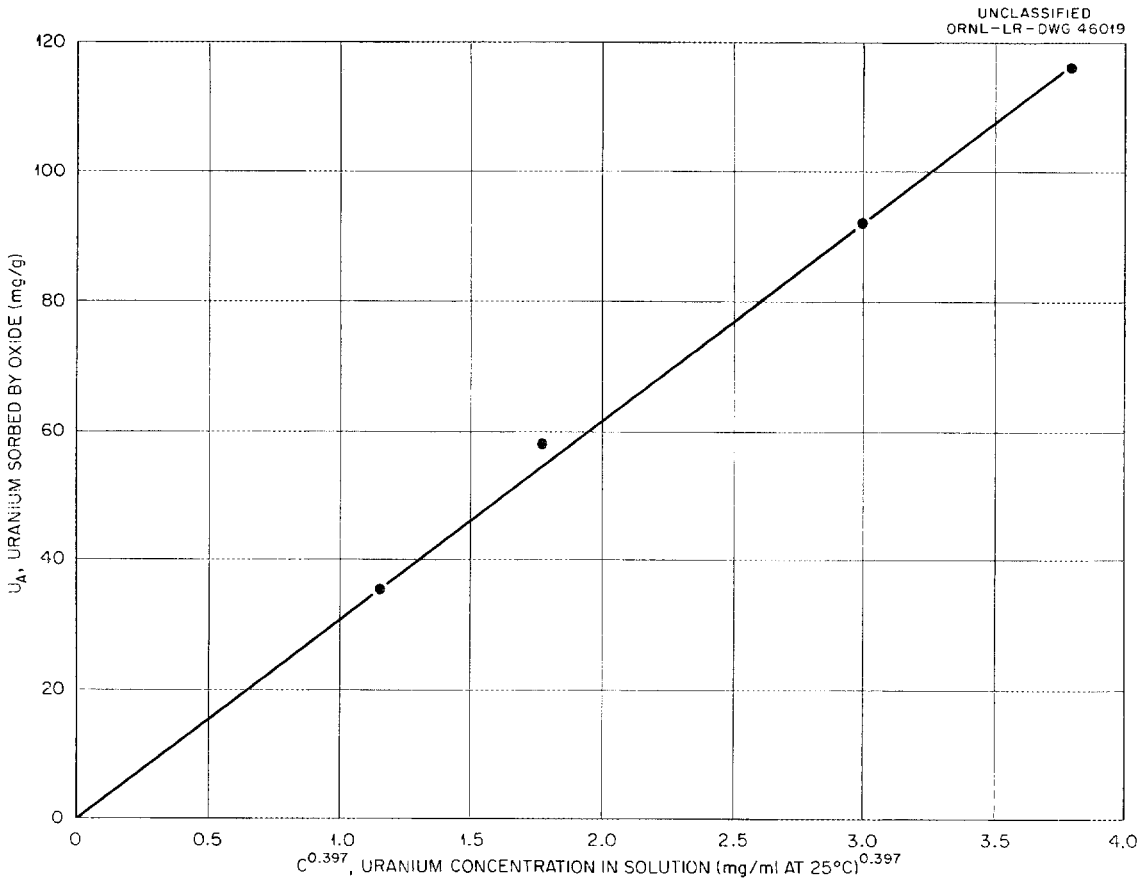

Fig. 13.2. Freundlich-Type Plot for Sorption of Uranium on Hydrous ZrO_2 at 250°C According to the Equation $U_A = 30.6\ C^{0.397}$.

Part IV

SLURRY FUELS

14. ENGINEERING AND PHYSICAL PROPERTIES

H. W. Hoffman

C. S. Morgan D. G. Thomas

14.1 RHEOLOGY OF SUSPENSIONS OF SPHERICAL ThO_2 PARTICLES

The laminar-flow characteristics of two suspensions of spheroidal ThO_2 particles (each of a different particle size) were measured by using a viscometer with a tube length of 1000 L/D and a diameter of 0.124 in. The smaller ThO_2 particles, which were prepared by flame calcination,[1] had a mean diameter of 1.4 μ, a logarithmic mean deviation of 1.9, and a particle density greater than 8.2 g/cc. The larger particles were "standard slurry" spheres refired at 1200°C; the mean diameter was 17 μ, the logarithmic mean deviation was 1.8, and the particle density was 9.1 g/cc.

Since the amount of material available was insufficient to determine the effect of concentration on the yield stress, the cubic relationship previously observed[2] has been assumed in order to compare the present data with earlier results[2] for irregular crystalline material. The two sets of data are shown in Fig. 14.1, with all the previous data being represented by the cross-hatched area. As can be seen, the effect of particle diameter appears to be the same regardless of whether the material is spheroidal or irregularly crystalline; however, the yield stress of suspensions of the spheroidal material may be as low as one-tenth the value for those prepared from irregular crystalline material of the same particle size.

14.2 LAMINAR HEAT-TRANSFER COEFFICIENTS OF NON-NEWTONIAN SUSPENSIONS

The correlation developed[3] for laminar heat-transfer coefficients with non-Newtonian suspensions used an approximate correction to compensate for the non-Newtonian velocity profile. The mean values for the experimental data were found to lie about 15% above this semitheoretical line; all the data fell within a scatter band of ±30% around the mean. Recently, a more detailed theoretical analysis has been presented by Hirai[4] which, when applied to these same data, results in the improved correlation shown in Fig. 14.2. The mean values for the data are now observed to be only 11% above those predicted by the Hirai line, and the spread of the data has been reduced to ±15%. The equation given in Fig. 14.2 is an approximation by Hirai of his exact solution and agrees closely with this exact solution for values of the Nusselt modulus (hd/k) greater than 8.

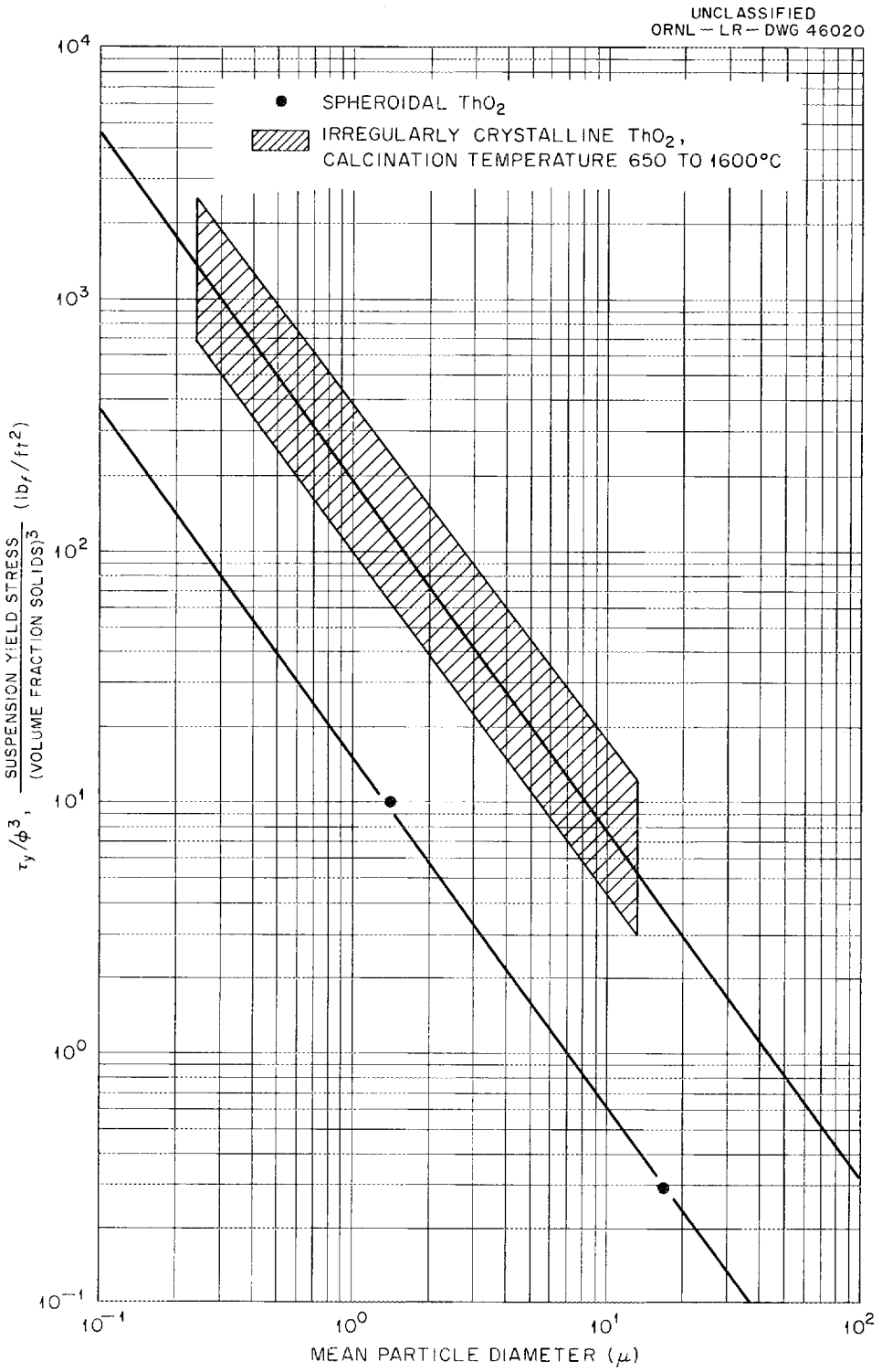

Fig. 14.1. Comparison of Effect of Particle Shape on Suspension Yield Stress.

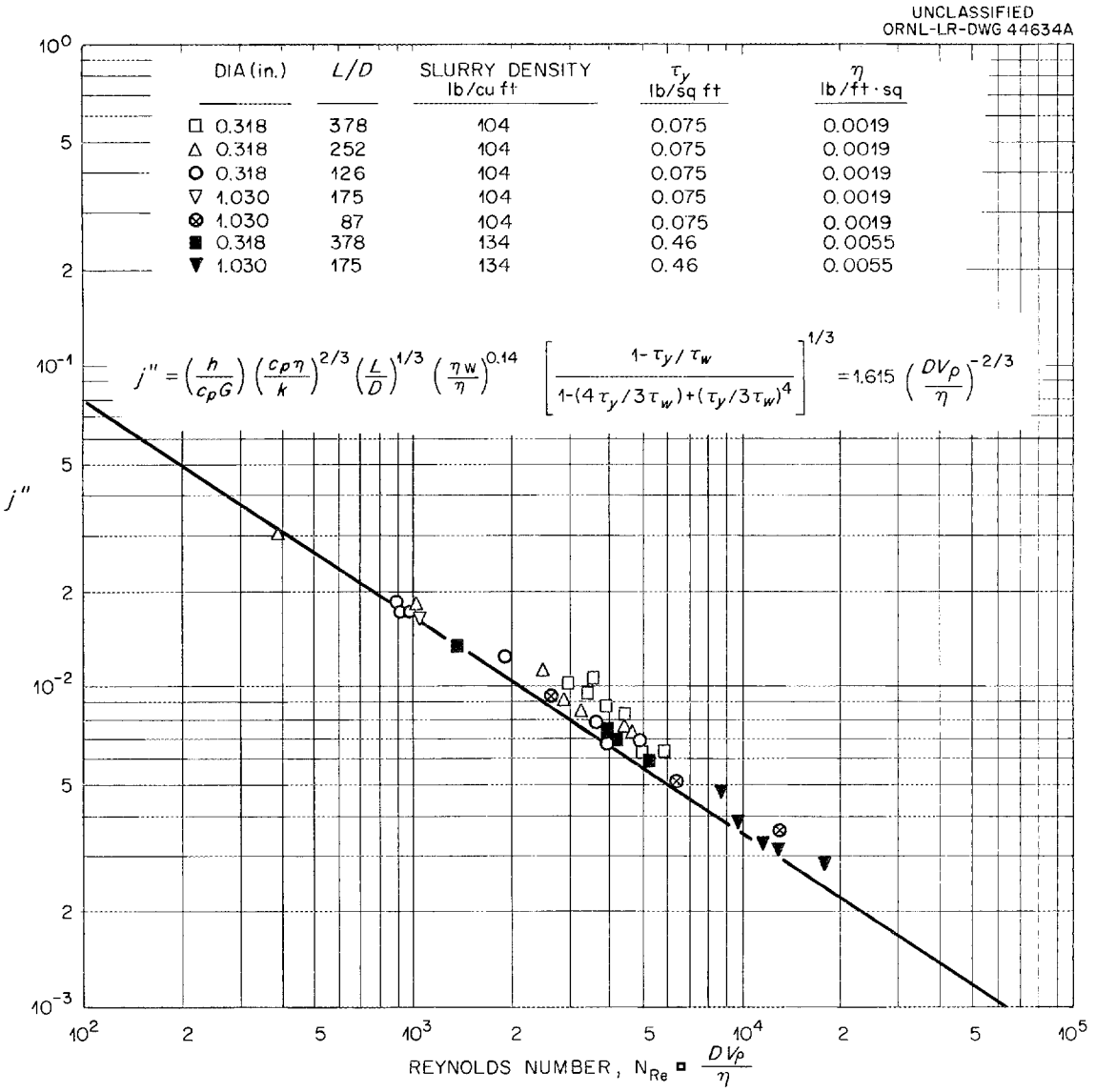

Fig. 14.2. Laminar Heat-Transfer Characteristics of ThO_2 Slurries Compared with Theoretical Equation of Hirai.

14.3 THORIA CAKING STUDIES

Investigation of the factors involved in cake formation during ThO_2 slurry circulation was continued with slurries composed of particles more resistant to degradation than the 800°C-calcined ThO_2 of the earlier studies. The two slurries used were (1) ThO_2 calcined at 1600°C and (2) ThO_2 - 8% UO_2 calcined at 1050°C. Spiewak et al.[5] have reported that the circulation of the latter composition resulted in deposition of a cake several microns thick on the cooled nickel-plated surface of a heat-transfer disk in the 200-gpm loop.

ThO_2 - 8% UO_2 was circulated in the 30-gpm loop to determine film or cake formation as a function of the slurry velocity and of the confining-metal surface. Stainless steel, copper, and nickel surfaces were included in each of the velocity sections of the multidiameter sample barrel (MDSB); nominal velocities in the sections were 5, 10, and 20 fps. Deposits in the various regions of the MDSB after 114 hr of circulation at 275°C with a slurry containing approximately 450 g of Th per kg H_2O are shown in Fig. 14.3. On 60% of the stainless steel surface in the 10-fps section and on nearly all of the nickel-plated surface in the 20-fps section, the ThO_2-UO_2 deposits were approximately 1.3 mils thick. Thinner, small-area deposits were observed on the copper surfaces of all three sections. A second circulation test with the same mixed-oxide batch exhibited similar behavior, although the deposition pattern was somewhat shifted. In contrast with the data for the 800°C-calcined ThO_2, Waring Blendor treatment of the mixed-oxide batch before circulation did not appreciably alter the deposition pattern.[6] An additional 200 hr of circulation in the cleaned MDSB resulted in no further deposits except for a very thin film on the nickel in the 5-fps section. There were no deposits in the pump.

Circulation of 1600°C-calcined ThO_2 for 100 hr yielded a thin thoria deposit on the stainless steel and copper (estimated 0.5-mil thickness) in the 10-fps section. No deposits were seen on the nickel in the intermediate-velocity section or on any surface in the 5- or 20-fps sections. After 300 hr of circulation, the entire 20-fps section (all nickel and copper plating had been eroded) and about 50% of the 10-fps section (without surface preference) were covered with a very thin oxide film. The thickness of this film was estimated to be between 0.1 and 0.3 mil. The film did not wash away in a stream of water but was easily removed by wiping with a sponge.

Examination of a small (1 in. long) water-cooled section in the external 1-in. piping of the loop (13 fps velocity) showed no detectable effect of cooling on oxide deposition.

The deposition of films from slurries composed of particles more resistant to degradation than 800°C-calcined ThO_2 seems to follow the caking behavior of 800°C-calcined thoria in that (1) deposits form during initial circulation[7] (presumably because fines generated by attrition of irregular-shaped particles are then most plentiful) and (2) the particle size of the redispersed films is smaller than that of the circulating slurry. It is probable that the film-forming mechanism for these oxides is essentially the same as that proposed for 800°C-calcined ThO_2; namely, the fine particles are pushed over each other by the fluid shear forces into positions of minimum energy where they are held together by van der Walls' forces.[8] Films from the higher fired oxides have usually been softer, presumably reflecting the reduced number of very small particles generated.

UNCLASSIFIED
PHOTO 35217

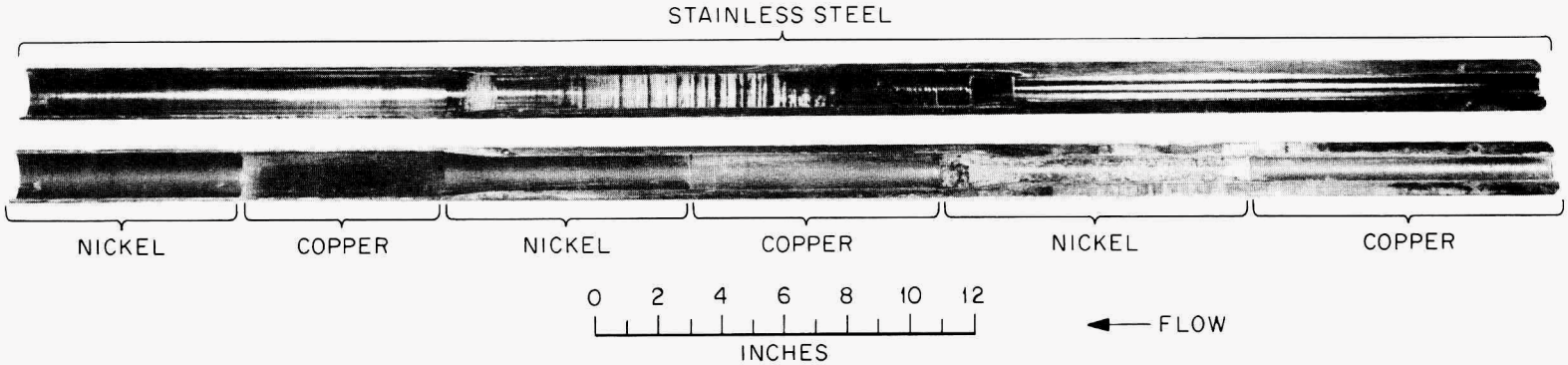

Fig. 14.3. Oxide Deposition in the Multidiameter Sample Barrel After 114 hr of Circulation of ThO_2–8% UO_2.

REFERENCES

1. C. C. Haws, Chemical Technology Division, Units Operations Section Monthly Progress Report, September 1959, ORNL CF-59-9-69, p 24-26.

2. H. W. Hoffman et al., HRP Prog. Rep. Oct. 31, 1959, ORNL-2879, p 159.

3. R. B. Korsmeyer et al., HRP Quar. Prog. Rep. Jan. 31, 1958, ORNL-2493, p 44-45.

4. E. Hirai, Chem. Eng. (Japan) 21, 17-25 (1957); see also AIChE Journal 5, 130-133 (1959).

5. I. Spiewak et al., HRP Prog. Rep. Oct. 31, 1959, ORNL-2879, p 65.

6. P. R. Kasten et al., HRP Quar. Prog. Rep. Oct. 31, 1958, ORNL-2654, p 74.

7. C. S. Morgan, Status Report on ThO_2 Caking Studies, ORNL CF-57-9-102 (Sept. 26, 1957).

8. R. N. Lyon, The Choice in Thorium Oxide Slurries for the Prevention of Caking in Circulating Systems, ORNL CF-57-4-77 (April 22, 1957).

15. SLURRY IRRADIATION STUDIES

J. P. McBride N. A. Krohn

15.1 SLURRY IRRADIATIONS IN THE LITR

A long-term irradiation of a settled slurry of thoria spheres containing 0.5% uranium was begun. The spheres were prepared by adsorbing uranium from ammonium uranyl carbonate solution on Houdry thoria spheres classified to >25μ. The spheres were then fired at 1000°C for 4 hr in air. The number of fine particles was decreased by several sedimentation classifications in water. The material was then dried and put into the irradiation test autoclave. After ~100 hr in-pile at 180°C the autoclave apparently went dry and was irradiated in this condition at 280°C for about three weeks. Then the isolation chamber at the top of the irradiation facility was opened, all accessible connections and valves were tightened, and water was added to the autoclave through the pressure-sensing capillary tube. The irradiation is continuing.

15.2 GAS SOLUBILITY IN AQUEOUS SLURRIES

The solubilities of hydrogen and oxygen gases in aqueous slurries containing 250, 500, and 1000 g of Th per kg of H_2O as 650°C-fired thorium oxide (surface area, 32 m^2/g) were measured by a method previously described.[1] The results indicated that no appreciable amount of hydrogen was adsorbed by the thoria, the observed solubilities of hydrogen for all concentrations of slurry being no greater than that corresponding to the amount soluble in the water phase alone. A relatively large amount of oxygen, however, was adsorbed by fresh thoria surfaces in an irreversible or very slowly reversible manner. Once the slurry had been pretreated with oxygen, the solubility of oxygen was higher than that in water. At 250°C with a slurry containing 1000 g of Th per kg of H_2O, approximately twice as much oxygen was taken up by the slurry as by pure water equal in volume to the aqueous phase of the slurry.

REFERENCE

1. H. F. Soard, Solubility of Oxygen, Hydrogen, and Iodine in Thorium Oxide Slurries, ORNL CF-59-2-97 (Feb. 2, 1959).

16. DEVELOPMENT OF GAS-RECOMBINATION CATALYSTS

J. P. McBride L. E. Morse

16.1 PALLADIUM AS A CATALYST

Reaction rates of stoichiometric H_2-O_2 mixtures were measured at 280°C in aqueous thorium oxide - 8% uranium oxide slurries (100 g of Th per kg of H_2O) containing palladium-on-ThO_2 catalyst and pressurized with O_2 (200 psi at 26°C). This work is a part of the general program to study the properties of this recently developed catalyst suspension[1] and is also in support of the REED LTTR in-pile slurry corrosion studies.[2]

With palladium concentrations of 60 and 120 ppm, based on thoria, the rates were equivalent to CPI's (catalyst performance index) of 0.4 and 1.2 w/ml at 280°C and a partial pressure of 100 psi H_2. This is a threefold increase in reaction rate where the catalyst concentration was doubled at constant slurry concentration. In previous work[1] with a similar catalyst suspension and the same conditions except that the slurry was pure ThO_2 (100 g of Th per kg of H_2O) and the palladium concentration was 275 ppm, the rate was equivalent to a CPI of 100 w/ml at 280°C and a partial pressure of 100 psi H_2.

In the proposed in-pile slurry loop experiment, which will be carried out at a concentration of 1000 g of Th per liter, the minimum acceptable reaction rate at 280°C would be equivalent to a CPI of 12.5 w/ml at a partial pressure of 100 psi D_2. This rate would be almost attained with a palladium concentration of 120 ppm, assuming that the rate varies linearly with slurry concentration.

Studies were also made of the effect of oxygen overpressure on the reaction rate of the H_2-O_2 mixtures in slurries containing 120 ppm of palladium. There was no appreciable change in the 280°C reaction rate when the O_2 overpressure (measured at 26°C) was decreased from 200 to 100 psi. However, in the absence of any O_2 overpressure, the reaction rate increased by a factor of almost 10, to a rate equivalent to 10.8 w/ml at 280°C and a partial pressure of 100 psi H_2. The increased rate was preceded by an induction period of about 5 min.

The thorium oxide - 8% uranium oxide used in these experiments was prepared by the adsorption method. After calcination at 1000°C for 8 hr the composition was 81% Th and 7% U; the surface area was 2.5 m^2/g.

16.2 DEVELOPMENT OF CONTINUOUS GAS PRODUCTION-RECOMBINATION APPARATUS

Minor changes in the recombiner vessel were made to improve the operation of the continuous gas production-recombination apparatus.[1] The thermocouple well was removed from the top plug and inserted through the bottom of the vessel. The 20-mil-ID, 65-mil-OD gas delivery tube which passes through the top plug and baffle plate and extends into the slurry mixture is now the only tube that extends through the steam draft tube. This should decrease the steam velocity and help to control entrainment of solids, which is a major operational problem. It should also eliminate the throttling of gas transfer from the generator caused by steam diffusing from the recombiner vessel and condensing in the gas transfer line.

A four-plate stainless steel baffle was fabricated to decrease the steam velocity in the draft tube still further if it should be found necessary. Insulation of the top plug of the recombiner vessel against heat loss may also be used to control boilup of water to the condenser section.

REFERENCES

1. J. P. McBride and L. E. Morse, HRP Prog. Rep. Oct. 31, 1959, ORNL-2879, p 174-179.

2. E. L. Compere, H. C. Savage, et al., HRP Prog. Rep. Oct. 31, 1959, ORNL-2879, p 207-209.

17. SLURRY CORROSION

E. L. Compere H. C. Savage

J. M. Baker
S. E. Bolt
V. A. DeCarlo
R. B. Gallaher
W. J. Leonard
R. A. Lorenz
R. E. McDonald
A. R. Olsen
S. A. Reed
L. Rice
A. J. Shor
L. F. Woo

17.1 OUT-OF-PILE TESTS

17.1.1 Introduction

The development of flame calcination of thoria particles by the Chemical Technology Division has led to interest in the circulation properties of such materials. These more rounded shapes might lead to more durable particles, with lowered aggressiveness and improved rheological properties. A number of small-scale preparations were tested in toroids, and good results led to the preparation of sufficient material for the 100A-pump-loop test discussed below.

Circulation tests on a thoria-urania slurry representative of a high-power-density blanket material for a proposed experimental reactor gave high corrosion rates. A comparison test on pure thoria is also reported.

The hydriding of Zircaloy-2 in circulating-slurry service is of considerable interest. Examination of a Zircaloy-2 pump impeller after substantial slurry service under both hydrogen and oxygen atmospheres is reported.

17.1.2 Evaluation Tests with Slurries of Flame-Calcined Oxides of Thorium, Thorium-Uranium, and Thorium-Uranium-Aluminum

During the past year a test program was conducted in cooperation with the Chemical Technology Division to evaluate experimental thoria preparations made by the flame-calcination method.[1] Samples of over 20 preparations were examined in a series of toroid tests to determine the relative corrosion-erosion properties and integrity of the oxides during circulation as aqueous slurries at 280°C. The program culminated in a 100A-loop test of 240 hr duration which was made at 250°C with a slurry of a ternary oxide containing 3.2% U/Th and 1.6% Al/Th.

17.1.3 Toroid Screening Tests

Materials produced by the experimental flame-calcination method for toroid tests were divided into three general categories: (1) those of pure ThO_2, (2) binary oxides containing nominally 6% U/Th, and (3) ternary oxides containing

nominally 6% U/Th and 2% Al/Th. The estimated calcination temperature of the preparations was 1500°C. The materials were spherical or semispherical due to fire-polishing. The apparent mean Stokes' diameters of the preparations ranged from 1.1 to 2.2 μ.

All preparations were circulated as aqueous (D_2O) slurries in 300-hr toroid tests at 280°C at a flow velocity of 26 fps. Each preparation was circulated in an oxygen atmosphere. Preparations containing uranium were also tested in an atmosphere of deuterium, when a sufficient quantity of sample was available. A slurry concentration of 500 g of Th per kg of D_2O was used in the majority of the tests, although because of a limited amount of material, four of the preparations were tested at 200 g of Th per kg of D_2O. Corrosion-pin specimens of type 347 stainless steel, Inconel, titanium-75A, and Zircaloy-2 were exposed in each test.

The attack data were examined by use of ratio analysis[2] (Table 17.1), which permitted separation of the effects of major variables into multiplicative factors. The reference condition was taken as the average for the Th-U oxide preparations. All attack data were normalized to 500 g of Th per kg of D_2O. The relative attack of the alloys under each atmosphere was normal and in agreement with previous experience using ThO_2 prepared by other methods.

In oxygenated tests of flame-calcined materials, slurries of the Th-U oxide preparations were generally most aggressive. Stainless steel was attacked at approximately the same rate by slurries of pure ThO_2 and Th-U-Al oxides; however, attack of Zircaloy-2 was moderately higher in tests with the ternary oxides.

In tests with deuterium atmospheres, attack by slurries of the Th-U-Al oxide was an average factor of 2 greater than with slurries of the Th-U oxide preparations. No tests with pure thoria were made with a reducing atmosphere.

No correlation between attack rate and particle size of the preparations was manifested in the test series. None of the preparations was detectably degraded.

17.1.4 Pump-Loop Test with Slurry of Flame-Calcined Th-U-Al Oxide

Subsequent to the series of toroid tests of flame-calcined oxides, one 100A-loop test, CS-51, was conducted to evaluate further a slurry of Th-U-Al oxide. The batch, 76-82RD, contained 3.2% U-Th and 1.6% Al/Th and had a mean particle size of 1.3 μ after classification.

The test loop was charged to a slurry concentration of 452 g of Th per kg of H_2O and operated at 250°C, using an oxygen atmosphere, for a period of 239.8 hr. Pertinent operating conditions and results of the test are shown in Table 17.2.

During the first 166 hr of the test, at a pipeline flow velocity of 6.5 fps, the circulating concentration was in excellent agreement with the charged concentration. However, over the following 24-hr period ~37% (~3 kg) of the solids was lost from circulation. No further loss occurred. In the final 1.4 hr of the test, the pipeline velocity was increased to 9 fps, but no change in circulating concentration was noted.

Table 17.1. Effect of Variables in Attack by Slurries of Flame-Calcined Mixed Oxides, Expressed as Multiplicative Factors Obtained by Ratio Analysis

Test Conditions: 280°C, 500 g of Th per kg of D_2O, 26 fps

Atmosphere:	Oxygen					Deuterium				
Metal:	347 SS	Toroid	Ti-75A	Inconel	Zircaloy-2	347 SS	Toroid	Ti-75A	Inconel	Zircaloy-2
Reference Rate, mpy:*	11	2.8	1.3	51	0.3	12.8	3.3	3.3	2.2	0.6
	Average Effect of Oxide Expressed as Ratio to Reference Rate									
Thorium oxide	0.17	0.29	0.58		1.02					
Th-U oxide	1.0	1.0	1.0	1.0	1.0	1.0	1.0	1.0	1.0	1.0
Th-Al-U oxide	0.2	0.22	0.96	0.21	1.55	2.1	1.6	4.5	1.7	1.35

* Reference condition: average Th-U oxide, given atmosphere.

Table 17.2. Summary of 100A-Loop Tests with Slurries of Thoria, Thoria-Urania, and Th-U-Al Oxides

	Run CS-51 (Th-U-Al oxides, flame calcined)		Run ES-14 (Th-U oxides)		Run ES-15 (Pure thoria)	
Operating temperature, °C	250		250		250	
Slurry circulating hours	239.8		340.5		339.4	
Atmosphere (std cc/liter slurry)	O_2 (394)		O_2 (662)		O_2 (778)	
Range of slurry pH	6.1-8.2		4.9-6.9		4.6-6.1	
Concentrations, g Th/kg D_2O						
Avg. inventory (max.)	453 (457)*		628 (764)		622 (746)	
Avg. circulating (max.-min.)	410 (490-288)*		729 (884-476)		669 (810-454)	
Batch number	76-82RD		MO-67		DT-46	
	Pre	Post	Pre	Post	Pre	Post
Surface area, m^2/g (N_2)	1.3	1.4	2.1	3.7	0.8	0.8
Crystallite size, Å	>2500	1900	1200	800	>2500	>2500
Mean particle diameter, μ	1.3	1.2	2.5	1.8	2.4	2.0
σ	1.67	1.74	1.31	1.39	1.35	1.37
g U/kg Th	32	31	28	29		
$U^{+4}/\Sigma U$, % (±4%)	48	32	44	24		
g Al/kg Th	16	16				
Attack rates, mpy						
Loop piping (SS), 6-7 fps, initial, average	1.7, 0.2		24, 13		29, 3.0	
Impeller (Zircaloy-2)	1.2		50		2.5	
Coupon specimens:						
Velocities, fps	20	40	19	38	19	38
329 SS	0.4	1.6	0.6	9.0	0.2	2.6
347 SS	0.1	0.9	1.6	18.	0.2	4.6
PH 15-7 Mo	1.1	1.1				
17-7 PH	0.1	0.7				
USS Corex (18 Cr, 24 Ni)	0.1	1.3	0.8	14.	0.2	5.6
Croloy 16/1			0.5	7.8	0.1	1.0
Croloy 9M			0.5	8.2	0.1	0.2
Croloy 5	1.1	1.4	2.6	6.8	0.8	0.8
Croloy 2	2.0	2.0	6.4	7.8	1.1	1.1
ASTM A285	5.9	3.6	12.	11.	3.1	2.5
Armco Iron			11.	8.8	1.7	1.6
Incoloy			0.4	12.		
Inconel	2.8	4.7	7.6	25.	5.5	32.
INOR-8	5.0	11.	13.	25.	1.8	18.
Pt-5% Ir	WG	0.8	0.2	5.8	<0.1	1.2
Ti-B120-VCA (13V, 11 Cr, 3 Al)	WG	0.7			0.2	0.8
Ti-MST Grade III	0.1	0.7	0.5	5.1	0.1	0.4
Zircaloy-2	WG	0.2	WG	1.7	WG	<0.1

* Grams of Th per kg of H_2O.

After hydrocloning solids from the loop at 250°C, the system was cooled to room temperature and rinsed once with water. When the system was opened for inspection, no deposits were found.

The U/Th and Al/Th ratios remained constant at 0.032 and 0.016, respectively, during the run. A maximum of 3 ppm of Al and 7 ppm of U was detected in the slurry supernatant liquid. The $U^{+4}/\Sigma U$ ratio decreased from 0.48 to 0.32 ($\pm$ 0.04) during the first 22.3 hr and then remained constant. No appreciable changes occurred in the mean particle size, surface area, or crystallite size of the mixed oxide. A marked increase (a factor of ~10) in the room-temperature settling rate occurred between the 70-hr and 116-hr samples. The pH of the slurry decreased from 8.2 to 6.4 during the first 70-hr period and remained essentially constant thereafter.

The pre- and the postrun yield stress of the material at a slurry density of 2.26 (1350 g of Th per kg of H_2O) were computed from pseudo-shear diagram data[3] to be 0.027 and 0.072 lb/ft^2, respectively. These values are substantially below the levels for thorias produced by furnace-calcination of thorium oxalate.

System attack rates were quite low. Incremental rates, including the attack on the stainless steel pump scroll and thermal barrier, were 1.7 mpy for the first 2 hr, 0.3 mpy during the next 68 hr of circulation, and constant thereafter. The attack rate on the stainless steel loop piping was 0.2 mpy. The cast Zircaloy-2 impeller lost 0.5 g, which was equivalent to an attack rate of 1.2 mpy.

Coupon-specimen corrosion rates at 20 and 40 fps were quite low, generally agreeing (although lower in proportion to slurry concentration) with results from run ES-15 (Table 17.2), which was made with a regular-production pure thoria.

17.1.5 Loop Tests Comparing Attack by Slurries of Th-U Oxide and Pure Thoria

Recent interest in a two-region breeder reactor which might contain 2 to 4% U/Th in a circulating slurry blanket[4] prompted one 100A-loop test (ES-14) which was made to evaluate the general properties and corrosion-erosion characteristics of such a material. Slurry for the test was prepared from experimental batch MO-67 prepared by the Chemical Technology Division by adsorption of uranium (2.8% U/Th) on 650°C-fired thoria[5] with subsequent calcination at 1075°C and classification to a mean particle size of 2.5 μ.

Slurry was circulated for the initial 167-hr period of the test at a charge concentration of 498 g of Th per kg of D_2O. Additional material was then injected into the loop, which increased the concentration to 757 g of Th per kg of D_2O.

The indicated attack rate of the stainless steel system during the first period of operation was 12 mpy. After increasing the slurry concentration, incremental system attack rates fluctuated between 10 and 46 mpy. Therefore the test was terminated after 173 hr of circulation at the higher concentration. The attack rate of the stainless steel components of the system for the total period of circulation (340.5 hr) was 13 mpy.

When the loop was disassembled, it was found that the attack had occurred principally in the circulating pump and was localized in areas of greatest

turbulence in the pump impeller hub and thermal barrier. Based on chemical analyses, the attack rate on the titanium pump scroll was 37 mpy; from weight-loss data, the Zircaloy-2 impeller was attacked at a rate of 50 mpy.

During the run, the U/Th ratio remained constant at 28 g of U per kg of Th. The $U^{+4}/\Sigma U$ ratio decreased from 0.44 to 0.26 ($\pm$0.04) in the first 8 hr of circulation and then remained essentially constant. Less than 3 ppm of uranium was found in the supernatant liquid. The pH of the slurry decreased from 6.9 to 4.9, and the pH of the supernatant liquid fluctuated without trend between 4.3 and 6.4.

The Th-U oxide particles degraded from a mean size of 2.5 to 1.8 μ, and a slight decrease in the crystallite size from 1200 to 800 Å was detected.

A comparison test, run ES-15, was made with a slurry of pure thoria (regular-production) at conditions approximating as closely as possible those of run ES-14. The test consisted of 168 hr of circulation at a slurry concentration of 541 g of Th per kg of D_2O followed by 171 hr of circulation at a concentration of 797 g of Th per kg of D_2O. Pertinent data for both tests are shown in Table 17.2.

During the first portion of the test, the mean 168-hr attack rate of the stainless steel components of the system was 3.3 mpy. At the higher concentration the mean 171-hr rate was 3.8 mpy. The over-all attack rate of the piping during the total period of circulation (339.4 hr) was 3.0 mpy, which was a factor of about 4 lower than in run ES-14 with the Th-U oxide slurry. Attack on the titanium scroll was <3 mpy. The Zircaloy-2 impeller lost 1.5 g, which was equivalent to 2.5 mpy. As shown in Table 17.2, lower rates were also noted for the corrosion specimens exposed in run ES-15.

A further comparison of slurry aggressiveness in terms of specimen data from the two tests is presented in Table 17.3, which shows for various metals the relative aggressiveness of the two preparations at 20 and 40 fps in terms of the ratio of attack rates (after adjustment by proportion to a common slurry concentration). At 20 fps the mean (geometric) ratio was 3.7 and at 40 fps, 4.9. Thus a consistent indication of increased aggressiveness for the thoria-urania preparation was obtained.

The results were consistent with previous experience which has shown that higher attack rates result with slurries whose particles are degraded during circulation. The poorer integrity of the mixed oxide was possibly due to the material being calcined at too low a temperature.[6,7,8]

17.1.6 Hydriding of Zirconium-Base Alloys

Discussions were presented previously concerning variables associated with the hydriding of zirconium-base alloys[9,10] observed in tests using small, pin-type corrosion specimens exposed to circulating slurries in toroids. It was of interest to examine other zirconium-base materials which had been exposed to slurries at different operating and flow conditions. Therefore a section from a cast Zircaloy-2 impeller which had been in routine use in one of the 100A slurry corrosion-test loops was examined by the Metallurgy Division for evidence of hydriding.[11]

The service history of the impeller is shown in Table 17.4.

Table 17.3. Relative Attack by Oxygenated Slurries of 1075°C-Calcined Th-U Oxide and 1600°C-Calcined Thoria at 250°C

Rates expressed as ratio of attack by slurry of Th-2.8% U oxide to attack by ThO_2 slurry (after proportionate adjustment to equal slurry concentration).

Material	20 fps	40 fps
329 SS	3.5	3.0
347 SS	9.0	3.1
USS Corex SS	4.5	2.0
Croloy 16/1	6.0	6.2
Croloy 9M	6.0	55
Croloy 5	3.0	8.3
Croloy 2	4.9	6.2
ASTM-A285 steel	3.4	3.9
Armco Iron	5.5	4.6
Inconel	1.1	0.64
Inor-8	5.8	0.96
Pt-5% Ir	2.0	4.6
Ti-MST III	6.0	11
Zircaloy-2	1.0	23
Mean, geometric	3.7	4.9

Table 17.4. Service History of Cast Zircaloy-2 Impeller from 100A Slurry Corrosion-Test Loop

Temperature (°C)	Media	Test Atmosphere	Time (hr)
280	H_2O	Oxygen	336
280	ThO_2 slurry	Oxygen	1452
200	H_2O	Oxygen	151
200	H_2O	Hydrogen	169
200	ThO_2, Th-U oxide slurry	Oxygen	901
200	ThO_2, Th-U oxide slurry	Hydrogen	981
		Total hours	3990

The vendor's analysis showed the composition of the cast impeller to be: 1.4% Sn, 0.005% C, 0.004% nitrogen, balance zirconium.

The section for metallographic examination was cut from the outer surface of the suction port of the impeller (see Fig. 17.1). Scored groove in the surface were a result of normal wear from rubbing adjacent sealing rings in the pump scroll.

Hydride needles were found throughout the specimen but were most concentrated near the scored circumferential surface. About 10% by volume of an inner dendritic constituent containing some hydride was noted. From metallographic consideration the hydrogen in the circumferential region was estimated as about 350 - 400 ppm. A gradient in hydride concentration was observed over about 40 mils toward the axis. Interior portions were fairly constant at an estimated 1 - 3 volume percent inner dendritic constituent which also contained zirconium hydride. The average hydrogen content of this region was estimated metallographically as 150 ppm, which is greater than that normally expected in

Fig. 17.1. Cast Zircaloy-2 Pump Impeller Showing Location from Which a Section Was Removed for Examination for Evidence of Hydriding.

Zircaloy-2. The average hydrogen content, over the 115 mil thick specimen, was 300 ppm by chemical analysis. No information is available as to the original hydrogen content of the Zircaloy-2.

After repair, the impeller will be used in subsequent loop runs in hydrogen atmospheres to determine the effect on hydride penetration.

17.2 IN-PILE AUTOCLAVE SLURRY CORROSION STUDIES

17.2.1 Introduction

The first type 347 stainless steel autoclave containing thoria-urania slurry at 280°C was irradiated, with fission-power densities of ~7.2 w/ml being maintained. Evidence of slurry deposition on the internal thermowell was developed during the 1118 in-pile hours of the experiment. Measurements of the recombination activity of the palladium catalyst were made, and corrosion rates during the course of the run were estimated from oxygen consumption. Postirradiation examination of the autoclave contents was made.

An unusual attack on corrosion specimens occurred during the out-of-pile pretreatment periods of two autoclave slurry experiments, which were consequently terminated. The investigation of the attack is reported.

17.2.2 Irradiation of Stainless Steel Autoclave Containing Thoria-Urania Slurry

Irradiation of the first type 347 stainless steel autoclave containing thoria-urania at 280°C in the HB-6 facility of the LITR was completed. Experiment L6S-151S contained thoria-urania slurry at a concentration of 1100 g of Th per kg of D_2O with 4.8 wt % enriched uranium, based on thorium, and 0.017 m Pd added as a recombination catalyst. The autoclave, charged with an overpressure of oxygen, was operated out-of-pile for 257 hr and in-pile for 1118 hr at 280°C. With the exception of brief periods to perform recombination experiments, the autoclave was operated at all times in the fully inserted position with the LITR at 3 Mw reactor power. The maximum fission-power density achieved at 280°C was 7.2 w/ml with the autoclave in the fully inserted position of the HB-6 facility assuming a neutron flux of 5.6×10^{12}, as obtained from neutron activation of Zircaloy-2 specimens in the previous experiment, L6Z-129S.[12] Pressure measurements at 25°C were made during periodic reactor shutdowns in order to follow the consumption of oxygen and thereby the generalized corrosion of the autoclave. Irradiation of the autoclave in the retracted position began after 264 hr at temperature.

Abnormal Temperature Behavior.--After 7 hr rocking at temperature under irradiation in the retracted position, the experiment was inserted to the position of maximum neutron flux. Because temperature control of the autoclave at 280°C was based on a thermocouple in a thermowell in the center of the squirrel-cage pin-specimen rack, the added radiation heating changed the temperature distribution, and some cooling of the autoclave walls was required. The exterior autoclave-wall thermocouple reading thereby fell to 271°C.

As shown in Fig. 17.2, over the subsequent period of 208 hr the temperature of the exterior autoclave wall fell steadily, accompanied by a steady drop in autoclave pressure. During this time, the control thermocouple was maintained at 280°C. At temperature-hour 480, a total decrease in pressure of 520 psi had been observed. It was concluded that the control-thermocouple temperature was

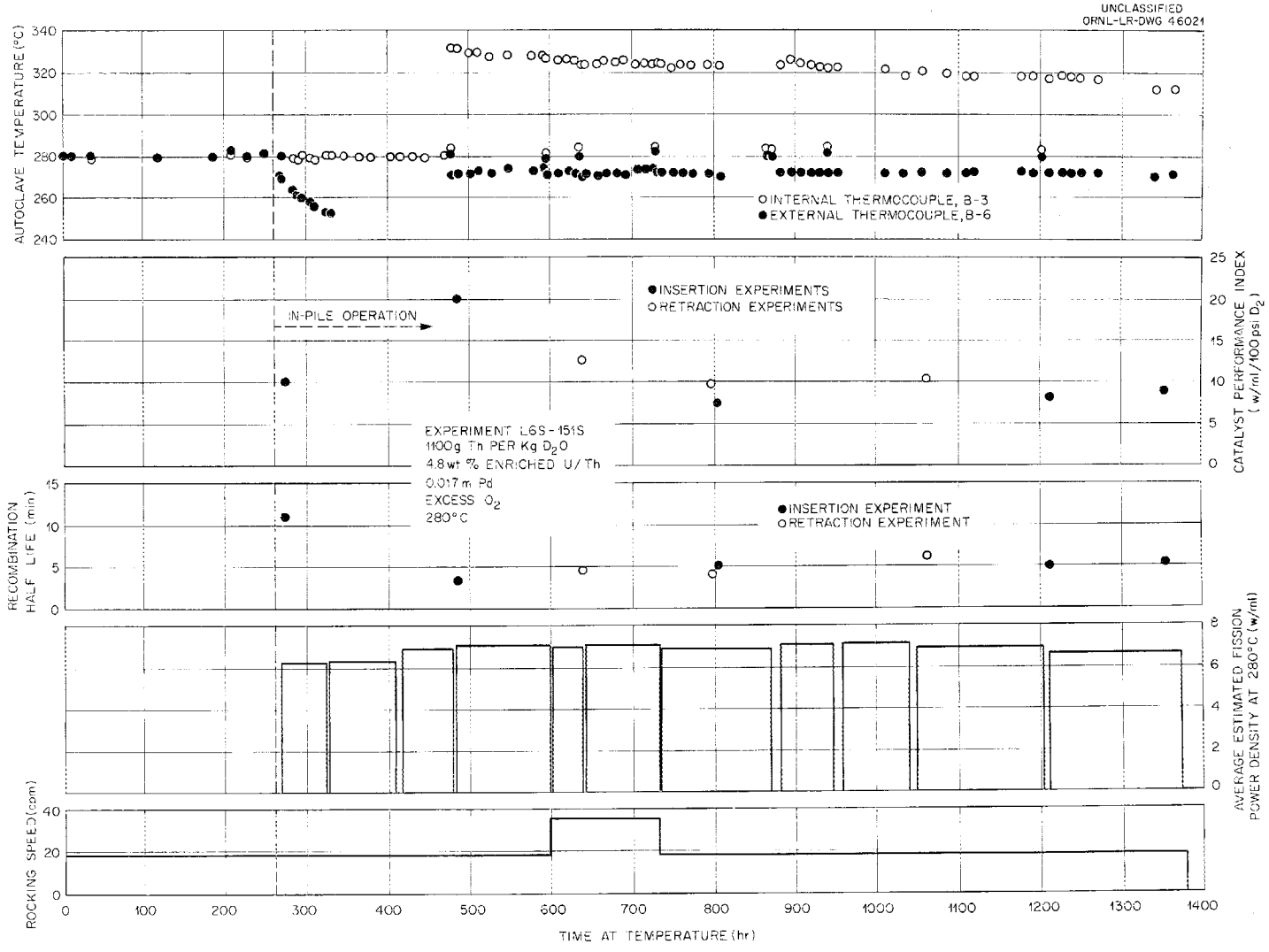

Fig. 17.2. Operating History of Experiment L6S-151S.

substantially higher under radiation than the true slurry temperature. During a reactor shutdown, this effect was not observed. In order to maintain the slurry temperature at 280°C, control was shifted to the exterior autoclave-wall thermocouple which was set at 271°C. Pressure rose to a level near that observed originally, and the thermocouples in the interior thermowell registered a rise to 332°C. Throughout the remainder of the experiment, which terminated at temperature-hour 1375, the temperature slowly decreased to 312°C. Increasing the rocking frequency from 19 to 36 cpm did not affect the temperature differential.

At the termination of the experiment, the relationship between the pressure at 280°C and that at 25°C indicated a normal volume of liquid (slurry) in the autoclave.

17.2.3 Postirradiation Examination

When the autoclave was dismantled 52 days later, slurry that was apparently moist was observed on the pin rack; but no liquid could be poured from the autoclave. Some particles (small lumps) of solids were later dislodged from the interior of the autoclave, which then appeared to be covered with an ordinary corrosion film. It is possible that water was lost through the crimped capillary during the 52-day cooling period.

Most of the slurry accumulation remained on the pin-rack assembly, even though the assembly was rinsed by immersion in distilled water several times. Figure 17.3 shows the pin-rack assembly after rinsing. The accumulation dried

Fig. 17.3. Middle Section of Pin Rack After Irradiation of Experiment L6S-151S.

under the heat of photographic lamps, developing into rosin-appearing material which cracked and popped off the assembly. The particles were not crushed when picked up with remotely manipulated tongs.

It should be noted here that the same thoria-urania preparation was used in a number of previous in-pile experiments (L6Z-126S, -127S, and -129S) without indication of similar accumulations.

Specimen-corrosion results are discussed in Sec. 17.2.6. Postrun physical and chemical characterization of the slurry has not been completed.

17.2.4 Catalyst Activity and Gas Production

Recombination experiments, in which the autoclave was inserted into or retracted from the high-flux region of the HB-6 beam hole, with observation of the ensuing pressure changes, were performed to measure the activity of the 0.017 *m* Pd catalyst and the pressure of equilibrium radiolytic gas. The results of these experiments are presented in Fig. 17.2. The equilibrium radiolytic gas is expressed in terms of the catalyst performance index, which is related to the catalyst activity and gas production rate by the following expression:

$$\text{Catalyst performance index} = \frac{(\text{power density, w/ml})}{(P_{equil}\ D_2/100)} =$$

$$= \frac{(\text{catalyst activity, moles } D_2\text{/liter-hr at 100 psi } D_2)}{0.38\ G_{D_2}} .$$

Upon the first insertion experiment, the generation of 107 psi radiolytic gas, (72 psi D_2), was observed. Based on a fission-power density of 7.2 w/ml at 280°C for the fully inserted position of the autoclave, a catalyst performance index of 10 w/ml at 100 psi D_2 was obtained. During the period of increasing temperature differential between internal- and external-autoclave thermocouples, no reliable measures of catalyst activity were obtained. After temperature control was based on external autoclave-wall temperature, a number of measurements were obtained, ranging between 7.5 and 20 w/ml at 100 psi D_2, as shown in Fig. 17.2.

17.2.5 Correlation of Time and Radiation Effects on the Corrosion of Type 347 Stainless Steel

Corrosion in experiment L6S-151S was followed in the usual manner[13,14] by the consumption of oxygen as measured at 25°C during periodic reactor shutdowns. The incremental corrosion rate and the average fission-power density for each irradiation period are presented in Fig. 17.4. When the autoclave was first heated out-of-pile to 280°C, a rapid corrosion rate was observed which decreased substantially as the autoclave was maintained at 280°C in the 257-hr out-of-pile period. Initial exposure of the autoclave to reactor irradiation resulted in a small increase in the corrosion rate. The fission-power-density level was maintained, and the corrosion rate decreased steadily to less than 0.1 mpy at the end of the experiment.

A correlation of the effect of time and radiation on generalized corrosion in the experiment is shown in Fig. 17.4. The data were fitted by the following equation, obtained by successive approximations:

$$\text{Instantaneous corrosion rate, mpy} = \frac{31 + 13 \times (\text{power density, w/ml})}{\text{hr at temperature}}$$

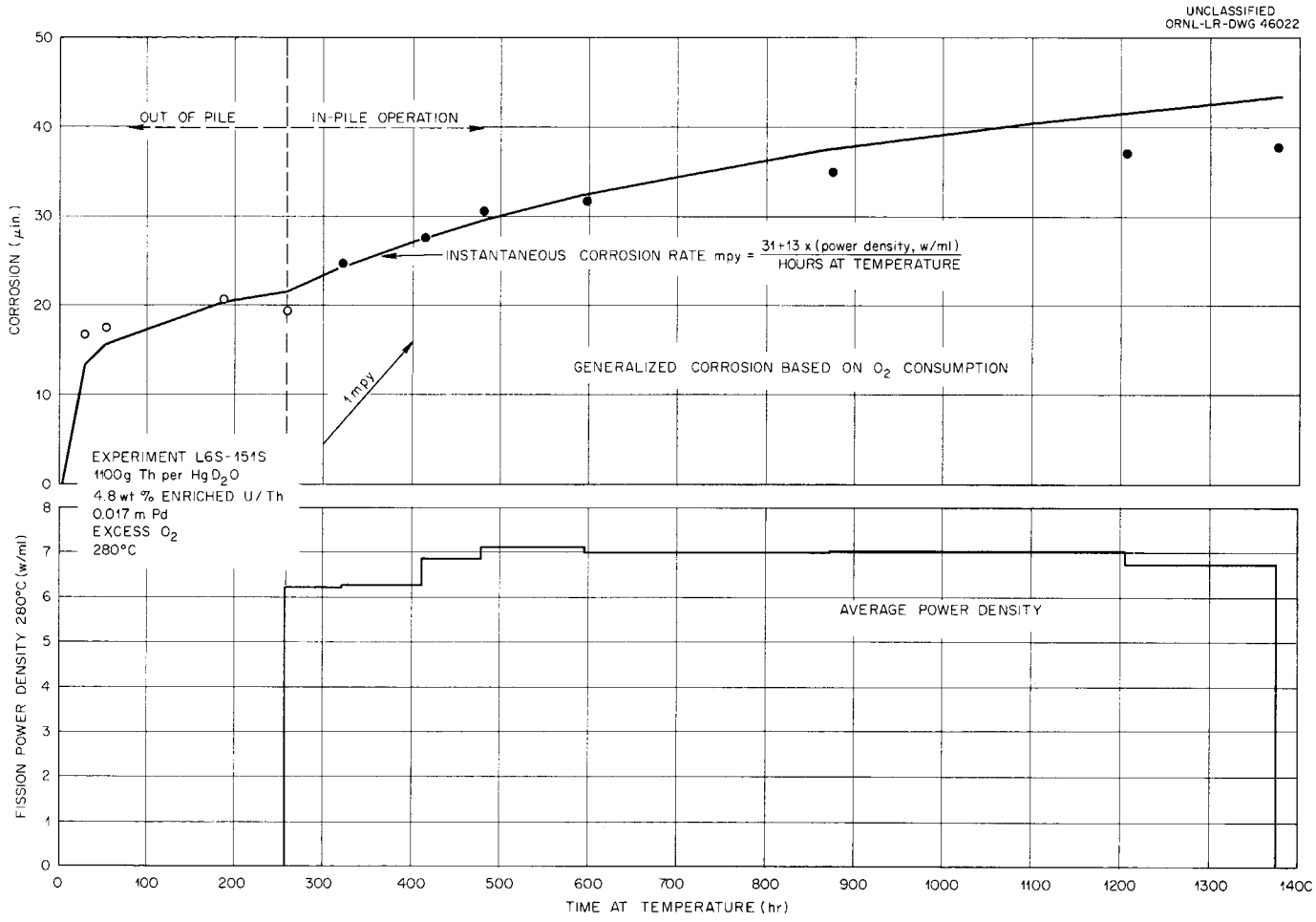

Fig. 17.4. Generalized Corrosion and Average Fission-Power Density in Experiment L6S-151S.

It will be noted that both the corrosion rate and the effect of power density on the corrosion rate are not great. Based on 1375 hr at 280°C, the over-all corrosion rate was 0.24 mpy.

17.2.6 Pin-Specimen Corrosion in Experiment L6S-151S

A comparison of the autoclave generalized corrosion as measured by oxygen comsumption in experiment L6S-151S and the corrosion of the pin specimens as measured by weight changes is shown in Table 17.5. The corrosion of the type 347 stainless steel pin specimens indicated fairly good agreement with the oxygen data. The corrosion of the Zircaloy-2 pin specimen appeared to be higher than that of the type 347 stainless steel specimen, while the corrosion of the titanium-75A specimen appeared to be lower.

Table 17.5. Radiation Corrosion of Pin Specimens: Experiment L6S-151S

280°C, 1100 g of Th per kg of D_2O, 4.8 wt % U/Th, 0.017 *m* Pd, Excess O_2, Type 347 Stainless Steel Autoclave

Hours at temperature, preirradiation (257 hr out-of-pile)	264
Total hours at temperature	1375
Hours irradiated	1028
Effective fraction of full irradiation time, fully inserted flux	0.96
Assumed neutron flux,* (in the fully inserted position)	5.6×10^{12}
Maximum power density, w/ml at 280°C	7.2
Average power density while irradiated, w/ml at 280°C	6.9
Autoclave generalized corrosion rate, μin.	
Out-of-pile	19
Total	38
Pin-specimen corrosion,** μin.	
Type 347 stainless steel	35, 30
Zircaloy-2	76
Titanium-75A	13

* Flux as determined by neutron activation of the Zircaloy-2 pin specimen is not yet available; presently using value obtained from experiment L6Z-129S.

** Corrosion of type 347 stainless steel pin specimen based on weight loss; that of Zircaloy-2 and titanium-75A based on weight gain.

17.2.7 Out-of-Pile Corrosion in Autoclave Experiments

During preirradiation testing at 280°C, unusually high rates of oxygen consumption occurred in two Zircaloy-autoclave slurry experiments containing a new thoria - enriched urania (8.0 % U/Th) preparation and a new palladium catalyst preparation (in ThO_2 suspension). Experiment Y6Z-150S lost 1270 μmoles of oxygen in 260 hr; and experiment Y6Z-150SA, which continued 602 hr, lost 1570 μmoles. In each case the most rapid loss occurred during the first three days.

The autoclaves were subsequently opened for examination without having been irradiated. Severe corrosion of several pin specimens of Zircaloy-2 and type 347 stainless steel was found, but the titanium pins were not attacked. Metallography[15] indicated that the Zircaloy-2 suffered localized intergranular attack, in one case disintegrating one section of a pin. The stainless steel was attacked by a severe pitting characterized by overlapping craters.

Chemical analysis of the pins did not show abnormal compositions. Analysis of the thoria-urania and the D_2O did not detect significant amounts of F^-, Cl^-, or NO_3^-. In the original preparation of palladium catalyst the concentration of F^- was 30 ppm and NO_3^- was 184 ppm, but the material was diluted approximately 1:16 by the other materials used in the preparation of the autoclave slurry.

A third autoclave experiment, Y6Z-150SB, was loaded with the same thoria-urania preparation but with a new catalyst preparation which, after oxygen and hydrogen treatments at 450°C, contained 90 ppm F^- and 50 ppm NO_3^-. This preparation was diluted 1:27 in use. The experiment was terminated after 207 hr at 280°C due to mechanical breakage of the capillary tubing. No evidence of unusual corrosion was found. Therefore, Zircaloy-2 and stainless steel pin specimens from the same and similar batches of metal were then subjected to several small-scale static autoclave tests to learn the effects of the thoria-urania, palladium catalyst, D_2O, and added F^- on the attack.

Localized surface attack was observed on Zircaloy-2 pins in tests with added F^- up to 100 ppm, but no intergranular attack was detected. Ends of a type 347 stainless steel pin were corroded in a test with thoria-urania slurry duplicating the original conditions. Other than these cases, none nearly as severe as those observed in experiments Y6Z-150S and Y6Z-150SA, no noteworthy attack was found.

No definitive conclusion has been reached as to the cause of the original attack. Attack on both Zircaloy and stainless steel implied chemical attack by the slurry. Inasmuch as both slurry and catalyst preparations involved solids, it is possible that unknown impurities, concentrated in a few grains, were sufficient to contaminate a system as small as the 4 ml contained in the autoclaves.

17.3 IN-PILE SLURRY LOOP

17.3.1 Introduction

Test operation of a prototype 5-gpm in-pile slurry loop was continued during the quarter. Run 3, previously described,[16] was terminated after 945 hr of operation; run 4, still in progress, has accumulated more than 1500 hr of slurry circulating time to date. For both runs, the loop was charged with a D_2O slurry of thorium oxide from batch DT-18, containing ~1/2 wt % uranium; a loop mainstream temperature of 280°C was maintained during slurry circulation. System

overpressure was obtained by operating the loop pressurizer at 295°C. The pressurizer and pump bearing region were maintained essentially free of slurry by utilizing the thoria-free filtrate from a sintered-metal filter,[16] mounted in the main stream of the loop, as the pressurizer feed and pump purge.

In addition to evaluation of the loop performance with regard to slurry circulation, tests have been carried out to determine the effectiveness and stability of a palladium catalyst proposed for use in recombining radiolytic gas (D_2 + 1/2 O_2) produced during reactor irradiation.

17.3.2 Slurry Circulation

Slurry was circulated at a rate of ~5 gpm, which gave a velocity of ~8.5 fps in the 3/8-in. sched-40 main loop piping and ~2 fps in the core section,[17] which is enlarged to expose an appreciable fraction of the slurry to the highest neutron flux.

During run 3 the slurry concentration ranged between 250 and 500 g of Th per kg of D_2O, and for the first 600 hr of operation the concentration of circulating slurry obtained from slurry samples was in good agreement with that obtained from inventory calculations. For the remainder of the run, loss of thoria from the circulating stream was indicated by slurry samples, and radiographs of the loop core section showed that thoria had been deposited in the low-velocity core section.

Particle-size determinations on material removed periodically from the loop indicated that pumping degraded the thoria. The initial mean particle size of 1.9 μ decreased to 1.1 μ after 600 hr of operation in run 3, as shown in Fig. 17.5. Also shown in Fig. 17.5 is a comparison of the circulating concentration, based on inventory, with that obtained from loop samples.

For run 4, which followed, the slurry velocity in the core section was increased to ~4 fps by installing filler pieces to reduce the cross-sectional flow area of the core. The concentration of circulating slurry was maintained in agreement with inventory during the initial 750 hr of operation, but as in run 3, a partial loss of thoria was then noted from sample analyses, and again radiographs revealed a deposit of thoria in the core section. Degradation of the thoria particles was also observed. The initial mean size decreased from 1.9 to 0.7 μ during 600 hr of operation, as shown in Fig. 17.6, which also gives a comparison of circulating-slurry concentration as based on inventory calculations and sample analyses.

In an effort to eliminate deposition of thoria in the core section, a core consisting of bent piping (1/2-in. sched-40) for increased velocity (~5 fps) and improved flow geometry is planned for future test runs. Improvement in particle integrity has been indicated in toroid tests when the firing temperature of the thoria was increased from 1225 to 1500°C, and a quantity of 1500°C-recalcined thoria-urania from batch DT-18 has been prepared for testing in this loop.

17.3.3 Catalyst Additions

In order to evaluate the effectiveness and long-term stability of a palladium catalyst proposed for recombination of radiolytic gas in thorium oxide slurries, seven batchwise additions of the catalyst were made to the circulating slurry during run 4. At each catalyst concentration level, measurements of the rate of recombination of D_2 and O_2 in the loop were made by injecting deuterium

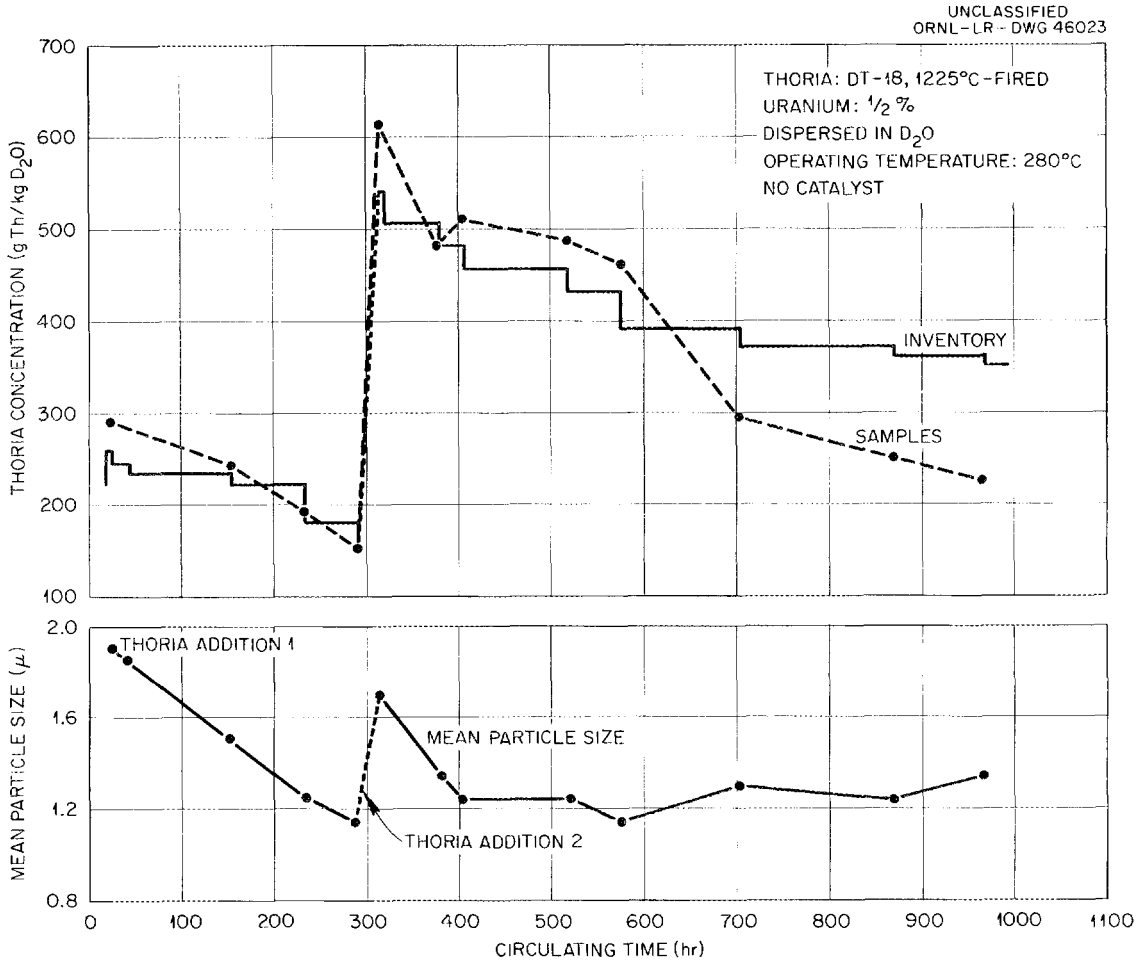

Fig. 17.5. Particle-Size Degradation and Circulating Thoria Concentration, Loop L-2-26S, Run 3.

gas into the loop in which an oxygen atmosphere is maintained. These additions have resulted in a catalyst concentration of ~100 ppm palladium, based on slurry. The palladium remained associated with the slurry under present loop operating conditions, according to chemical analyses of slurry samples removed periodically from the loop.

Results obtained from measurements of the recombination rate are discussed in Sec. 17.3.6.

17.3.4 Filter Performance

The sintered-metal (type 347 stainless steel) filter which provides a thoria-free feed to the pressurizer and a purge stream to the pump bearing region has performed satisfactorily for the ~2500 hr of loop operation with thoria slurry in runs 3 and 4. The filter is in the form of a cylinder, 12 in. long and 3/8 in. in internal diameter (14 in.^{2} inside surface area), with a mean pore diameter of 8 μ.

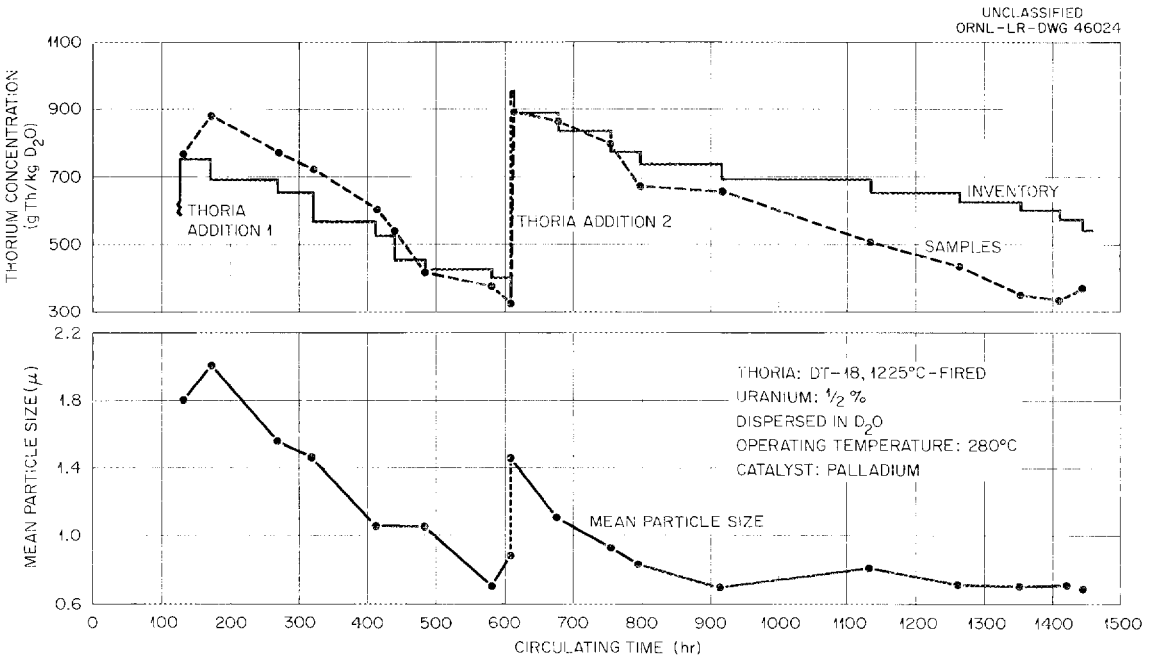

Fig. 17.6. Particle-Size Degradation and Circulating Thoria Concentration, Loop L-2-265, Run 4.

Initially, the filtrate flowed at 22 cc/sec. However, after 140 hr of operation this rate had decreased to 7 cc/sec and has remained at 3 to 7 cc/sec for more than 2000 hr. Operating conditions were 280°C in the loop main stream, circulating slurry concentrations varying from 200 to 800 g of Th per kg of D_2O with a pressure drop across the filter of ~30 ft of H_2O. The particle size of the unpumped thoria was 1.9 μ, which was reduced to 0.7 μ during circulation (refer to Figs. 17.5 and 17.6).

17.3.5 Over-All Loop Corrosion

The corrosion-erosion of the type 347 stainless steel loop and sintered-metal filter for the 1500 hr of operation of run 4 resulted in removal of 4 g of stainless steel, based on the oxygen consumed, which was in agreement with that calculated from the soluble chromium associated with the slurry. However, the amount of stainless steel attack calculated from iron pickup by the circulating slurry was only 2 g. This difference may have resulted from the insoluble iron oxide produced by corrosion of the sintered-metal filter being retained in the filter matrix.

The corrosion-erosion rate of loop surfaces exposed to circulating slurry, based on the above iron pickup, was 0.2 mpy. In any event, the quantity of stainless steel removed from the loop and sintered-metal filter surface was small and indicated that there was no serious corrosion-erosion.

17.3.6 Catalysis Studies

The activity and stability of palladium catalyst for the recombination of radiolytic gas in an in-pile slurry loop were studied in a series of tests performed in conjunction with the out-of-pile development runs on the prototype loop, described above.

An estimate of the catalytic activity required for the first in-pile slurry loop was made. A radiolytic-gas generation rate of 0.06 mole of D_2 per hour in a circulating-slurry volume of 0.7 liter was estimated, assuming operation at 280°C with a 500 g of Th per kg of D_2O slurry, 0.5% U/Th, 93% enriched, $G_{D_2} \sim 0.6$, with the given loop geometry in beam hole HB-2 at an LITR power of 3 Mw. At a catalyst activity of 0.22 mole of D_2 per liter-hr at 100 psi D_2, a D_2 pressure of 35 psi in the 295°C pressurizer gas space would be developed at equilibrium. For the specific loop geometry and operating conditions of the prototype, a corresponding pressure-decay half life of about 18 min was estimated for transient experiments in which no gas was generated or continuously injected.

Tests were made at a main-stream temperature of 280°C, using thoria - 0.5% urania from batch DT-18 as described in Secs. 17.3.2 and 17.3.3. Excess O_2 pressures during the recombination tests varied between 50 and 200 psi.

Recombination rates for uncatalyzed slurry were first determined. Subsequently, several different incremental additions of palladium were made to the loop, and the catalytic activity was observed by suitable experiments for a number of days after each addition. The experiments consisted of the rapid injection of a quantity of D_2 gas into the pressurizer vapor space while the loop operated with oxygenated slurry at 280°C, followed by observation of the rate and manner of pressure decay. Previous calculations have indicated[18] that recombination kinetics would be controlling at pressurizer flow rates of 3 cc/sec, and such rates were maintained in the experiments. Pressure decay was found to be first order with respect to "radiolytic gas" in all cases, after a short induction period attributed to distribution of injected D_2 within the system. The fastest rates observed were characterized by pressure half lives of about 10 min.

Figure 17.7 shows catalyst activities observed at various palladium concentrations as a function of time after catalyst loading. The catalytic activity decreased with time at all catalyst levels studied. With the final catalyst addition to a level of 177 mg of palladium per liter of circulating slurry, a catalyst activity of 0.45 mole D_2 per liter-hr at 100 psi D_2 was obtained, and values below 0.22 mole D_2 per liter-hr were not indicated until about 240 hr after addition.

It was concluded that palladium-catalyst activities sufficient for operation of the first in-pile slurry loop were demonstrated. Supplemental additions of catalyst may be required for extended in-pile operating periods.

REFERENCES

1. C. C. Haws et al., HRP Quar. Prog. Rep. July 31, 1958, ORNL-2561, p 297.

2. E. L. Compere, Multifactor Ratio Analysis (Factor Analysis) of Corrosion Data Using Logarithmic Transformations, ORNL CF-58-9-3 (Sept. 3, 1958).

3. Memorandum from D. G. Thomas to C. C. Haws, Properties of Flame-Calcined Thoria Containing 4% Urania and 2.5% Alumina, (Dec. 15, 1959).

4. P. R. Kasten et al., HRP Prog. Rep. Oct. 31, 1959, ORNL-2879, p 45.

5. J. P. McBride et al., HRP Quar. Prog. Rep. Oct. 31, 1958, ORNL-2654, p 211.

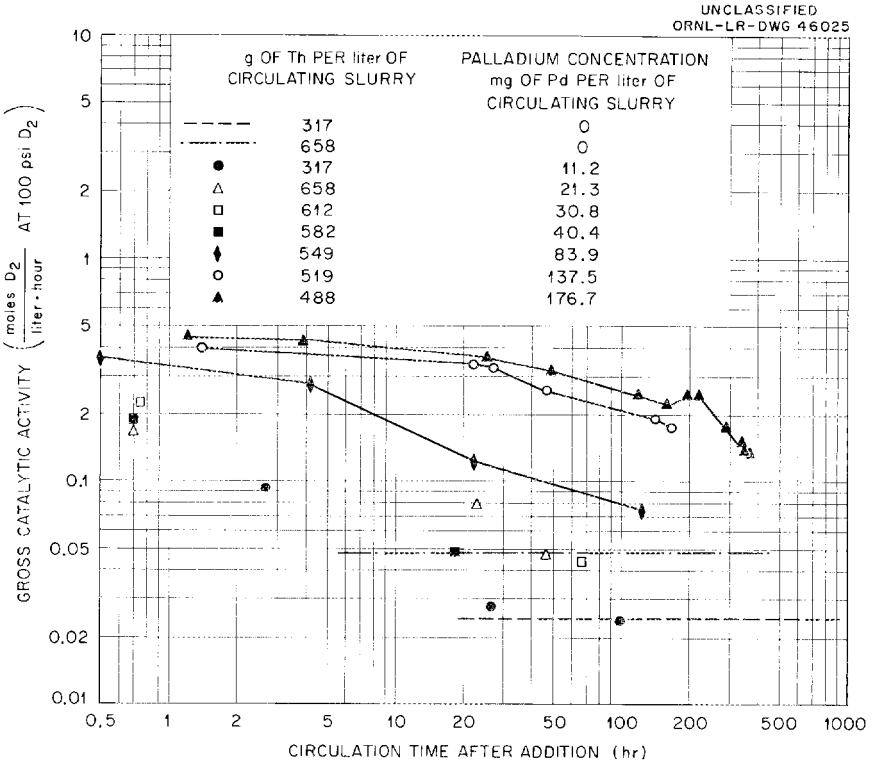

Fig. 17.7. Variation of Catalytic Activity with Time After Successive Palladium Additions.

6. G. E. Moore and E. L. Compere, Small-Scale Dynamic Corrosion Studies in Toroids--Aqueous Slurry Systems, ORNL-2502 (to be published).

7. E. L. Compere et al., Dynamic Slurry Corrosion Studies: Quar. Ending Jan. 31, 1956, ORNL CF-56-1-168, p 33.

8. E. L. Compere et al., HRP Quar. Prog. Rep. Apr. 30, 1957, ORNL-2381, p 109.

9. E. L. Compere et al., HRP Quar. Prog. Rep. Apr. 30, 1959, ORNL-2743, p 134.

10. E. L. Compere et al., HRP Prog. Rep. Oct. 31, 1959, ORNL-2879, p 191.

11. W. J. Leonard, Metallographic Examination of Zircaloy-2 Impeller from 100A Slurry Corrosion Loop, HRP-MET-101 (to be issued).

12. E. L. Compere et al., HRP Prog. Rep. Oct. 31, 1959, ORNL-2879, p 200.

13. E. L. Compere et al., HRP Quar. Prog. Rep. Jan. 31, 1958, ORNL-2493, p 113.

14. K. S. Warren and R. J. Davis, In-Reactor Autoclave Corrosion Studies--LITR I--Outlines of Methods and Procedures, ORNL CF-57-5-110 (May 22, 1957).

15. T. M. Kegley, Jr., Metallurgical Examination of Specimens from In-Pile Autoclave Experiment L6Z-150S and L6Z-150SA, ORNL CF-59-11-35 (Nov. 9, 1959).

16. H. C. Savage et al., HRP Prog. Rep. Oct. 31, 1959, ORNL-2879, p 205.

17. H. C. Savage et al., HRP Quar. Prog. Rep. Oct. 31, 1958, ORNL-2654, p 165, Fig. 15.5.

18. E. L. Compere et al., HRP Prog. Rep. Oct. 31, 1959, ORNL-2879, p 208.

Part V

FUEL MANUFACTURE AND PROCESSING

18. THORIUM OXIDE PREPARATION AND PRODUCTION

O. C. Dean

A. T. Kleinsteuber K. H. McCorkle C. E. Schilling

18.1 EVALUATION OF THORIA AND THORIA-URANIA POWDER PREPARATIONS FOR BLANKET SLURRIES

18.1.1 Jet Abrasion Testing

From previous work with the jet abrasion tester,[1] it was concluded that by observing the time required for a jet of ThO_2 slurry to penetrate a metal foil, the tendency of the thoria particles to degrade could be determined. Further tests have confirmed that it is possible to differentiate between a material that is easily degraded and one that does not significantly degrade. However, it was not found possible to detect mild degradation (a change in particle size of less than a factor of 2).

It was also expected that a marked effect of particle shape on abrasiveness could be demonstrated with the jet abrasion tester. This was not the case. A small reduction of abrasiveness could be detected for Houdry spheres and flame-calcined materials, but this effect was insignificant compared with the effect of firing temperature of an oxide made from oxalate precipitated thorium.

Additional experiments are in progress to define more clearly what properties of an oxide can be measured with the jet abrasion tester.

18.1.2 Studies of Thoria-Urania

Slurries containing 0.5 and 3 mole % urania were shown to be degraded and to abrade surfaces badly in loop and toroid tests. Some formed plugs in vertical sections. Experiments were started to determine the effect of increased firing temperature on degradation and abrasion tendencies of the adsorbed mixed oxides prepared by the Pilot Plant. The following original powders were obtained from the Pilot Plant, all prepared by the adsorption of uranyl ammonium carbonate from solution onto a 650°C-fired oxalate-precipitated thoria and fired for 4 hr: MO-81 (3% urania), fired at 650°C; MO-75 (3% urania), fired at 1100°C and then classified and dried at 650°C; MO-76 (8% urania), fired at 1050°C and then classified and dried at 650°C; MO-75 (0.5% urania), fired at 1050°C and then classified and refired at 1225°C for 4 hr.

The program consisted of firing at 1000, 1100, 1200, and 1400°C those powders not having reached that temperature previously. Samples of the 1000°C-fired materials were to be further fired at the higher levels to determine the

variation in effects of slow and fast approach to maximum temperature. Clinker tests were applied to each sample. Only the initial powders received jet abrasion and particle-size testing. The results of the clinker tests are shown in Table 18.1.

Table 18.1. Clinker Formation in Thoria-Urania Powders
(All firings conducted in oxyacetylene furnace, 4 hr)

Firing Temp. (°C)	Percentage Clinker[a] in Samples				
	MO-81	MO-75	MO-76	MO-69	MO-81-1000[b]
1000	10.4				10.4[c]
1050			9.5[c]		
1100	13.1	10.2[c]	15.9		
1200	18.8	6.4	9.8	3.7[c]	8.5
1400	25.0	14.4	8.8	7.0	16.4

[a]Percentage of powder having particles >10 μ, according to a sedimentation procedure.

[b]MO-81 powder previously fired to 650°C then refired at 1000°C.

[c]Original test powders, as received.

All original powders except MO-69 and MO-81 contained about 10% clinkers; therefore the results were evaluated on the basis of the increase in percentage of clinker. The MO-81 (3% urania) powder, initially fired to only 650°C, could not be rapidly fired to temperatures higher than 1100°C without an excessive increase in clinker content. However, if held at an intermediate 1000°C for 4 hr, it could be fired to 1200°C without extreme clinker formation. After initial firing to 1050°C for 4 hr, the MO-76 (8% UO_2) powder was fired to 1400°C without a significant increase in clinker content. MO-75 (3% urania) was fired to 1200°C and MO-69 (0.5% UO_2) to 1400°C without a significant increase.

In studies on the effect of firing atmospheres on the particle densities of adsorption-prepared mixed-oxide powders containing 3 and 5 mole % urania, air firing was found to exert a greater densifying effect than hydrogen firing.

18.2 PREPARATION OF THORIA FOR HOMOGENEOUS REACTOR BLANKET

18.2.1 Preparation of Thoria Microspheres

The study of the preparation of thoria microspheres of approximately 3-μ diameter by a gel-forming technique was continued. In this technique, a thoria sol is prepared by careful neutralization or denitration of 2 M $Th(NO_3)_4$ solution.[2] Gel beads are formed by pumping sol and isopropyl alcohol - water simultaneously through an orifice. The optimum alcohol - water to sol ratio for sols formed by neutralization is controlled by the final optimum water content of the mixture. Bead size is controlled by the relative flow rates of the two phases during spraying. Since the newly formed beads are plastic, and when formed from ammonia-neutralized sols contain about 50 wt % ammonium nitrate, it is necessary to leach the ammonium nitrate out of the bead and

into the isopropyl alcohol - water phase before drying and firing the residual solid bead, in order to avoid forming porous beads.

The highest bead densities (9-10) were obtained when the water content of the system in the forming step was 17% and when the beads were washed repeatedly with isopropyl alcohol containing decreasing amounts of water. With a water content of 22-23%, the beads soften and then disperse in the isopropyl alcohol. For 2- to 3-μ beads, if the water concentration is decreased to less than 12%, the walls of the beads tend to be thin and hard (eggshell), which retards outward diffusion of ammonium nitrate and promotes porosity. When these beads were washed on the filter, they tended to become deformed and stick to each other when dried and fired. The use of concentrated isopropyl alcohol, hexamethylene tetramine, or citric acid in the final wash hardened the beads but also decreased densities. Those washed with hexamethylene tetramine solution exhibited slight pyrophoricity at 250 to 300°C, indicating that nitrate still remained. It is thought that continuous washing with isopropyl alcohol containing 15% water, in a fluidized bed of the beads, and recycling of part of the wash liquor may give high densities without the agglomeration difficulties experienced when washing on the filter.

18.2.2 Preparation of Thoria-Alumina by Coprecipitation

The presence of small percentages of alumina in thoria may decrease the yield stress of thoria slurries. An attempt was made to prepare thoria containing 2% alumina by coprecipitation of the oxalates from thorium-aluminum nitrate solutions with various ratios of oxalic acid from 10% deficient to 35% excess. Only 6 to 10% of the initial aluminum precipitated with the thorium.

In another experiment an aluminum oxalate - oxalic acid solution (0.618 M oxalic acid, 0.0585 M Al) was added to 0.7 M $Th(NO_3)_4$ with oxalates in 10% deficient, stoichiometric, and 10% excess quantities. Eleven, 47, and 14% of the aluminum was precipitated with the thorium oxalates, producing 650°C-calcined oxides containing 0.21, 0.80, and 0.21 wt % aluminum.

The above stoichiometric precipitations were repeated, and the pH of the slurry was adjusted to 3.0-3.4 with ammonium hydroxide before filtering. Four per cent of the aluminum was precipitated with the thoria when aluminum was added to the oxalic acid, and 1.5% when it was added to the nitrate. It was concluded that aluminum cannot be quantitatively coprecipitated with thorium in the oxalic acid system.

18.3 OXIDE PREPARATION DEVELOPMENT

18.3.1 Flame Denitration

Studies of the preparation of thoria particles by the flame denitration of solutions of thorium nitrate in methanol were continued. Approximately 30 lb of thoria-urania, prepared to give spherical particles of U/Th = 0.08 and containing 2.5 wt % Al_2O_3 (ref 3), was classified to remove large particles (>10-μ diameter) and was submitted to REED for tests. Preliminary results indicate that the material has desirable characteristics (see Sec. 17.1).

One run was made with a mixture containing 40 mole % thorium nitrate and 60 mole % beryllium nitrate in methanol. This should produce an oxide mixture having a melting point near 2100°C. A photomicrograph (Fig. 18.1) of the

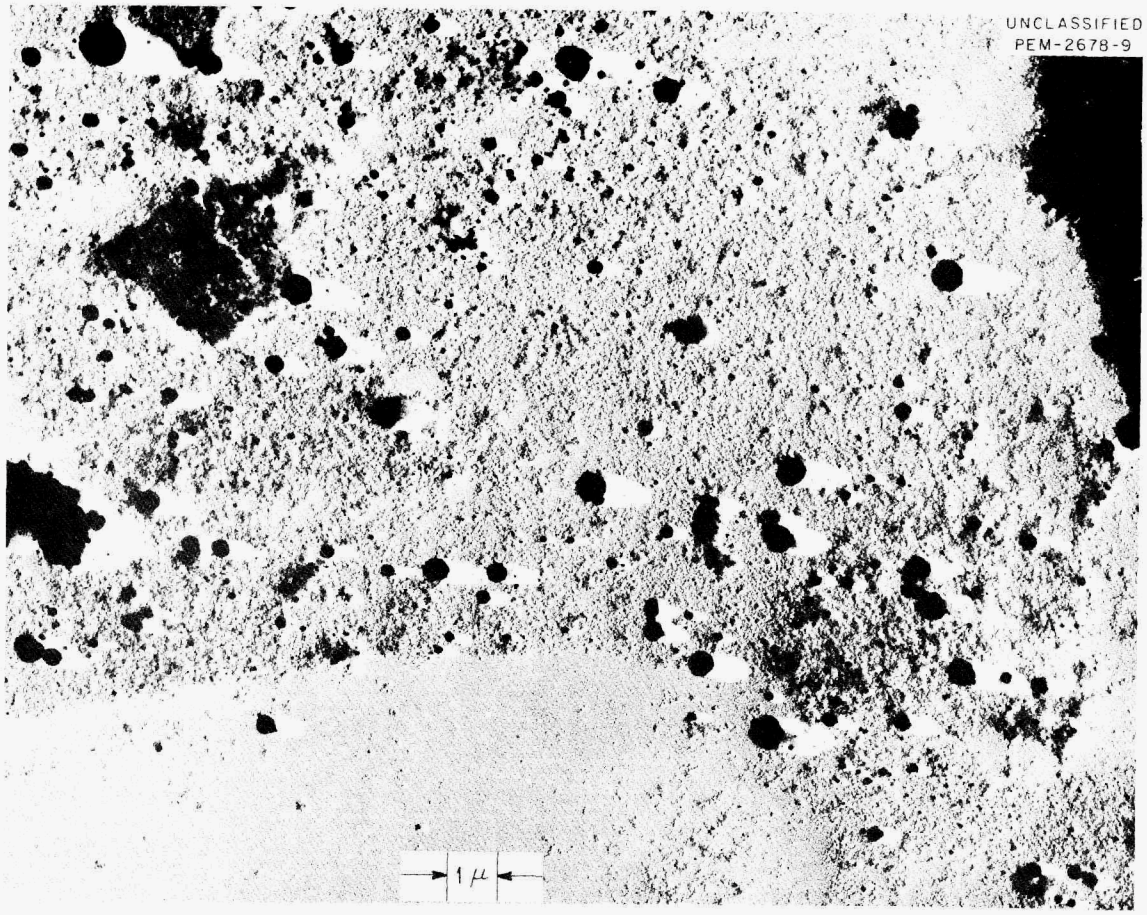

Fig. 18.1. Shadowgraph of $BeO-ThO_2$ Particles Produced by Flame Denitration. Conditions: outer reflector wall at 1475°C; 60 mole % (12 wt %) BeO, 40 mole % (88 wt %) ThO_2.

product showed definite rounding of the oxide particles. Because of the hazards involved in the handling of beryllium compounds, only a few grams of material were prepared, and the number of tests which can be made on this product will be limited.

The runs to compare the effect of adding Al_2O_3 or SiO_2 to thoria or urania in flame calcination were completed. Table 18.2 presents the data from the runs, and Figs. 18.2 and 18.3 are photomicrographs of typical products. From the photomicrographs it appears that thoria containing 0.5 to 5.0% of either alumina or silica forms predominately rounded particles. The same additives with urania produced much smaller particles, the shape of which is uncertain (run 86). The addition of SiO_2 to the thoria-urania mixture produced spheroids (run 90).

Fig. 18.2. Typical Flame-Calcination Product Containing Thoria Plus an Additive. See Table 18.3 for data.

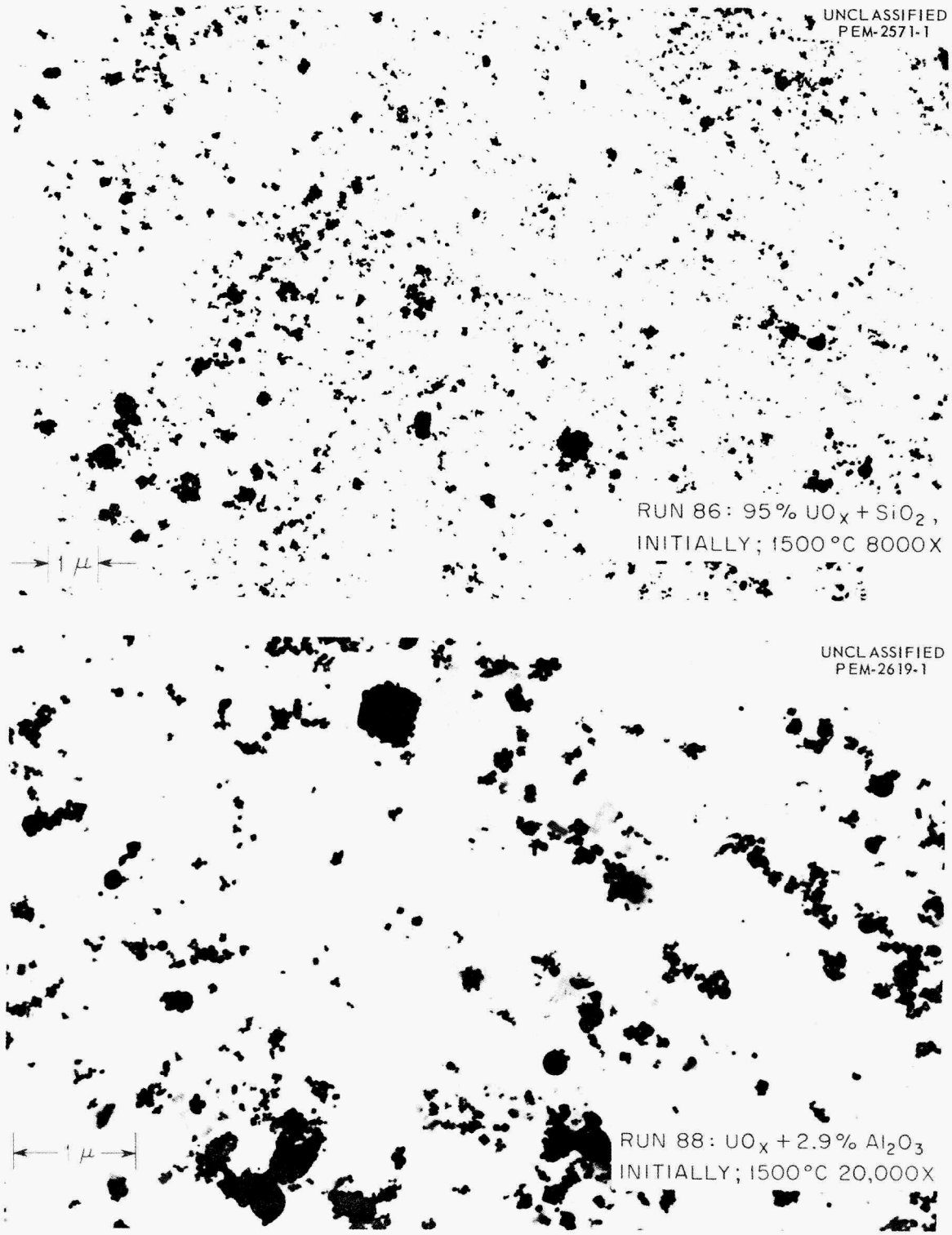

Fig. 18.3. Typical Flame-Calcination Product Containing Urania Plus an Additive. See Table 18.3 for data.

Table 18.2. Flame Calcination of Uranium and Thorium Oxides with Additives

Run	Composition(wt %)				Reflector Temp. (°C)	Surface Area, (m^2/g)	Mean Dia. (μ)	Slurry Yield Stress* (lb/ft^2)	Powder Bulk Density (g/cc)
	Th	U	Al	Si					
84	85.83			0.80	1200	1.5	1.2	<0.02	4.56
85	87.31			0.51	1200	4.0	1.0	<0.02	2.47
86		78.38		2.12	1500	6.2	1.2	<0.02	2.26
87		82.52		0.42	1500	6.1	1.0	<0.1	2.10
88		78.66	2.88		1500	7.4	0.6	>0.1	1.93
89		82.97	0.90		1500	8.5	0.6	>0.1	2.18
90	72.55	12.2		0.94	1500	1.9	1.2	<0.02	3.46

*Measured at a slurry density of 2.0.

REFERENCES

1. J. P. McBride et al., HRP Quar. Prog. Rep. July 31, 1957, ORNL-2379, p 150-151.

2. R. L. Pearson and A. T. Kleinsteuber, HRP Prog. Rep. Oct. 31, 1959, ORNL-2879, p 227-231.

3. P. A. Haas, C. C. Haws, and K. O. Johnsson, HRP Prog. Rep. Oct. 31, 1959, ORNL-2879, pp 223, 227.

Part VI

METALLURGY

19. METALLURGY

A. Taboada

F. W. Cooke
T. M. Kegley
W. J. Leonard
M. L. Picklesimer
P. L. Rittenhouse
R. L. Stephenson
C. H. Wodtke

19.1 ZIRCALOY-2 FABRICATION STUDY

The anisotropy of mechanical properties of Zircaloy-2 plate and sheet is known to be a function of the preferred orientation and of the mechanical fibering which occurs during fabrication.[1] A study is in progress to evaluate the various fabrication procedures and to determine the effects of specific fabrication variables on the final state of this anisotropy. The aims, experimental procedures, variables studied, experimental data, and a number of conclusions have been reported previously.[2-5]

A series of specimens from two schedules have been broken to determine the reproducibility of the experimental determinations of tensile properties and k values. For each set of six specimens from each major sheet direction for the two schedules, all the tensile and yield strengths fell within a band 500 psi wide, the limit of accuracy for reading the individual values from the recorded load-elongation curves. An examination of the values determined for all the specimens in the entire study indicates that a more reasonable value for the accuracy of an individual determination of yield and tensile strengths for the particular test is ±1200 psi. The mean error in the k values was found to be ±0.015 or less for a range of k values from 0.115 to 0.885.

Strain-strain data for all the tensile specimens pulled at 150 and 300°C have been calculated and are undergoing analysis. No striking differences from the room-temperature data are apparent.

Careful examination of the tensile- and yield-strength data for those schedules for which specimens were taken every 22.5° from the rolling direction to the transverse direction has shown that for most of the schedules, the directions for maximum and minimum yield and tensile strengths are not in the rolling and transverse directions. The same is true for elongation and reduction-of-area values. For several schedules the anisotropic axes for yield strengths are at 45 to 90° to those for the tensile strengths. No explanation of such observations can be made at present.

Sheet-type tensile specimens have been machined and broken for three schedules for which strain-strain and tensile-property data were available for round specimens. The yield strengths for the sheet-type specimens were

consistently 12,000 psi lower and the tensile strengths were consistently 10,000 psi lower than for the corresponding round specimens for all specimen axis directions and fabrication schedules. The strain and necking behavior of the sheet-type specimens was consistent with the ellipticity of cross section produced in the corresponding round specimens. No strain-strain data can be obtained from the sheet-type specimens because of the roughened surface condition and strain pattern (more thinning of the specimen along the center line than along the edges) produced in the fractured specimens.

The collection of data for the fabrication study is complete, and the final portion of data is being examined. A final report is in preparation.

19.2 ZIRCONIUM ALLOY DEVELOPMENT

Zirconium-base alloys containing niobium and copper have shown considerable promise for the development of a more corrosion-resistant alloy to replace Zircaloy-2 as the core-tank material for aqueous homogeneous reactors. The information necessary for the development of these alloys is being procured by basic physical metallurgical studies and in-pile corrosion tests.

Considerable data have been obtained and reported[4,5] on the beta-quench and reheat transformations. Recent reruns of some of the tests with the Zr-15% Nb alloy (for the determination of differences due to a new lot of iodide zirconium-base melting stock) revealed several discrepancies in the time required for the formation of the first omega phase in the retained beta phase. Incubation times as long as 3 hr were found for reaction at 400°C, instead of the 2 to 6 min previously found. A series of quenching-rate experiments was performed to determine the effects of quenching rate and quenching temperature on the incubation time at 400°C for the formation of omega phase. Two lots of iodide zirconium of the same reported analyses were used for base-melting stock. Specimens from four ingots were quenched from 900°C in cold water, hot water, oil, and air. Other specimens were quenched from different beta temperatures after soaking at 900°C. Not all the data have been collected or analyzed. However, it has been established that the fastest quenching rates and highest quenching temperatures lead to earliest formation of omega phase. The slowest quenching rates and lowest quenching temperatures result in the longest incubation times, provided that no appreciable amounts of omega phase have been formed during the quench. The study is continuing. The variation in niobium contents (small) has been found to be in the wrong direction to explain the behavior observed.

19.3 FORMING OF ZIRCALOY-2

As part of the effort to develop techniques for forming core vessels and piping of Zircaloy-2, a study was conducted to determine the amenability of this material to hot pressing. The specific purpose of the study was to demonstrate the feasibility of forming a transition between a pipe and a spherical vessel that would require a minimum of welding.

A pair of carbon steel dies (see Fig. 19.1) was used to press pipes and hemispheres preheated with an oxyacetylene torch to 1200 to 1400°F. The pipes were easily formed, and the wall thinout was 35% of that calculated for a simple stretching model.[6]

UNCLASSIFIED
ORNL-LR-DWG 46026

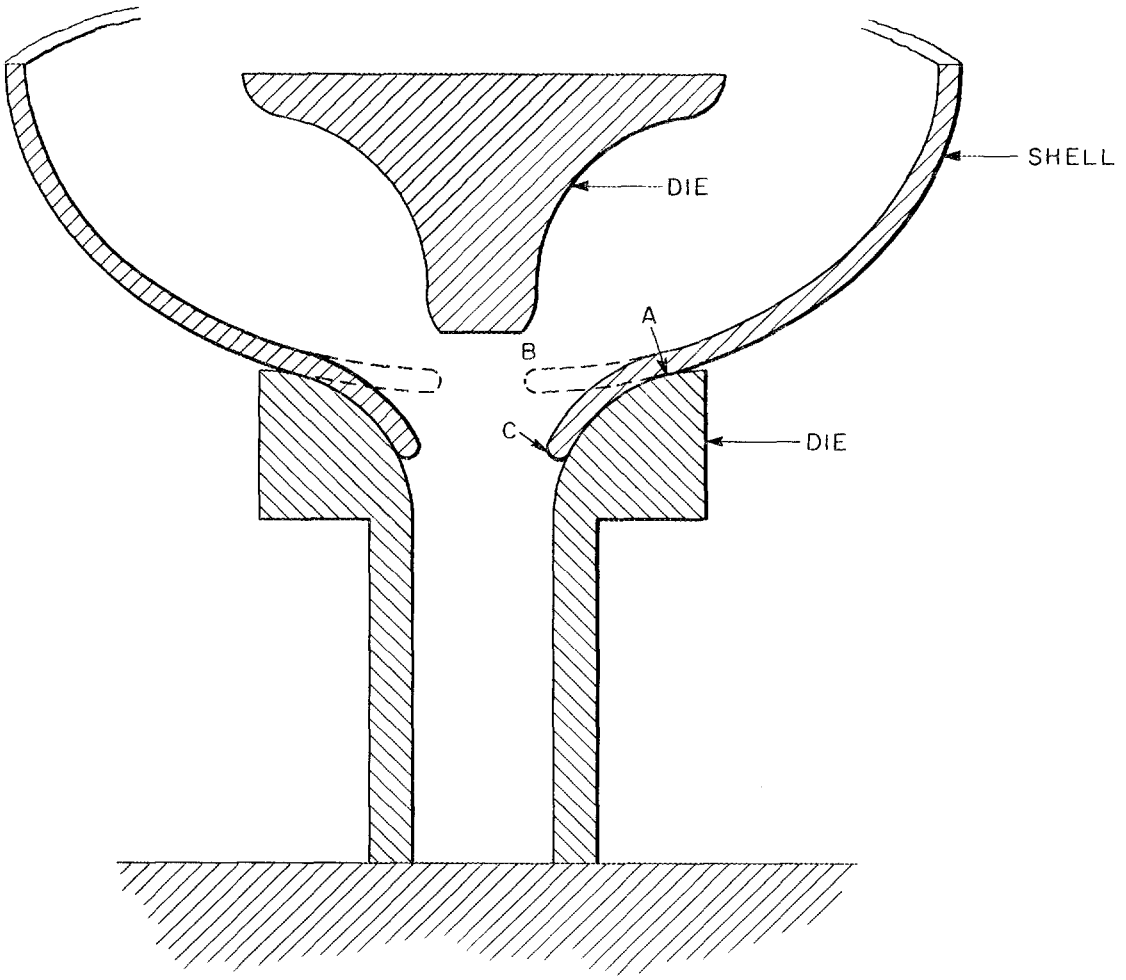

Fig. 19.1. Pressed Zircaloy-2 Shell in Dies.

A 0.226-in.-thick shell, preheated to 1200 to 1400°F, was thinned by only 13% when formed to a shape with a 68% increase in hole diameter. This diametral change would require about 50% thinout based on a simple stretching model. The reduced thinout was compensated for by a decrease in the meridional dimension of the deformed area. Before pressing, the dimension A-B in Fig. 19.1 was 2.0 in.; after pressing, A-C was 1.9 in. No completely satisfactory mechanism has been devised to explain this phenomenon, though it is probably related to the preferred orientation of Zircaloy-2. Since the wall thickness of the vessel must be maintained throughout the transition, the amount of thinout should be small.

This work further substantiates the belief that a full-size transition could be made by this simple process and would require only a modest development program.

REFERENCES

1. M. L. Picklesimer and G. M. Adamson, Development of a Fabrication Procedure for Zircaloy-2, ORNL CF-56-11-115 (Nov. 21, 1956).

2. G. M. Adamson et al., HRP Quar. Prog. Reps. Oct. 31, 1958, ORNL-2654, p 184-186; April 30, 1959, ORNL-2743, p 182-191; Oct. 31, 1959, ORNL-2879, p 240-241.

3. M. L. Picklesimer et al., Met. Div. Ann. Prog. Rep. Sept. 1, 1959, ORNL-2839, p 115-127.

4. G. M. Adamson et al., HRP Quar. Prog. Reps. Oct. 31, 1956, ORNL-2222, p 114-116; Jan. 31, 1957, ORNL-2272, p 119-123; April 31, 1957, ORNL-2331, p 124-128; July 31, 1957, ORNL-2379, p 122-126; Oct. 31, 1957, ORNL-2432, p 131-133; Jan. 31, 1958, ORNL-2493, p 141-143; April 30 and July 31, 1958, ORNL-2561, p 245; Oct. 31, 1958, ORNL-2654, p 188.

5. M. L. Picklesimer et al., Met. Div. Ann. Prog. Rep. Sept. 1, 1959, ORNL-2839, p 113-114.

6. G. M. Adamson et al., HRP Quar. Prog. Rep. April 30, 1959, ORNL-2743, p 192.

Part VII

ANALYTICAL CHEMISTRY

20. ANALYTICAL CHEMISTRY

O. Menis H. P. House

G. Goldstein
D. L. Manning

20.1 DETERMINATION OF TOTAL SULFATE IN SOLUTIONS OF URANYL SULFATE

A nonaqueous titrimetric method was devised for the rapid determination of sulfate in solutions containing cations, such as UO_2^{++}, Fe^{+++}, and Zr^{+4}, which interfere in conventional methods for sulfate. The sulfate is precipitated in an acetic acid medium by the addition of a known amount (excess) of barium acetate, after which the excess reagent is titrated potentiometrically with a strong acid, such as perchloric acid. This titration is possible because barium acetate is a moderately strong base in an acetic acid medium. Typical titration curves for several sulfate salts are shown in Fig. 20.1.

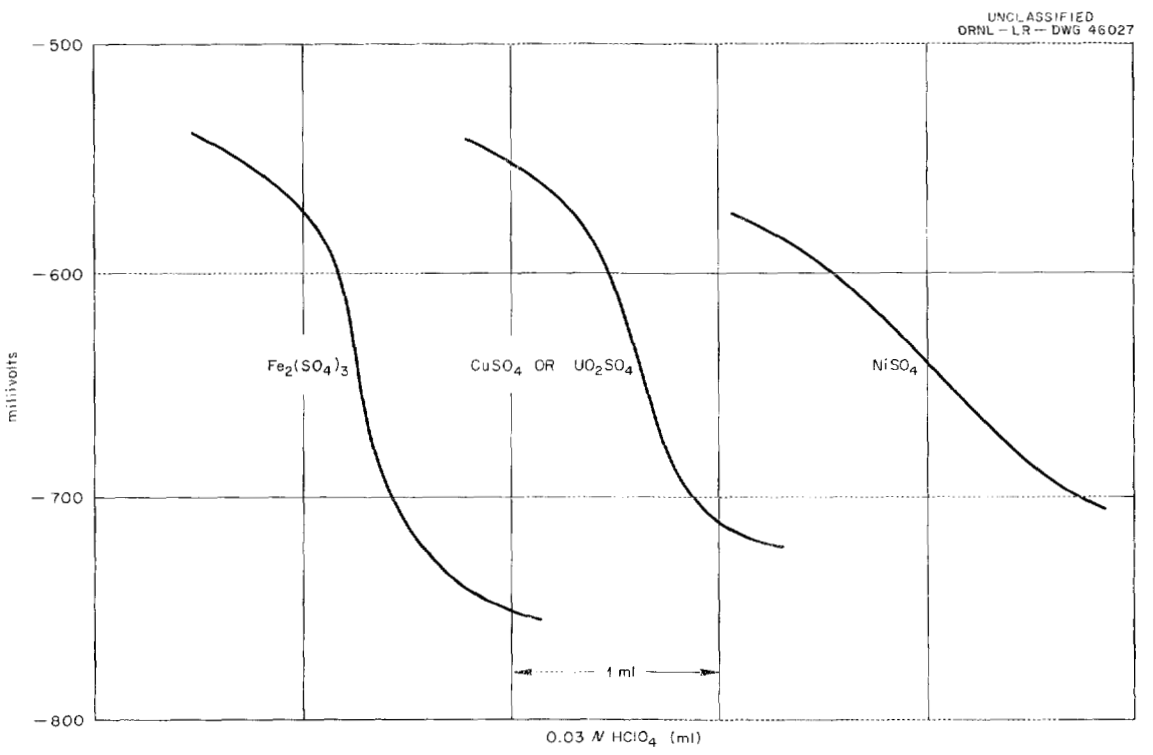

Fig. 20.1. Titration Curves in the Determination of Sulfate in Various Salts.

No interference is encountered with UO_2^{++}, Cu^{++}, Fe^{+++}, Zr^{+4}, or, in general, tri- or tetravalent cations, whereas sulfates of uni- or divalent cations, such as Na^+, K^+, or Ca^{++}, which form strongly basic acetates, interfere. Some nitrate, phosphate, and fluoride salts may be tolerated, while others interfere, depending on the associated cation. Free HNO_3 or HCl interfere and are to be avoided; HF and H_3PO_4 do not interfere.

The method was applied specifically to the determination of total sulfate in solutions simulating homogeneous reactor fuels which contain uranyl and copper sulfate, sulfuric acid, and corrosion products of stainless steel as minor components. By replicate titrations of samples of this type, the coefficient of variation was found to be less than 1%. The results were in good agreement with the known sulfate content of synthetic samples and with values obtained previously by a conventional method.

20.2 DETERMINATION OF FREE ACID IN URANYL SULFATE SOLUTIONS

Free acid in impure uranyl sulfate solutions under test as simulated fuels for the homogeneous reactor cannot be titrated by conventional means because of the interference of uranyl and other easily hydrolyzable cations. For this purpose, a modification of a conductometric method suggested by Pepkowitz, Sabol, and Dutina[1] was successfully utilized. The H_2SO_4 is conductometrically titrated with NaOH after the addition of NaF to form slightly dissociated fluoride salts (or complexes) with uranyl and other hydrolyzable cations. Excess NaF over that required to react with the hydrolyzable ions should be avoided since it reacts with H_2SO_4 to form weakly ionized HF, which obscures the end point. By the use of electrodes of large surface area, the end point can be readily established with a conventional conductance bridge.

The precision of the method was evaluated by titrating a series of synthetic homogeneous reactor fuel solutions which contained 0.04 meq of H_2SO_4, and also (as sulfates) U, 6 mg/ml; Cu, 0.8 mg/ml; and Ni, 0.4 mg/ml. The coefficient of variation for H_2SO_4 was found to be better than 1%. The method is easily adaptable to operations involving remote control.

20.3 DISSOLVED-OXYGEN ANALYZER*

J. M. Wright of the Advanced Development Chemistry Section of Bettis Atomic Power Division, Westinghouse Electric Corporation, has developed an instrument for the determination of low concentrations of oxygen in water which promises to be of use to the HRP.[2] Mr. Wright kindly sent working drawings and instructions for the analyzer to ORNL, and a unit was constructed and tested, and was installed at the HRT.

The analyzer works on the principle that thallium metal will react with oxygen in water, but not with water alone, to form soluble and ionized thallium hydroxide. Measurement of the conductivity of the water before and after passing over thallium metal can be related quantitatively to the dissolved oxygen. A mixed-bed ion exchange column is incorporated in the unit before the first conductivity cell in order to remove ionized species present in the

*This section contributed by J. C. Griess, H. C. Savage, S. E. Bolt, R. S. Greeley, and P. D. Neumann of the Solution Corrosion Section, REED.

water, and a similar column is incorporated after the second conductivity cell to remove the thallium hydroxide from the water before disposal.

The analyzer was calibrated, as directed, on air-saturated water and tested on the letdown stream from 100A-loop D circulating water at 200°C and 500 psi (steam plus hydraulic pressure). Changes in oxygen content of the letdown stream caused by adding oxygen or oxygen scavengers, such as hydrazine or sodium sulfite, to the loop were indicated quickly by the analyzer; oxygen concentrations calculated from the analyzer conductivity readings were in agreement with concentrations determined by chemical analysis on water samples taken simultaneously.

The analyzer was also tested at the HRT on the laboratory distilled water and on ORNL plant-steam condensate. Then the analyzer was installed to take reactor-steam condensate, and measurements were made with the reactor at 3.4 and 4.0 Mw. (During this period, excess hydrazine was added to the boiler feed water, as has been the practice at the HRT.) Simultaneous water samples were taken for chemical analysis of the dissolved oxygen by the Winkler method.[3] Table 20.1 gives the results of the measurements at the HRT. It is felt that the agreement between the analyzer values and the Winkler values is reasonable. The analyzer readings on reactor-steam condensate were particularly valuable since some doubt had been cast on the validity of the Winkler method by variations in the results depending on the time of adding the reagents.[4] It is not believed that the difference between the values obtained with the analyzer during power operation at 3.4 and 4.0 Mw is indicative of a real trend in oxygen concentration

The analyzer is easy to use and gives rapid, accurate values of dissolved-oxygen concentration. It could also be conveniently set up to give continuous and automatic recording of the oxygen level.

Table 20.1. Comparison of Results Obtained with the Oxygen Analyzer and the Winkler Method of Analysis

Condition	O_2 Concentration (ppm)	
	Analyzer	Winkler Method
Laboratory distilled water	0.92	0.79
X-10 steam condensate	0.019	0.00
HRT steam condensate		
Reactor at 3.4 Mw	0.035	0.048
Reactor at 4.0 Mw	0.019	-

REFERENCES

1. L. P. Pepkowitz, W. W. Sabol, and D. Dutina, "Determination of Free Acid in the Presence of Hydrolyzable Ions," Anal. Chem. 24, 1956 (1952).

2. J. M. Wright, Instructions for the Installation, Operation, and Maintenance of the Bettis Dissolved Oxygen Analyzer, Model 3, WAPD-CDA(AD)-453 (Sept. 4, 1958).

3. W. W. Scott, Standard Methods of Chemical Analysis, p 2079, ed. by N. H. Furman, Collective Vol. II, 5th ed., D. Van Nostrand, New York, 1939.

4. D. M. Richardson, private communication.

OAK RIDGE NATIONAL LABORATORY
HOMOGENEOUS REACTOR PROJECT

JANUARY 1, 1960

PROGRAM DIRECTOR
R. B. BRIGGS — D
A. L. GUNNELS, SEC. — REE

PROGRAM EDITOR
W. D. REEL — TI

DESIGN AND ENGINEERING
R. N. LYON, ASSOCIATE DIRECTOR — REE
P. A. HICKEY,* SEC. — REE

DESIGN
W. R. GALL,** SECTION CHIEF — REE
M. I. LUNDIN,** ASSISTANT SECTION CHIEF — REE

DESIGN AND SPECIFICATIONS
R. C. ROBERTSON, GROUP LEADER — REE
J. E. JONES, JR — REE

DRAFTING
J. P. GILL,** GROUP LEADER — REE
W. B. KRICK — REE
L. E. PENTON — REE
T. E. HAYNES — REE

REACTOR ANALYSIS
P. R. KASTEN,** SECTION CHIEF — REE

REACTOR PHYSICS
M. TOBIAS, GROUP LEADER — REE
D. R. VONDY — REE
H. A. MASCOLL — REE

ENGINEERING RESEARCH
H. W. HOFFMAN,** SECTION CHIEF — REE

AQUEOUS HOMOGENEOUS REACTOR SLURRY STUDIES
D. G. THOMAS — REE
P. H. HAYES** — REE
R. M. SUMMERS** — REE

ENGINEERING DEVELOPMENT
I. SPIEWAK, SECTION CHIEF — REE
F. N. PEEBLES, ASSISTANT SECTION CHIEF — REE

MAINTENANCE DEVELOPMENT
E. C. HISE,* GROUP LEADER — REE
R. BLUMBERG — REE
P. P. HOLZ — REE
C. JONES — REE

COMPONENT DEVELOPMENT
C. H. GABBARD, GROUP LEADER — REE
E. C. HISE* — REE
J. C. MOYERS — REE
H. R. PAYNE — REE
J. P. HIRST — REE
G. A. WINDLE — REE

CORE AND BLANKET DEVELOPMENT
C. G. LAWSON, GROUP LEADER — REE
R. J. KEDL — REE
M. RICHARDSON — REE
W. P. WIDMIER — REE
T. L. CASTILE — REE
B. J. YOUNG — REE

SYSTEM DEVELOPMENT
L. F. PARSLY, GROUP LEADER — REE
P. H. HARLEY — REE
R. E. CARNES — REE

SLURRY LOOP PROGRAM
D. M. EISSENBERG, GROUP LEADER — REE
A. N. SMITH — REE
J. T. DICKEY — REE
C. A. GIFFORD — REE
H. C. MOORE — REE

INSTRUMENTATION AND CONTROLS
R. L. MOORE,** SECTION CHIEF — I&C

REACTOR I&C SYSTEM DESIGN
J. R. BROWN,** GROUP LEADER — I&C
R. W. BORGERS** — I&C

HRP SUPPORTING SERVICES
H. D. WILLS, GROUP LEADER — I&C
P. G. HERNDON — I&C
R. M. BURNETT — I&C

VALVE DEVELOPMENT AND SPECIFICATION
A. M. BILLINGS,** GROUP LEADER — I&C
B. J. JONES** — I&C

INSTRUMENT DEVELOPMENT AND EVALUATION
D. G. DAVIS,** GROUP LEADER — I&C
T. M. CATE** — I&C

REACTOR MATERIALS RESEARCH
E. G. BOHLMANN, ASSOCIATE DIRECTOR — REE
P. A. HICKEY,* SEC. — REE

SOLUTIONS
J. C. GRIESS,** SECTION CHIEF — REE
J. L. ENGLISH** — REE
L. L. FAIRCHILD** — REE
R. S. GREELEY — REE
P. D. NEIMANN** — REE
H. L. BARKER** — REE
W. H. HINDS — REE
B. L. JOHNSON** — REE

SLURRIES
E. L. COMPERE, SECTION CHIEF — REE

OUT-OF-PILE STUDIES
S. A. REED — REE
R. B. GALLAHER — REE
R. F. DENSON — REE
F. E. MCDANIEL* — REE
G. G. WARNER — REE

IN-PILE LOOPS
A. J. SHOR — REE

IN-PILE AUTOCLAVES
L. F. WOO — REE
F. E. MCDANIEL* — REE

MATERIALS EXPERIMENT ENGINEERING
H. C. SAVAGE, SECTION CHIEF — REE

OUT-OF-PILE OPERATIONS
S. F. BOLT* — REE
T. H. MALINEY** — REE

100A LOOPS
J. F. WINSETTE — REE
C. R. BENSON — REE
C. M. BURCHELL — REE

IN-PILE EXPERIMENT FABRICATION
S. E. BOLT* — REE
J. R. HART* — REE
R. W. RAY — REE

IN-PILE SLURRY LOOP
R. A. LORENZ* — REE
J. M. BAKER — REE
J. R. HART* — REE

REACTOR OPERATIONS
R. A. LORENZ* — REE
V. A. DECARLO — REE
K. G. CHANDLER — REE
E. H. GUINN — REE
J. W. MOSIER — REE
J. W. MYERS — REE
D. G. PEACH* — REE
C. E. ROBERTS — REE
W. C. ROSS — REE
A. L. SUTTON — REE
W. E. TEICHERT — REE
R. M. WALLER* — REE

RADIATION
G. H. JENKS, SECTION CHIEF — REE

IN-PILE LOOPS
J. E. BAKER — REE
S. H. WHEELER — REE

IN-PILE BOMBS
R. J. DAVIS — C
J. L. RUTHERFORD — REE

SUPPORTING RESEARCH
A. L. BACARELLA — C
J. C. BANTER — REE

METALLURGY
A. TABOADA, SECTION CHIEF — M
F. W. COOKE — M
W. J. LEONARD — M
M. L. PICKLESIMER** — M
P. L. RITTENHOUSE** — M
C. H. WOOTKE — M
P. J. JONES** — M
G. C. NELSON** — M
E. M. SMITH — M

METALLOGRAPHY
T. M. KEGLEY,** LEADER — M
E. R. BOYD** — M
B. F. DAY** — M
T. J. HENSON** — M

SUBCONTRACTS

UNIVERSITY OF UTAH

NON-CITIZEN ASSIGNEE

P. VIGNET
COMMISSARIAT A L'ENERGIE ATOMIQUE
CENTRE D'ETUDES NUCLEAIRES DE SACLAY FRANCE

AC — ANALYTICAL CHEMISTRY DIVISION
C — CHEMISTRY DIVISION
CT — CHEMICAL TECHNOLOGY DIVISION
D — DIRECTOR'S DIVISION
I&C — INSTRUMENTATION AND CONTROLS DIVISION
M — METALLURGY DIVISION
RC — REACTOR CHEMISTRY DIVISION
REE — REACTOR EXPERIMENTAL ENGINEERING DIVISION
TI — TECHNICAL INFORMATION DIVISION
* — DUAL CAPACITY
** — PART TIME

PERSONNEL SUMMARY

	FULL TIME	PART TIME	NON-CITIZEN ASSIGNEE	TOTAL
ADMINISTRATION	5	4	0	9
ANALYTICAL CHEMISTRY	24	19	0	43
CHEMICAL RESEARCH	0	10	0	10
CHEMICAL TECHNOLOGY	13	11	0	24
DESIGN AND ENGINEERING	37	14	0	51
HOMOGENEOUS REACTOR TEST	36	0	1	37
REACTOR MATERIALS RESEARCH	30	7	0	37
TOTAL	145	65	1	211

CHEMICAL TECHNOLOGY
D. E. FERGUSON,** PROBLEM LEADER — CT
J. MAYES, SEC. — CT

CHEMICAL DEVELOPMENT
D. E. FERGUSON,** SECTION CHIEF — CT

OXIDE PREPARATION
O. C. DEAN,** GROUP LEADER — CT
A. T. KLEINSTEUBER** — CT
K. H. MCCORKLE** — CT
C. E. SCHILLING** — CT
C. W. GREENE** — CT

THORIUM OXIDE STUDIES
J. P. MCBRIDE, GROUP LEADER — CT
R. A. KROHN, PROBLEM LEADER, *IRRADIATION STUDIES* — CT
L. E. MORSE — CT
P. P. HAYDON — CT
W. L. PATTISON — CT
H. F. SOARD — CT

SURFACE CHEMISTRY
C. H. SECOY, GROUP LEADER — CT
H. F. HOLMES — CT
F. H. SHEETON — CT

DESIGN
W. E. UNGER,** ASSISTANT SECTION CHIEF — CT

ThO_2 DEVELOPMENT AND HRT-CP DESIGN SUPPORT
H. O. WEEREN** — CT

INSTRUMENTATION
C. S. LISSER** — CT

PILOT PLANT
J. C. BRESEE,** SECTION CHIEF — CT

THORIUM OXIDE PREPARATION
W. H. LEWIS,** GROUP LEADER — CT
K. H. WINGET, PROBLEM LEADER — CT

UNIT OPERATIONS
P. A. HAAS,** GROUP LEADER — CT

SLURRY PREPARATION DEVELOPMENT
C. C. HAWS, JR. — CT
K. O. JOHNSSON — CT
V. L. FOWLER — CT

CHEMICAL RESEARCH
H. F. MCDUFFIE,** ASSISTANT DIRECTOR — RC
T. F. KELLY, SEC. — RC

HETEROGENEOUS EQUILIBRIA IN AQUEOUS SYSTEMS
W. L. MARSHALL,** GROUP LEADER — RC
J. S. GILL** — RC
E. V. JONES** — CONSULTANT
R. M. USHER** — RC
J. E. SAVOLAINEN** — RC

REACTIONS IN AQUEOUS SOLUTIONS
G. H. WATSON,** SUPERVISOR — RC
M. J. KELLY,** GROUP LEADER — RC
D. R. CUNEO** — RC
L. O. GILPATRICK** — RC
M. D. SILVERMAN** — RC
H. H. STONE** — RC

ANALYTICAL CHEMISTRY
MYRON T. KELLEY,** DIRECTOR
C. D. SUSANO,** ASSOCIATE DIRECTOR
K. A. ODOM,** SEC. — AC
H. E. ZITTEL, COORDINATOR HRP ANALYTICAL CHEMISTRY — AC

CORROSION ANALYTICAL LABORATORY
O. MENIS,* SECTION CHIEF — AC
H. P. HOUSE,** ASSISTANT SECTION CHIEF — AC

RESEARCH
O. MENIS,* GROUP LEADER — AC
C. M. BOYD — AC
D. L. MANNING, GROUP LEADER — AC
G. GOLDSTEIN — AC

DEVELOPMENT AND SPECIAL ANALYSES
T. C. RAINS, GROUP LEADER — AC
N. M. FERGUSON — AC

SERVICE
C. K. TALBOTT, SUPERVISOR — AC
F. L. LAYTON — AC
T. P. DACON — AC
C. A. CLARK — AC
P. S. GOODWIN — AC
T. G. MILLER — AC
E. ONKST — AC

SPECTROCHEMICAL SERVICES
C. FELDMAN,** SUPERVISOR — AC
W. R. MUSICK** — AC
A. H. MARSHALL** — AC
J. A. NORRIS,** GROUP LEADER — AC
J. J. MUROZAK** — AC

HRT AND IN-PILE LOOP ANALYSIS
U. KOSKELA, SUPERVISOR — AC
L. G. FARRAR, ASSISTANT SUPERVISOR — AC
C. P. BAKER — AC
S. R. DINSMORE — AC
G. M. CAMPBELL — AC
F. E. HAGA — AC
F. K. HEACKER — AC
M. H. MCCORQUODALE — AC
J. L. SHARP — AC
H. L. WEBB — AC
A. D. WILSON — AC

RADIOCHEMICAL ANALYSIS
E. I. WYATT,** SUPERVISOR — AC

HRT DEVELOPMENT
P. F. THOMASON,** GROUP LEADER — AC
R. E. BIGGERS** — AC
F. J. MILLER** — AC
S. A. REYNOLDS,** GROUP LEADER — AC
J. S. ELDRIDGE** — AC
T. H. HANDLEY** — AC
W. S. LYON** — AC

HIGH RADIATION LABORATORY
J. E. MORTON,** SUPERVISOR — AC

NUCLEAR ANALYSIS LABORATORY
G. W. LEDDICOTTE,** SUPERVISOR — AC
L. C. BATE** — AC
W. W. HARVEY** — AC

OPTICAL AND ELECTRON MICROSCOPY
T. E. WILLMARTH,** GROUP LEADER — AC

HOMOGENEOUS REACTOR TEST
S. E. BEALL, PROJECT ENGINEER — REE
H. HUMAN, SEC. — REE
D. SCOTT, JR., SPECIAL ASSIGNMENT — REE

J. W. HILL, JR., ASSISTANT SECTION CHIEF — REE
J. R. BUCHANAN, ASSISTANT FOR PLANNING — CT
R. H. GUYMON, CHIEF OF OPERATIONS — CT
H. C. ROLLER — REE
J. D. JONES — REE
R. J. HARVEY, SHIFT SUPERVISOR — REE
R. SMITH, JR., CONTROL ROOM SUPERVISOR — REE
D. T. GODWIN — REE
T. G. HILL — REE
A. L. JOHNSON — REE
H. F. BAUMAN, SHIFT SUPERVISOR — CT
E. W. BROWN, CONTROL ROOM SUPERVISOR — CT
E. D. BOLLING — REE
W. T. BOSTIC — CT
F. L. KOUSER — REE
D. F. FRECH, SHIFT SUPERVISOR — REE
R. J. SHANNON, CONTROL ROOM SUPERVISOR — CT
J. E. EVE — REE
L. J. SHEPSKY — CT
J. E. WOLFE — REE
N. C. BRADLEY, SHIFT SUPERVISOR — CT
J. L. STEPP, CONTROL ROOM SUPERVISOR — REE
J. D. BARNES — REE
H. D. CURTIS — REE
T. W. HERGE — REE

MAINTENANCE PLANNING
W. TERRY, SUPERVISOR — REE
G. H. JOHNSTONE — REE
L. P. PUGH — REE

INSTRUMENTATION
J. L. REDFORD, GROUP LEADER — I&C

P. N. HAUBENREICH,* ASSISTANT SECTION CHIEF — REE

REACTOR ANALYSIS
P. N. HAUBENREICH,* GROUP LEADER — REE
S. R. BUXTON — REE
J. O. KOLB — REE
H. B. PIPER — REE
P. VIGNET — FRENCH ATOMIC ENERGY COMMISSION
J. A. WATTS — REE

REACTOR CHEMISTRY
D. M. MCHARRISON, GROUP LEADER — REE
D. G. PEACH* — REE
R. M. WALLER* — REE

CHEMICAL PLANT
W. D. BURCH, GROUP LEADER — CT

INTERNAL DISTRIBUTION

1. C. E. Center
2. Biology Library
3. Health Physics Library
4. Metallurgy Library
5-6. Reactor Experimental Engineering Library
7-9. Central Research Library
10-14. Laboratory Records Department
15. Laboratory Records, ORNL R. C.
16. G. M. Adamson
17. A. L. Bacarella
18. J. E. Baker
19. S. J. Ball
20. J. C. Banter
21. S. E. Beall
22. L. L. Bennett
23. A. M. Billings
24. D. S. Billington
25. E. P. Blizard
26. R. Blumberg
27. E. G. Bohlmann
28. S. E. Bolt
29. C. J. Borkowski
30. G. E. Boyd
31. J. C. Bresee
32. F. R. Bruce
33. J. R. Buchanan
34. W. D. Burch
35. C. A. Burchsted
36. S. R. Buxton
37. A. D. Callihan
38. T. A. Carlson
39. W. L. Carter
40. G. H. Cartledge
41. R. H. Chapman
42. R. A. Charpie
43. R. D. Cheverton
44. C. J. Claffey
45. H. C. Claiborne
46. T. E. Cole
47. C. W. Collins
48. E. L. Compere
49. F. L. Culler
50. D. G. Davis
51. R. J. Davis
52. V. A. DeCarlo
53. W. K. Eister
54. L. B. Emlet (K-25)
55. J. L. English
56. D. E. Ferguson
57. D. F. Frech
58. J. H. Frye, Jr.
59. C. H. Gabbard
60. J. L. Gabbard
61. W. R. Gall
62. R. B. Gallaher
63. E. H. Gift
64. H. E. Goeller
65. R. S. Greeley
66. A. T. Gresky
67. J. C. Griess
68. W. R. Grimes
69. E. Guth
70. R. H. Guymon
71. L. A. Haack
72. P. A. Haas
73. J. Halperin
74. P. H. Harley
75. R. J. Harvey
76. P. N. Haubenreich
77. D. N. Hess
78. J. W. Hill
79. E. C. Hise
80. A. Hollaender
81. P. P. Holz
82. H. P. House
83. A. S. Householder
84. S. Jaye
85. G. H. Jenks
86. D. T. Jones
87. E. V. Jones
88. W. H. Jordan
89. P. R. Kasten
90. C. P. Keim
91. M. T. Kelley
92. F. Kertesz
93. J. O. Kolb
94. U. Koskela
95. K. A. Kraus
96. N. A. Krohn
97. J. A. Lane
98. C. G. Lawson
99. S. C. Lind
100. R. B. Lindauer
101. R. S. Livingston
102. R. A. Lorenz
103. M. I. Lundin
104. R. N. Lyon
105. J. L. Marsh (C&CC, South Charleston)
106. W. L. Marshall

107. J. P. McBride
108. H. F. McDuffie
109. H. A. McLain
110. J. R. McWherter
111. O. Menis
112. E. C. Miller
113. R. L. Moore
114. C. S. Morgan
115. K. Z. Morgan
116. L. E. Morse
117. J. P. Murray (Y-12)
118. M. L. Nelson
119. P. D. Neumann
120. A. R. Olsen
121. L. F. Parsly
122. F. N. Peebles
123. M. L. Picklesimer
124. B. E. Prince
125. L. R. Quarles
126. S. A. Reed
127. W. D. Reel
128. P. M. Reyling
129. S. A. Reynolds
130. L. Rice
131. D. M. Richardson
132. R. C. Robertson
133. W. Robinson
134. H. C. Roller
135. M. W. Rosenthal
136. H. C. Savage
137. C. E. Schilling
138. H. E. Seagren
139. C. H. Secoy
140. C. L. Segaser
141. E. D. Shipley
142. M. D. Silverman
143. M. J. Skinner
144. A. N. Smith
145. E. S. Snavely
146. A. H. Snell
147. I. Spiewak
148. H. H. Stone
149. R. W. Stoughton
150. C. D. Susano
151. J. A. Swartout
152. A. Taboada
153. E. H. Taylor
154. W. Terry
155. D. G. Thomas
156. P. F. Thomason
157. M. Tobias
158. W. E. Unger
159. W. C. Ulrich
160. R. Van Winkle
161. D. W. Vroom
162. R. E. Wacker
163. H. O. Weeren
164. A. M. Weinberg
165. S. H. Wheeler
166. E. P. Wigner (consultant)
167. H. D. Wills
168. G. C. Williams
169. J. C. Wilson
170. R. H. Winget
171. C. E. Winters
172. L. F. Woo
173. F. C. Zapp
174. ORNL - Y-12 Technical Library, Document Reference Section
175. HRP Director's Office, Y-12

EXTERNAL DISTRIBUTION

176. Division of Research and Development, AEC, ORO
177-753. Given distribution as shown in TID-4500 (15th ed.) under Reactors-Power Category (75 copies - OTS)

Reports previously issued in this series are as follows:

ORNL-527	Date Issued, December 28, 1949
ORNL-630	Period Ending February 28, 1950
ORNL-730	Feasibility Report - Date Issued, July 6, 1950
ORNL-826	Period Ending August 31, 1950
ORNL-925	Period Ending November 30, 1950
ORNL-990	Period Ending February 28, 1951
ORNL-1057	Period Ending May 15, 1951
ORNL-1121	Period Ending August 15, 1951
ORNL-1221	Period Ending November 15, 1951
ORNL-1280	Period Ending March 15, 1952
ORNL-1318	Period Ending July 1, 1952
ORNL-1424	Period Ending October 1, 1952
ORNL-1478	Period Ending January 1, 1953
ORNL-1554	Period Ending March 31, 1953
ORNL-1605	Period Ending July 31, 1953
ORNL-1658	Period Ending October 31, 1953
ORNL-1678	Period Ending January 31, 1954
ORNL-1753	Period Ending April 30, 1954
ORNL-1772	Period Ending July 31, 1954
ORNL-1813	Period Ending October 31, 1954
ORNL-1853	Period Ending January 31, 1955
ORNL-1895	Period Ending April 30, 1955
ORNL-1943	Period Ending July 31, 1955
ORNL-2004	Period Ending October 31, 1955
ORNL-2057	Period Ending January 31, 1956
ORNL-2096	Period Ending April 30, 1956
ORNL-2148	Period Ending July 31, 1956
ORNL-2222	Period Ending October 31, 1956
ORNL-2272	Period Ending January 31, 1957
ORNL-2331	Period Ending April 30, 1957
ORNL-2379	Period Ending July 31, 1957
ORNL-2432	Period Ending October 31, 1957
ORNL-2493	Period Ending January 31, 1958
ORNL-2561	Periods Ending April 30 and July 31, 1958
ORNL-2654	Period Ending October 31, 1958
ORNL-2696	Period Ending January 31, 1959
ORNL-2743	Period Ending April 30, 1959
ORNL-2879	Period May 1 Through October 31, 1959